JIMMA UNIVERSITY

JIMMA INSTITUTE OF TECHNOLOGY

SCHOOL OF GRADUATE STUDIES

FACULTY OF CIVIL AND ENVIRONMENTAL ENGINEERING

GEOTECHNICAL ENGINEERING PROGRAM

GEOTECHNICAL INVESTIGATION AND STABILITY ANALYSIS OF LANDSLIDE USING NUMERICAL METHODS: THE CASE OF CHIRA TOWN, SOUTH-WESTERN ETHIOPIA

A Thesis Submitted to the School of Graduate Studies of Jimma University, Jimma Institute of Technology, Faculty of Civil and Environmental Engineering in Partial Fulfillment of the Requirements for the Degree Master of Science in Geotechnical Engineering

By:

MULATU TAMIRU TEREFE

July 2021

Jimma, Ethiopia

JIMMA UNIVERSITY

JIMMA INSTITUTE OF TECHNOLOGY

SCHOOL OF GRADUATE STUDIES

FACULTY OF CIVIL AND ENVIRONMENTAL ENGINEERING

GEOTECHNICAL ENGINEERING PROGRAM

GEOTECHNICAL INVESTIGATION AND STABILITY ANALYSIS OF LANDSLIDE USING NUMERICAL METHOD: THE CASE OF CHIRA TOWN, SOUTH-WESTERN ETHIOPIA

A Thesis Submitted to the School of Graduate Studies of Jimma University, Jimma Institute of Technology, Faculty of Civil and Environmental Engineering in Partial Fulfillment of the Requirements for the Degree Master of Science in Geotechnical Engineering

Advisor: Dr. DAMTEW TSIGE (Ph.D.)

Co-Advisor: Engr. HASHIM WARE (MSc)

July 2021

Jimma, Ethiopia

DECLARATION

I declare that this research entitled "**Geotechnical Investigation and Stability Analysis of Landslide Using Numerical Method: The Case of Chira Town, South-Western Ethiopia**" is my original work and has not been sent to Jimma University or elsewhere as a prerequisite for the award of any degree.

    Mr. MULATU TAMIRU TEREFE   _____   _____

        NAME   SIGNATURE   DATE

As research Advisor, I now certify that I have read and evaluated this research paper under my guidance, by Mr.Mulatu Tamiru Terefe entitled "**GEOTECHNICAL INVESTIGATION AND STABILITY ANALYSIS OF LANDSLIDE USING NUMERICAL METHOD: THE CASE OF CHIRA TOWN, SOUTH-WESTERN ETHIOPIA**" and recommend and would be accepted, as a fulfilling requirement for the Degree Master of Science in Geotechnical Engineering.

    Advisor: Dr. DAMTEW TSIGE (Ph.D.)   _____   _____

        NAME   SIGNATURE   DATE

    Co-Advisor: Engr. HASHIM WARE (MSc)   _____   _____

        NAME   SIGNATURE   DATE

ABSTRACT

Landslide is a natural disaster in which earth mass materials like rock, debris, or earth move down a slope and cause damage to living things, as well as the natural environment. In 2020, the landslide occurred in Chira town following heavy rainfall. As a result, Residential houses, internal roads of the towns, pipelines, and natural environment were damaged following the land subsidence of the study area. Therefore, this research aimed to conduct geotechnical conditions and stability analysis of landslide occurred in Chira Town. The main objective of the study was include investigation on geotechnical conditions and their role in landslide occurrence, identification of the main triggering factors, slope stability analysis by using Plaxis 2D and Slide software's, and propose remedial measures to safeguard future failure in the study area. To achieve the objective of this study, experimental and analytical methods were conducted. To determine subsurface condition, Geophysical test was conducted. Soil samples were taken from the crest and toe of the affected and unaffected slope area at different depths and test on index and engineering properties of soils was conducted following the ASTM procedure. Three slopes were analysed by plaxis 2D and slide softwares on affected and unaffected slopes. Based on laboratory tests and geophysical investigation, the soil types of the study area were dominated by fine-grained soils (Clay &silt) and they initiate the occurrence of landslide since they are weaker soil when contact with water. Rainfall is the major triggering factor and from prediction rate of causal factors, the soil type, land use, elevation, distance to stream, slope, aspect and curvature were a reason for the occurrence of Chira landslide by 22.03%, 18.89%, 15.75%, 15.46%, 10.87%, 9.7%, and 7.5% respectively. FS varied between 1.34 to 1.95 (by plaxis) and 1.35 to 1.93 (by slide) for affected slopes and 0.66 to 0.98 (by plaxis) and 0.67 to 0.97 (by slide) in saturated and dry state respectively. Hence, they are considered as unstable slopes. FS for unaffected slope varied between 1.83 to 3.18 (by plaxis) and 2.02 to 3.17 (by slide), which is stable. The LE overstimate the FS from 5% - 20% over FE analysis in dry and partially saturated conditions respectively. Groundwater increament decreases the FS by 42.45% - 50.75% (by plaxis) and 35.94% - 49.93% (by slide) software's. Surface drainage, planting vetiver vegitation, and proper landuse management were the proposed remedial measures for Chira town landslide.

Keywords: *Geotechnical Investigation; Landslides; Mitigation Measures; Slope Stability.*

ACKNOWLEDGEMENT

TABLE OF CONTENT

Contents	Page No.

LIST OF FIGURE

LIST OF TABLE

ABBREVIATION

ASTM	American Standard Test Method
BGL	Below Ground Level
Cf	Corrected Factor
CH	Highly Plastic Clay
CHR	Corrected Hydrometer Reading
DSP	Diameter of Soil Particles
ECDSWC	Ethiopian Construction Design & Supervision Works Corporation
EP	Electrical Profiling
FEM	Finite Element Method
FOS	Factor of Safety
FR	Frequency Ratio
GCP	Ground Control Points
GIS	Geographic Information System
Gp	Force Perpendicular to Gravity
GPS	Geographical Positioning System
Gt	Force Tangential to Gravity
GWT	Ground Water Table
Hr	Hour
HR	Hydrometer Reading
IITC	International Institute for Aerospace Survey and Earth Sciences
LEM	Limit Equilibrium Method
LL	Liquid Limit
LSI	Landslide Susceptibility Index
MH	Highly Plastic Silt
MR	Mass of Retained
Nci	Number of Cell Points of Class I
NCt	Total Number of Cell Points
Nli	Number of Landslides In Class I
NLt	Total Number of Landslides

NMC	Natural Moisture Content
OCHA	Office for the Coordination of Humanitarian Affairs
PL	Plastic Limit
PR	Prediction Rate
RF	Relative Frequency
SS	Sieve Size
T	Temperature
UU	Unconsolidated Un-drained
USCS	Unified Soil Classification System
VES	Vertical Electrical Sounding

CHAPTER 1

INTRODUCTION

1.1Background

Landslide is a natural disaster in which earth mass materials like rock, debris, or earth move down a slope and cause damage to living things as well as the natural environment (Serdarevic and Babic, 2019). It's composed of two words: land and slide. The first term is used to describe natural materials before they affected, and the second term implying that, the action taken on the first term, that is the movement of landmass from its original position (Lollino *et al.*, 2015; Serdarevic and Babic, 2019; Walker and Shiels, 2013). As clearly stated by Walker and Shiels (2013), landslides occur in all geographic regions of the world due to the principal natural drivers of landslides and triggering factors such as high rainfall intensity, soil erosion, earthquake, groundwater fluctuation, and human activities. Landslide is worldwide natural hazard since, it is responsible for direct and indirect losses of human lives and injuries, damages to roads, houses, other infrastructures, and bankrupt economy of the country (Gaurina-Medjimurec, 2014; Patra and Devi, 2018).

According to Highland and Bobrowsky (2008) and Serdarevic and Babic (2019), classifying landslide help us to estimate the rate of movement, the likely volume of displacement, the run-out distance, as well as the possible effects of the landslide and the appropriate mitigation measures to be taken into account. The same author points out that; landslide classification is based on the way of movement and type of material involved. Soil, rock, or debris are materials involved in landslide. The soil in landslide studies can be debris, or earth. Debris contains coarser in which 20% - 80% of particles are more significant than 2 mm, and earth materials are smaller than debris and contains 80% or more of the particles are smaller than 2 mm. The types of movement express how materials are displaced from their original position and moved to a stable position due to causal factors, and they can be listed as: fall, topple, slide, spread, or flow (Highland and Bobrowsky, 2008).

Landslide occurs along the slope of earth mass and more significant in mountainous terrain since the soil mass or rocks slides from an unstable position to a stable position by gravity load. According to Woldearegay (2013) and Liu *et al.* (2017), landslides are frequently occurr in

mountainous areas of tropical and temperate zones after heavy rainfall and cause instability along the slope of the earth's mass, which are known as a rainfall-triggered landslide. After heavy rainfall, the pore pressure becomes increases, and the effective stress of soil decreases, which leads to significant decreases in shear strength of the soil and eventually resulting in the failure of the slope (Liu *et al.*, 2017; Hulagabali et al., 2019). Extreme rainfall intensity was concentrated, and occurred in Ethiopia in July and August, which will cause high water percolation in the ground and initiate the occurrence of landslides (Abebe *et al.*, 2010; Hulagabali et al., 2019). Slope steepness, soft soils over the impermeable rocky materials, deforestation are among some triggering factors of landslides besides heavy rainfall (McColl, 2015).

Landslide issues can sometimes be avoided to make the slope more stable by using engineering techniques. Some of the engineering techniques used to overcome this challenge are proper land use, treatment such as constructing retaining walls, managing water through proper drainage for maintaining appropriate soil moisture, Internal slope reinforcement, and modifying slope geometry (Serdarevic and Babic, 2019; Choi and Cheung, 2013). Landslide mitigation measures to be considered mainly depend on the type of mass movement, condition of the environment, engineering and economic feasibility, the volume of displaced materials, etc.

1.2 Statement of the Problem

Landslide is a global problem and occurred throughout history under all climate conditions and terrains. It is responsible for economic loss estimated at billion dollars and deaths and injuries of thousands of people annually (Highland and Bobrowsky, 2008). Landslide problems are significantly affecting both developed and developing countries. In history, the landslides in japan cause direct and indirect losses of $4 billion annually. The USA, Italy, and India follow Japan with an estimated annual cost ranging between $1 billion to $2 billion (Popescu and Sasahara, 2009). Economic losses due to landslides in developing countries are sometimes equal to or exceed their gross national products (Wang and Sassa, 2003).

As stated by Abebe *et al.* (2010), Hulagabali et al. (2008), and Hearn (2019), Ethiopia considered a lot of landslide history, and there has been a massive loss in terms of properties and deaths of peoples in thousand across all corners of the country. Previous researchers, such as (Woldearegay, 2013; Tsige *et al.*, 2017) shown that the highlands of Ethiopia were frequently

affected by landslides, and detailed investigation should be needed to overcome the problem. Tsige *et al*. (2017) pointed that several infrastructures has been destroyed in south-Western Ethiopia as a result of landslides, and its consequences affect both community and government directly or indirectly. As mentioned by Abebe *et al.* (2010), an average high relief between 2000 m to 3000 m in highlands of Ethiopia, and high rainfall intensity up to 2000 mm in South-western of the country is considered as the most triggering factor for landslide occurrence. The report by OCHA (2020) indicated that as a result of high rainfall intensity from June to September, the flood occurred, and at least 151,828 people were affected, including 100,176 people were displaced from their homes; from this, 1,266 people were displace from Oromiya National Regional State.

In 2020 landslide have been occurred in Chira town and caused the displacement of many households, and damaged many infrastructures like houses, roads and pipelines in the town. Even though socio-economic study didn't studied in this study area, this problem bankrupt the socio-economic of the study area.This problem frequently occurred from year to year during the rainy season especially starting from 2014 in this study area. Concerning this, the geotechnical conditions and slope stability of the study area were investigated and analyzed, and the prevention, and mitigation measures of the affected area were proposed.

1.3 Research Questions

The research questions this thesis aimed to address was:-

1. What are the Geotechnical Conditions of the soils and their role in landslide occurrence of the study area?
2. What are the causes and triggering factors of the landslides of the study area?
3. What is the slope's condition from slope stability analysis using Plaxis 2D and Slide Software?
4. What is the remedial measures to safeguard future failure in the Chira town landslide?

1.4 Objectives

1.4.1 General Objective

The general objective of the research was to investigate geotechnical conditions and analysis of slope stability of landslide in Chira Town, Jimma Zone, South-western Ethiopia.

1.4.2 Specific Objectives

The basic goals of this study were to be:-

- ➢ To investigate the Geotechnical Conditions of the soils and their role in landslide occurrence of the study area.
- ➢ To find out the causes and triggering factors of landslides of the study area.
- ➢ To analyze the condition of the slope using Plaxis 2D and Slide Software.
- ➢ To provide remedial measures to safeguard future failure of Chira town landslide.

1.5 Scope of the Study

This research looked at the geotechnical conditions and slope stability analysis of a landslide in Chira Town, Jimma Zone. The study aims identification of geotechnical conditions and their role in landslide initiationas, determination of causal factors, stability conditions of slopes, and propose remedial measures to safeguard future failure in the study area. To achieve the goal, the geophysical test and laboratory test conducted to determine geotechnical conditions. Seven causal factors were investigated using GIS software based on stastical bivirate fruquency ratio method. After assessing Slope stability by using Plaxis 2D and Slide software, relevant remedial actions were given to reduce the effects of landslides in the study area.

1.6 Limitation of the Study

Even though this study has made a significant contribution to the landslide of Chira town, it has limitations owing to a lack of complete data, such as rainfall data, restricted morphological features, and deep digging equipment.

1.7 Significance of the Study

The findings of this study will have a valuable information on the Chira town landslide. The study area's primary cause of landslide and mitigation methods was recommended, and municipality office can use the findings to overcome the problem. This study will also serve as a resource for investigators looking into the landslide problem and a reference for other researchers looking into the origins and features of geotechnical conditions and slope stability analyses.

1.8 Organization of the thesis

This study was divided in to five chapters, each covering the specific topic of the study work. In chapter one the background of landslides as perspective to worldwide upto study area, statement of the problem, research questions, objective, limitations, scope, and significance of the study are presented. Chapter two deals with a detail literature review. Several causes of landslide, type of landslide, its effects as well as some of remedial measures regarding to landslide are discussed in this chapter. Different mechanisms of slope stability analysis by using numerical methods are also presented under this chapter. Chapter three deals with material and methods used for the study, chapter four contain result and discussion gained from laboratory and field test, visual observation and software results. The last chapter was conclusion and recommendations drawn from the study. Reference comes next to conclusion and recommendation, at the end Tables and Figures of laboratory result and standard are included in appendices.

CHAPTER 2

LITERATURE REVIEW

2.1 General

A landslide is a natural catastrophe in which earth mass materials like rock, debris, or earth move down a slope and cause damage to living things as well as the natural environment (Serdarevic and Babic, 2019). This issue is responsible for significant property damage, loss of human lives, and hundreds of injuries each year. Landslide disasters have a tremendous impact on both developed and developing countries. Landslides in Japan have historically resulted in direct and indirect losses of $4 billion per year, with the United States, Italy, and India trailing behind with yearly costs ranging from $1 billion to $2 billion. Landslide disasters in poor nations are projected to be equivalent to or greater than their gross national products (Wang and Sassa, 2003).

2.2 Responsible Factors for Causes of Landslide

Slope failure is another term used interchangeably with a landslide because of, most landslides occurred along a slope of earth mass (Highland and Bobrowsky, 2008). However, there are also different triggering factors responsible for the occurrence of a landslide in addition to slope steepness. We can categorize causes of the landslide as natural and human activities but, the two combinations can also cause the landslide. Natural causes of landslides are categorised into three. Those are water, earthquake, and volcanic activities because they alter the balance between the driving force and resisting force in slope areas (Walker and Shiels, 2013). They all depend on factors such as slope steepness, soil type, rainfall, underlying geology and, etc. Modifying slope geometry due to different construction purposes, such as undercutting for road embankments, deforestation, irrigation, etc., are among the most human activities responsible for the cause of landslide (Highland and Bobrowsky, 2008; Azeze, 2020).

2.2.1 Water Activities on Landslide

Water is one of the foremost triggering factors of the landslide, commonly in the highland terrain areas (Yifru and Ayehu, 2017). Water that comes from rainfall or snow melts onto the earth mass increase the weight to the slope (Serdarevic and Babic, 2019). Weight is force, and stress is force over the area that can be considered as driving force and resulting slope instabilities. When we

say water in landslide initiation factor, we need to talk about flooding because most of the moisture causes landslide arises from flooding which is related to precipitation, run-off, and saturation of ground by both flows on slope surface and water infiltration (Liu *et al.*, 2017).

2.2.2 Earthquake Activities on Landslide

Earthquake causes landslides due to ground shaking and liquefaction of soil (Geertsema and Highland, 2011). Slope surfaces are prone to damage during an earthquake because the shaking process or motion disrupts the ground mass, causing the soil to lose its shear strength, resulting in landslides (McColl, 2015).The higher the magnitude of an earthquake, the more energy it exerts on slope material, which can increase driving force along potentially slip planes (Walker and Shiels, 2013). If seismic and other driving forces exceed, the resisting forces, a landslide will occur (Fisseha and Mewa, 2016). Even if earthquake activities are the most responsible of triggering landslides factors worldwide, it is not common in Ethiopia.

2.2.3 Volcanic Activities on Landslide

Landslides occurred due to volcanic activities are considered as the most devastating earth mass failure (Highland and Bobrowsky, 2008; Walker and Shiels, 2013). The same author stated that the rock, soil, ash, and water formed from volcanic lava are accelerating rapidly on the steep slopes of volcanoes and devastating anything on its path. Like earthquake activity, this kind of triggering is also not expected in Ethiopia.

2.2.4 Human Activities on Landslide

A lot of activities are done on earth mass by human beings. As a result, they modify the geometry of earth mass, disturbing or changing drainage patterns, undercutting slope due to different construction of infrastructures, mining, quarrying, irrigation works, and removing Vegetation (Azeze, 2020; Highland and Bobrowsky, 2008). This disturbed natural environment reacts to the new modification depending on the amount and type of modification made to it (Senouci, 2020). During the modification of land profile, the resisting force against shear failure along with slope decreases, and mass movement will occur. Most of these activities have occurred during road construction since a large volume of soil that can take a long length undergoes the cutting and filling process.

2.3 Landslide Contributory Factors

2.3.1 Slope Geometry

Slope geometry is the general term used to describe words with the same meaning and close relation, such as slope angle, slope steepness, and gravity. It is the most landslide contributory factor that is why the mass movement is high in mountainous areas where there is a steep slope and unbalances of earth materials occur (Broothaerts *et al.*, 2012). It describes both relative relief and slope morphometric. Relative relief refers to the distance between a slope's highest and lowest points, whereas morphometric refers to the slope's angle or steepness (Mulatu et al., 2009). An increment in both cases increases the occurrence of landslides (Abebe *et al.*, 2010; McColl, 2015). The force of gravity on the slope can be resolve into a component acting perpendicular to the slope and a component acting tangential to the slope (Nelson, 2013).
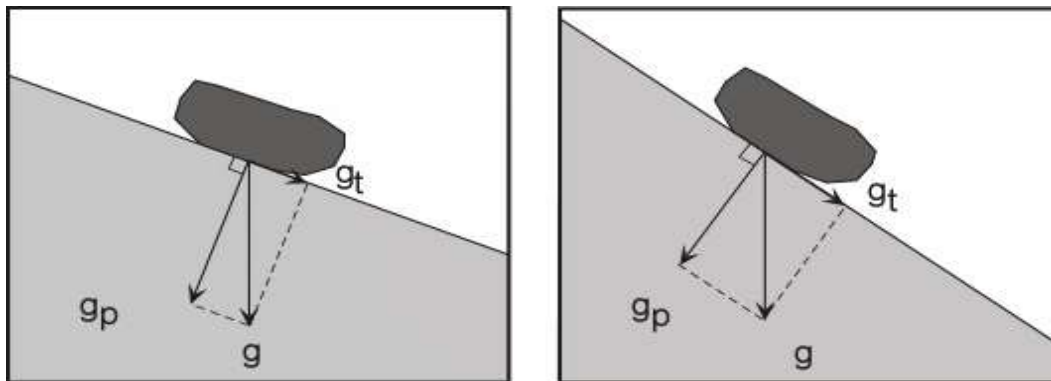
Figure 2.1 Slope geometry effect on the mass movement (Source: (Nelson, 2013)).

From Figure 2.1 above, the perpendicular gravity component, gp, tries to hold the object on the slope and keep it steady. A shear stress parallel to the slope in the down-slope direction that pulls the object is affected by the tangential gravity component, gt. The shear pressure or tangential component of gravity, gt, increases, and the shear stress or tangential component of gravity increases on a steeper slope (Nelson, 2013; McColl, 2015). As stated by Walker and Shiels (2013), slope geometry that is > 75° can be considered as a steep slope, and they are susceptible to landslide occurrence. The driving force in steep slope increases since the weight for a hilly slope is larger than the flat one.

2.3.2 Type and properties of Materials

Soil, rock, or their combinations are the primary materials of earth mass or slope. Depending on their formation, we can classify soil as residual soil and transported soils. Transported soils are more exposed to landslides since they are erodible ,and chemically and physically altered materials (Walker and Shiels, 2013). Pore pressures develop quickly in shallow soils and cause shallow debris or slide (Geertsema et al., 2009). Clay is more negatively charged particles, and in water, hydrogen has a positive charge, which results in the attraction of water by clay particles and saturates the slope. According to Walker and Shiels (2013), materials such as weathered basalt, tuff, and basalt are very sensitive to a landslide. The slope material, either soil or rock lose its strength due to discontinuities like faults, bedding surface, foliations, cleavages, joints, fissures, shears zones. Discontinuities make soil or rock mass anisotropic.

The void ratio is depending on the texture of the soil. Increasing the void ratio increases the probability of percolation runoff into the soil while, decrease in void ratio leads to produce pore pressure with that can initiate landslide (Budhu, 2011). It is known that particle arrangement and interlocking are probably the factors of their shape and size, which control the void ratio of the soil and allow the soils to stay in a more stable configuration. The shear strength parameter (internal friction angle) increases more rapidly on those materials having higher angularity, and increases the relative density.

According to McColl (2015), material type can define the shear strength of materials. The shear strength of materials depends on factors such as composition, fabric, size, texture, plasticity, angle of repose, density, bonding material, and other properties of slope material. The soil has high shear strength than rock because of the cohesive properties of soil (Walker and Shiels, 2013).

2.3.3 Rainfall

Most landslides have occurred after heavy rainfall intensity (Liu *et al.*, 2017). This is since during and after rainfall, the slope material saturated and increases in weight, which leads to a decrease in shear strength of the soil and causes a landslide. The differences in pore water pressures distributed in the soil differ depending on the hydraulic conductivity, topography, degree of weathering, and soil fracturing during high rainfall rates (Duan et al., 2019). Heavy

rainfall increases the positive pore pressure in the soil. A void space of soil in positive pore pressure has only water, and this water pushes the soils and disperses the soil particles that may cause landslides.

Rainfall-induced landslides are common in Ethiopia's highlands, where steep and mountainous terrains are regularly damaged by landslides due to high rainfall intensity (Woldearegay, 2013; Kabeta and Teshager, 2020).The same author points out that, rainfall that triggered a landslide in Ethiopia include debris/earth slides, debris/earth flows and, medium to large-scale rock slides. Even if rock falls are familiar in Ethiopian highlands, it does not have any relation with rainfall.

The mean annual rainfall in Ethiopia is between < 250 mm and 2000 mm, but some parts of the country, especially the south-western part of the country, may receive more than this amount of rainfall (Hearn, 2019; Abebe *et al.*, 2010; Woldearegay, 2013). This heavy rainfall also responsible for the occurrence of flooding, and its consequences decrease the stability of the slope in Ethiopia. As reported by OCHA (2020) as a result of high rainfall intensity from June to September, a landslide occurred, and at least 151,828 people were affected, including 100,176 people were displaced from their homes; from this, 1,266 people were displaced from Oromiya National Regional State.

2.3.4 Groundwater Fluctuation

Groundwater fluctuation is variation in groundwater level due to seasonal differences in rainfall. After heavy rainfall the runoff percolate into the ground and the groundwater fluctuation appears. Groundwater flow is different from region to region, and it is continuously in motion regions of recharge to discharge size (Yifru and Ayehu, 2017). It is a natural factor that hurts the stability of the slope, and rainfall is the primary supply source to groundwater fluctuation. During the dry season, the groundwater level is low, while after heavy rainfall in the winter period, the groundwater level becomes increased and groundwater fluctuation, as well as slope instability, occurs since the shear strength of slope material decrease as the weight of the materials due to the addition of water level above the weak zone of the earth mass increase. The posetive pore pressure is produced during increament of groundwater condition. Periodical swell-shrink behavir of expansive clay soils due to groundwater fluctuation is also one of the significant causes of slope instabilities (Duan et al., 2019).

2.3.5 Liquefaction of the Soil

Soil liquefaction develops when the vibrations or shaking from an earthquake cause the soil to behave like a liquid (Serdarevic and Babic, 2019). It tends to compact and decrease in volume when saturated sand is subject to ground vibration; if drainage is unable to occur, the tendency to decrease in volume results in an increase in pore water pressure, and when this becomes equal to the total stress, then effective stress is equal to zero. Soils lose its strength because of loss of effective stress.

2.3.6 Undercutting of slope Geometry

Due to population expansion, different infrastructures constructed in the natural environment. The natural environment may not suit to put the intended structure on it, and needs to modify its geometry. Undercutting the slope geometry for different purpose in the construction industry is one of these kinds of modification and is considered as an initiator for the occurrence of landslides (Coutinho *et al.*, 2019; Kabeta and Teshager, 2020). Human activities in the construction industry and related works such as the construction of roads, buildings, mines and quarries, dams and reservoirs, canals, an increase of groundwater levels, changes in vegetative cover, tunnels, and communication systems have a significant impact on the stability of the slope (Walker and Shiels, 2013).

2.3.7 Vegetation

Vegetation is a process in which ground is cover by plants. It may contain plantations and deforestation. Deforestation is the removal of different types of plants from the natural environment. It contains activities like the forestland conversation to farms, ranches, or urban use (Sharma and Ram, 2014; Walker and Shiels, 2013). Deforestation hurts the slope of earth mass. Landslide increases due to deforestation because of the removal of trees, which can anchor the soil with their roots. After deforestation in a specific area, the soil loses its capacity and ultimately leads to landslides during heavy rainfall (Sharma et al., 2014). On the other hand, planting additional vegetation's on slope surface may cause landslide since the weight or driving force of the soil increase but the root strength govern on earth mass and make it stable. The root should have to penetrate in deep and must greaterthan the depth of critical layer just to compromise the affected soil and the soil loses its strenth.

Table 2.1 Summary of Landslide Causes (Source: (Msilimba, 2012)).

External Causes	Internal Causes
➢ Geometrical change	➢ Progressive failure (internal
• Height	response to unloading)
• Gradient	• Expansion and swelling
	• Fissuring
• Slope length	• Straining, softening
	• Stress concentration
➢ Loading	➢ Weathering
• Natural	• Physical property changes
• Man-induced	• Chemical changes
➢ Unloading	➢ Seepage erosion
• Natural	• Removal of cement
• Man-induced	• Removal of fine particles
➢ Shocks and Vibrations	➢ Water regime change
• Single	• Saturation
• Multiple/continuous	• Rise in the water table
	• Excess pressures
	• Drawdown

2.4 Landslide Susceptability Mapping

Determining the susceptibility of landslide requires identification and estimation of the landslide causative factors contributions and their relationship (Hamza and Raghuvanshi, 2016). For landslide hazard mapping, statistical hazard mapping techniques considering various causative factors were used. There are different approaches used to determine the landslide susceptibility maps. They can becatagorized as qualitative approach, semi-quantitaive approaches, and quantitative approaches (Shan *et al*., 2020). Frequency ration is one of bivariate statical quantitative approaches and it is based on combinations of causal factors. Frequency Ratio (FR) is the ratio of the area where landslides occurred in the total study area and is the ratio of the

probabilistic of a landslide occurrence to a non-occurrence for a given attribute (Silalahi *et al.*, 2019). Mathematically, frequency ratio is expressed as,

$$FRi = \frac{(\frac{Nli}{NLt})}{(\frac{Nci}{Nct})}$$ (1)

After determining the FR, normalize the FRs in a range of probability values (0,1) as a relative frequency (RF). The RF for each class was calculated with the following formula,

$$RF = \frac{FRi}{\sum FRi}$$ (2)

The highest RF value shows the highest probability of the landslide occurrence in the corresponding classes (Acharya and Lee, 2019).

Prediction Rate (PR) was calculated to rate every conditioning factor with training data sets using the following empirical,

$$PR = \frac{(RFmax - RFmin)\ of\ each\ factor}{(RFmax - RFmin)min\ of\ all\ factor}$$ (3)

Landslide Susceptibility Index (LSI) was derived from the relative frequency ratio and prediction rate using raster calculator in ArcGIS spatial analysis too using equation 4 (Acharya and Lee, 2019).

$$LSI = \sum(PR * RF)$$ (4)

Where,

NLi is the number of landslides in class i

NLt is the total number of landslides

NCi is the number of cell points of class i

NCt is the total number of cell points

2.5 Classification of Landslide

According to International Institute for Aerospace Survey and Earth Sciences (IITC), the following criteria's can be used or have been used to classify landslides:

➢ Material: Rock, Soil Lithology, structure.

➢ Geotechnical properties

➢ Geomorphic attributes: Weathering, Slope form

> ➤ Landslide geometry: Depth, Length, Height, etc.

> ➤ Type of movements: Fall, Slide, Flow, etc

> ➤ Climate: Tropical, per glacial, etc.

> ➤ Water: Dry, wet, saturated

> ➤ Speed of movement: Very slow, slow, etc.

> ➤ Triggering mechanism: Earthquake, rainfall, etc.

According to J.Crozier (2004), classification of the landslide had been proposed based on the type of materials involved, kind of movements, causes, and many other factors. The same author categorizes the mass movement depending on the type of movement into six main groups, namely falls, topples, slides, lateral spreads, flows, the complex movement, which contain combinations of two or more of the other types of movement and besides he also subdivides the type of materials into bedrock, debris, and earth. The author gives this name by adding an adjective in front of the noun (Land) to describe more the condition of movement. As stated by (Highland and Bobrowsky, 2008; Mia et al,, 2016), classifying a landslide enable as to evaluate landslide hazards and propose remedial mitigation measures.

Table 2.2 Classification of Landslide (Source: (Crozier, 2005; Highland and Bobrowsky, 2008) as cited from Varnes, 1978))

Type of movement			Type of materials		
			Bedrock	Engineering soils	
				Predominantly coarse	Predominantly fine
Falls			Rock fall	Debris fall	Earth fall
Topples			Rock topple	Debris topple	Earth topple
Slides	Rotational	Few units	Rock slump	Debris slump	Earth slump
	Translational	Many units	Rockslide	Debris slide	Earth slide
Lateral spreads			Rock spread	Debris spread	Earth spread
Flows			Rock flow	Debris flow	Earth flow
Complex			Combination of two or more primary movement forms		

2.5.1 Fall

A fall of soil, rock, or both occurred from a steep slope along a surface where is no, or slight shear displacement has been occurred and descends mainly through the air by falling, saltation, or rolling due to triggering factors such as undercutting of the slope, differential weathering and earthquake shaking (Lollino *et al.*, 2015; Geertsema and Highland, 2011).
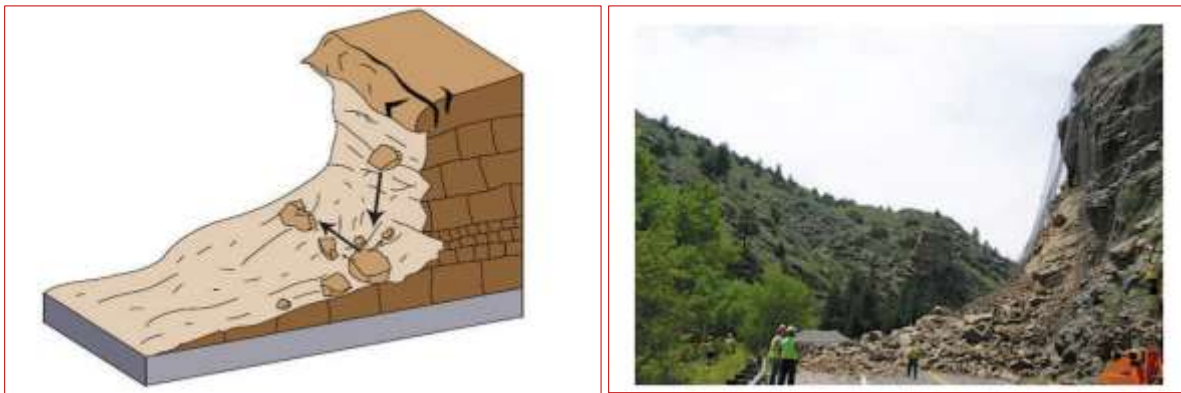
Figure 2.2 Schematic of Rockall in Colorado, USA, 2005: (Source, (Highland and Bobrowsky, 2008)).

2.5.2 Topple

A Topple failure is a complex and composite process that may range from extremely slow to extremely rapid (Highland and Bobrowsky, 2008; Geertsema and Highland, 2011). It's the forward motion of material out of the slope of a mass of soil or rock about a pivot point that may be driven by gravity and influenced by the fracture pattern in the rock, by abrupt falling, sliding, bouncing, and rolling (Highland and Bobrowsky, 2008; Lollino *et al.*, 2015).

Figure 2.3 Schematic of a topple failure in Canada (Source: (Highland and Bobrowsky, 2008)).

2.5.3 Slides

A slide type of failure is the down slope movement of earth material on the surface of the weak zone where there is a highly shear strain (Highland and Bobrowsky, 2008). It can categorize as a rotational or translational landslide. Lollino *et al.* (2015) and Walker and Shiels (2013) suggested that translational slides are relatively flat, planar movements along surfaces, and they have pre-existing slide planes that are activated during the slide event. In contrast rotational slides have a curved surface rupture and produce slumps by backward slippage.
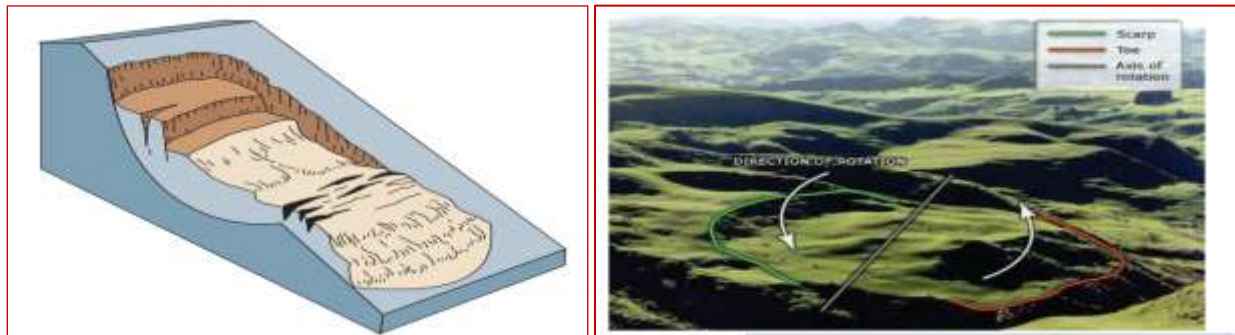
Figure 2.4 Schematic of slide failure occurred in New Zealand, 2007 (Source: (Highland and Bobrowsky, 2008)).

2.5.4 Lateral Spreads

A spread failure is an extension of cohesive materials that may result from the liquefaction of underlying materials. Spread commonly occurs in very gentle slopes, and it may be slow to moderate and increase in velocity in an earthquake triggering case (Lollino *et al.*, 2015).

Figure 2.5 Schematic of Spread Failures and Due to the 1989 Loma Prieta, California, USA earthquake, lateral spread damage to a roadway (Source: (Highland and Bobrowsky, 2008))

2.5.5 Flow

A flow type of failure in a landslide is the downslope movement of soil, bedrock, or debris in the form of a fluid (Lollino *et al.*, 2015). According to Highland and Bobrowsky (2008), based on the moisture content, mobility, and evaluation of the movement, there is a gradation of change from slides to flow.
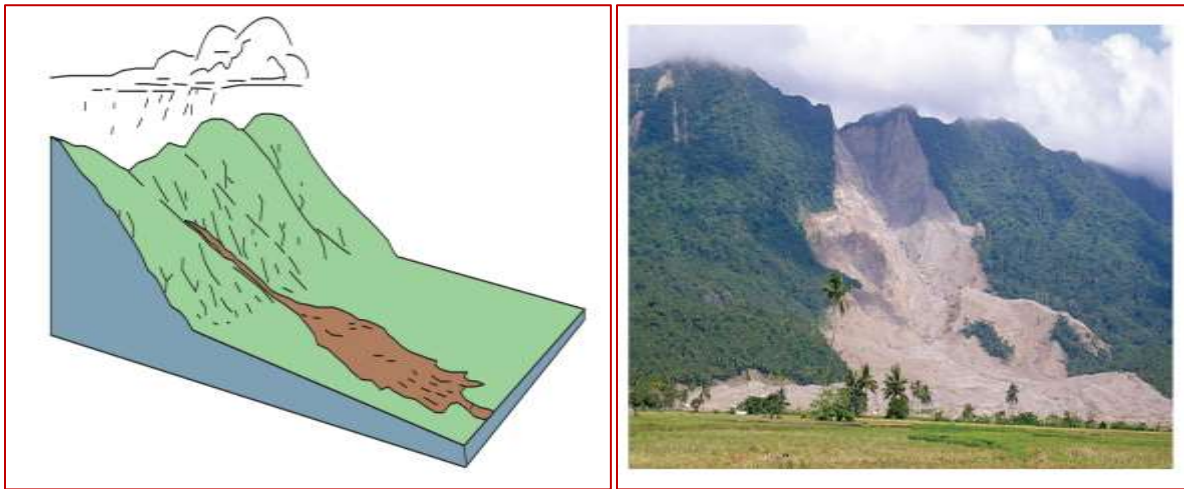
Figure 2.6 Schematic Failure of Flow Type Landslide and In February 2006, a debris avalanche buried the village of Guinsaugon, South Leyte, Philippines. (Source: (Highland and Bobrowsky, 2008))

2.6 Effect of Landslide

Landslide is a hazard when people, property, and livelihood become threatened (Tsige et al., 2017). All the researches on the landslide worldwide show that the occurrences of the mass movement have hazards on the economic, social, and natural environment. According to Woldearegay (2013), Ethiopian highlands have been affected frequently by a landslide due to high rainfall intensity. It is responsible for hazards such as damages of roads, hamper traffic, rarely car accidents, damage on other infrastructures like a power line, etc., repeated failures leading to repeated maintenance costs. One of the main reasons why landslide cause becomes distractive was due to its difficulty to predict whether landslide will occur or not in a given environment. For this reason this problem is known as a sudden distractive phenomenon. Landslide effects can occur in the natural environment and built environment (Highland and Bobrowsky, 2008). Tsige et al. (2017) further classifies Losses due to landslide as personal, economic, and environmental losses as follows.

2.6.1 Personal Losses

Thousands of people died and injured due to landslides worldwide annually. This type of loss does not limit to personal losses because of losses of productive human power also an adverse effect on the development of a country. Tsige et al. (2017), Stated that injuries on human beings have also continue consequence in the decline of the economy since an injured person needs medical treatment. This loss is very high when landslides occurred in populated areas.

2.6.2 Economic Losses

The volume of the affected area, type, and amount of properties on the affected area determines the extent of economic losses due to a landslide (Zumpano *et al.*, 2018; Tsige et., 2017). Different infrastructures like roads, buildings, communication towers, pipes under the ground, and crops on farmland destroyed due to landslides. Hence, a vast amount of economic losses may occur due to this destructive agent worldwide (Winter *et al.*, 2016). In addition to the losses of existing infrastructures, an additional cost invested in rebuilding was also considered as economic losses due to an occurrence of the landslide.

2.6.3 Environmental Losses

The landslide harms the environment and makes it out of function. According to Geertsema and Highland, (2011), damage on habitats, loss in productive soils from farmlands, reduced property lands, adverse effect on water quality, loss of natural resources, bank erosion within the stream channel, accelerated meander development, prevention of fish migration, and loses of scenic beauty of mountainous are some environmental losses due to landslide.

2.7 Landslide Controlling and Mitigation Measures

Conditions of landslide such as its scales, distribution, and causes are essential for proposing mitigation measures of the landslide. Mitigations can be reducing the driving force or increasing resisting forces or shear strength in the landslide-prone areas (Walker and Shiels, 2013). Mitigation measures taken on affected areas may aim to reusable the area by treating some engineering structures such as retaining walls and keep the earth mass in its position by increasing the resisting force of soil against driving force. But, many researchers use in appropriate remedial measures that can increase the driving force, like providing retaining on the above critical surface.

2.7.1 Modification of Slope Geometry

Reducing the steep angle slope and adding materials to the area maintaining stability is one of the slope geometry treatments in which a slope becomes more stable (Popescu and Sasahara, 2009). In addition, to making the slope more gentle and stable during slope modification, the weight of slope mass also declines, which decreases the driving force and increases the resisting force of slope material.

2.7.2 Providing Drainage

Providing drainage in the areas prone to landslides is the most effective method to mitigate mass movement since it is used to collect floods after heavy rainfall and avoid the probability of water triggering landslides (Popescu and Sasahara, 2009; Coutinho *et al.*, 2019; Abebe *et al.*, 2010). Surface drainage is used to divert water from flowing onto the slide area using collecting ditches and avoid the tendency of slope material to lose its resisting force against the mass movement.

2.7.3 Providing Engineering Structures

Providing retaining structures along landslide-affected areas is one of the controlling mechanisms of the mass movement. This Engineering structures may include retaining walls, gabion walls, embankments, individual geo-synthetic or geo-composite materials, and they are functional in areas limited in space and those near to other structures (Popescu and Sasahara, 2009).

2.7.4 Stabilization by Afforestation

Afforestation enhances the stability of the slope by increasing the shear strength of the soil or by decreasing the probability of the effect of an erosion on the slope. Planting fast-growing plants such as grasses, shrubs, bushes etc. are the beginning of this task (Forbes and Broadhead, 2013). The root of a tree on the slope of the earth the mass has a high contribution to anchor the soils together and increase by offering additional apparent cohesion that increases the cohesiveness of the soil mass due to its closely spaced root matrix system. Hulagabali *et al*. (2008) Come upon his work; Vetiver grass with row spacing of 1 m and clump spacing 10 -15 cm with penetration of root to a depth of 3 m and expand to 0.5 m can reduce the effect of erosion and tightens the soil particles. According to Forbes and Broadhead, (2013), deep-rooted trees and shrubs can reduce shallow landslides by reinforcing shallow soil layers and improving drainage.

2.8 Geophysical Exploration Survey

Geophysical subsurface exploration methods are a non-destructive means that is rapidly cover a large area and very cheap when compared with conventional exploration by drilling (Budhu, 2011; Marwa *et al.,* 2016). Seismic Refraction survey, Cross-hole seismic survey, and Electrical Resistivity Surveys are the main types of geophysical exploration survey.

2.8.1 Electrical Resistivity Survey

Electrical resistivity is an indirect technique that measures how much the flow of Electricity is resisted by the soil and used to characterize the subsurface information without soil disturbance (Marwa *et al*., 2016). Resistivity values of geological units may vary depending on their structures and the amount of water that they contain. Volcanic and metamorphic rocks have high resistivity values. The resistivity of these rocks mostly depends on the amount of faults and the percentage of the groundwater content of these faults. Sedimentary rocks, which have various clearances and high water content, usually have a low resistivity.

Hunt (2005) state the correlation of resistivity values and various earth materials in detail way as shown in Table 2.3 given below.

Table 2.3 Resistivity values and various earth materials (Badr and Anwar, 2015)).

Materials	Resistivity (Ω)m
Clay soils: wet to moist	1.5-3
Silty clay and silty soils: wet to moist	3-15
Silty and sandy soils: moist to dry	15-150
Bedrock: Well fractured to slightly fractured with moist soil filled cracks	150-300
Sand and gravel with silt	About 300
Sand and gravel with silt layers	300-2400
Bedrock: slightly fractured with dry soil filled cracks	300-2400
Sand and gravel deposit: course and dry	> 2400
Bedrock: Massive and Hard	>2400
Fresh water	20-60
Seawater	0.18-0.24

Basic geotechnical terms that are used in geotechnical investigation, like thickness of earth mass layers (lithology), weak zone, type of soil depending on resistivity value, location of groundwater level, and direction of groundwater flow was obtained from geophysical survey. One of the most advantage of resistivity method over traditional bore hole drilling of subsurface

exploration method is that, an information is only obtained for soils extracted from bore hole and for those soils found in between boreholes are assumed similar with soils sampled from boreholes, while in electrical resistivity method, it account all the soils found on that area.

2.9 Geotechnical Investigation

Geotechnical investigation is the process used to deeply understand the nature, behavior, and type of materials under the ground (Highland and Bobrowsky, 2008). In the landslide study area, geotechnical investigation means experimentally identify the geological, topographical, and hydrological nature of the soil, its types, degree of saturation, and unique properties of the soil, identifying triggering factors to slope failure, evaluating the socio-economic losses by a landslide, and proposed remedial measures (Coutinho *et al.*, 2019; Woldearegay, 2013). But, the main aim of the geotechnical investigation is to identify the cause of occurrences of landslides and propose the best remedial measures to overcome the problem temporarily or permanently. Grain size analysis, natural moisture content, specific gravity, Consolidation test, and shear strength parameters, Triaxial tests are the primary laboratory tests used in a geotechnical investigation. Slope stability analysis by using different methods like Limit Equilibrium Method and Finite Element Methods were also categorized under geotechnical investigation.

2.10 Slope Stability Analysis

Slope stability analysis is the process in which the stability of slope profile is determined whether stable, moderately stable, or unstable in terms of safety factor (Salunkhe *et al.*, 2017). It depends on driving force and resisting force. Driving forces are triggering forces that cause the slope to be unstable and initiate the movement of slope materials, especially in hilly areas, and cause distractive of earth mass and manufactured structure built on it. The driving force should be less than the shear strength force for a slope to be stable (J.Crozier, 2004). Some other factors that influence the conditions of slope stability like slope steepness, the strength of underlying soil, and slope geometry of slope (Walker and Shiels, 2013). In an assessment of landslide phenomena, before slope stability analysis, geotechnical investigation (Field exploration and laboratory test) are essential requirements since data used in the analysis were obtained from laboratory test results and field investigations. Different methods such as Limit Equilibrium Method (LEM) and Finite Element Methods (FEM) can be applied to determine the factor of safety for a given slope geometry (Azeze, 2020). The Finite Element Method, enables us to

discretize the geometry of slope profile into small finite elements and gives accurate result in stability analysis. In LEM, a soil profile that is non-homogeneous was considered as homogenous materials.

2.10.1 Finite Element Method

Today, there are two basic approaches used to calculate slope stability analysis. These are LEM and FEM. In slope stability analysis, the Limit Equilibrium Method is the oldest and simplest numerical method (Azeze, 2020). The Finite Element Method approach is very vital and more preferable than Limit Equilibrium Methods (Abderrahmane and Abdelmadjid, 2016; Azeze, 2020). The FEM approach contains stress-strain relationship and compatibility equations, which are the basic parameters required in different geotechnical structure analyses. For this reason, different complex geotechnical computations can simply be calculated by using the Finite Element Method approach. Even if many FEM software are available for different geotechnical commutations, Plaxis 2D software is the most applicable in slope stability analysis (Azeze, 2020).

2.10.1.1 Plaxis 2D Software

Plaxis 2D software is a FEM based software. It is used to analyze different geotechnical computations like slope stability analysis. The software contains four main sub-routines; inputs, calculations, outputs, curve plots, and the Factor of safety versus displacement is plotted from the curve plots sub-routine (Jacob *et al.*, 2018). The first step in plaxi software analysis is to set basic parameters like the description of the problem, the type of analysis, the primary type of elements, the basic units, and the size of the draw area.

Finite element models may be either Plane strain or Axisymmetric. The slope was analyzed as a plane strain model. Different soil layers below the slope surface will model on this software, and all the necessary parameters will define for each soil layer. For soil interfaces, Mohr-Columb criteria were used and the Factor of safety was computed by using the Phi-C reduction procedure (Jacob *et al.*, 2018) and deformation was computed by plastic analysis. The intensity parameters are successively reduced before structure failure occurs. The Factor of safety keeps on changing until the ultimate state of the system was attained, and the corresponding ΣMSf will be FOS of the slope.

2.10.2 Limit Equilibrium Method

Limit Equilibrium Method is one of the most known numerical method in slope stability analysis. Limit equilibrium method subdivide the landslide body into slices to calculate the forces for each slice and uses the principle that a slope is stable when driving forces exceeded by resisting forces and factor of safety, FOS is equal or larger than 1. The main disadvantage of conventional LEM is that it requires pre-assumptions to complete the solution. Some of the well-known and widely used LEM methods are Bishop Method (1955), Janbu method (1954) and GLE-Morgensterm slice method (1986). The stability of a slope in a c', ϕ soil is usually analysed by discretizing the mass of the failure slope into smaller slices and treating each individual slice as a unique sliding block.

2.10.2.1 Slide Software

Slide Software is a 2D LEM based computer program that is used to analysis the stability of soil and rock. The software is used to analysis both circular and non-circular failure surfaces. It has some features over other Limit equilibrium based software's like groundwater analysis, back analysis for support forces (Krishna, 2006). The software is easy to uses and able to model the slopes with different loading conditions like surcharge, groundwater conditions, and support conditions.

CHAPTER 3

MATERIALS AND METHODS

3.1 Study Area

The study area of this research (Chira Town) was located in south-western part of Ethiopia, Oromia Regional State, Jimma zone. Chira town was considered as a town in 2007. The capital of the zone, Jimma City, is locating 345 km from the capital of Addis Ababa while Chira town located at 100 km to the south-west part of Jimma city. The altitude of the town ranges 1390 - 2980 meters above sea level.
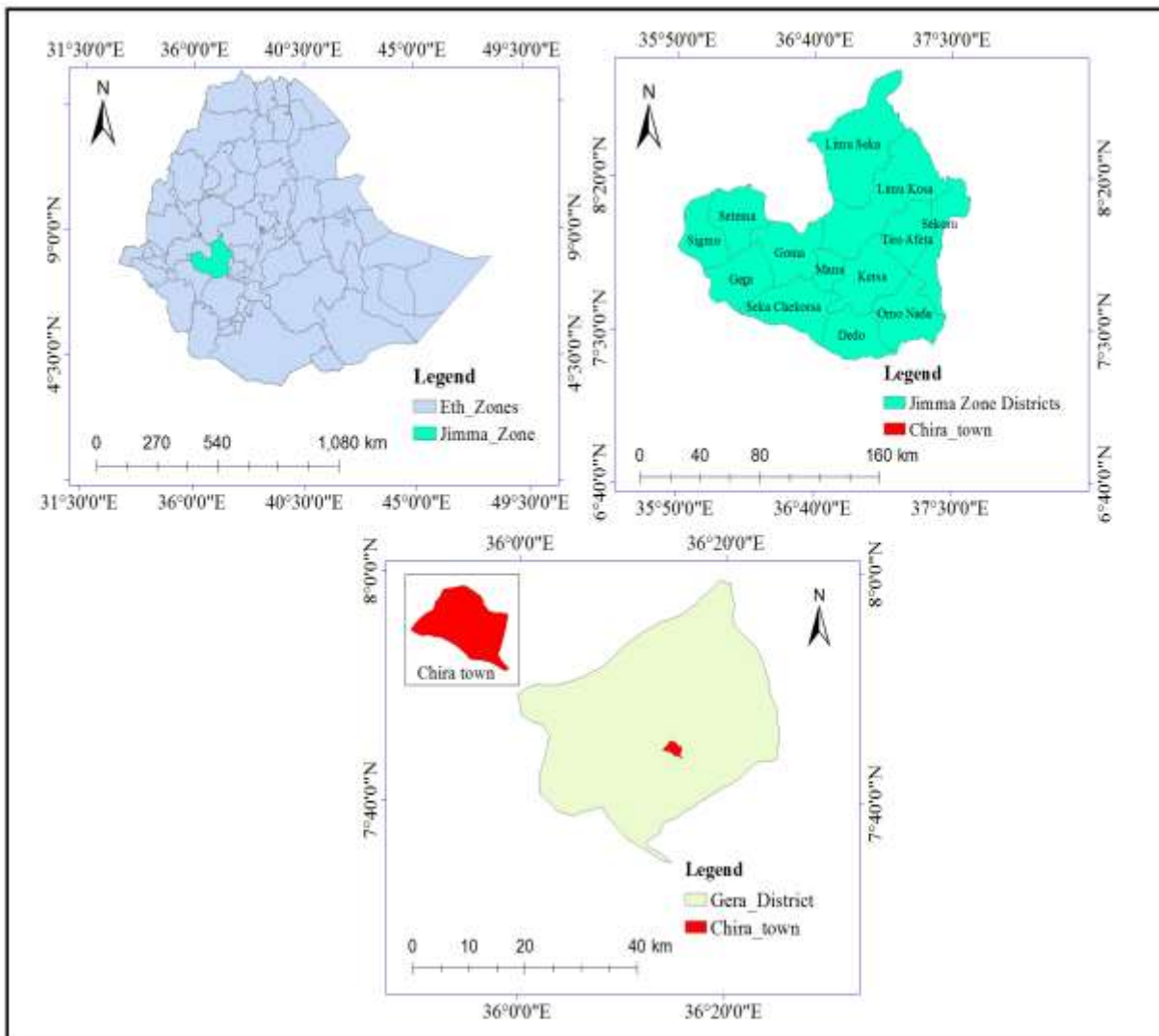
Figure 3.1 Map of the study area (Source: GIS)

3.2 Climate and Topography of study Area

Chira town is categorized under the warmed humid and wet subtropical weather conditions. The average mean annual rainfall of Chira was 1955.4 mm with a maximum and minimum rainfall of 2967.8 and 1414.1 mm respectively (Figure 4.8). The Monthly Analysis of Chira Rainfall shows, the area will get rainfall throughout the year with a small rainfall in January, February and December. Whereas the main rainfall seasons of the area were May, June, July, August and September with the highest rainfall records in June, July and August (Figure 4.9). The study area was characterized by rugged volcanic mountainous terrain comprising of high to low relief hills and an Elevation range from 1390 -2980 m.

3.3 Research Design

The study included both experimental and simulation approaches, as well as quantitative and qualitative investigations. In contrast to the qualitative research, which was used to acquire information about the event from residents through interviews and visual inspection, the quantitative research will explain the numerical aspects of the findings.

Soil samples were collected via systematic random sampling. Field observation was applied to the study area to visualize the affected area and its extent. Geophysical survey (Electrical resistivity method) also conducted on the field to determine the subsurface formation of the study area. Laboratory experimental programs were performed to investigate the geotechnical conditions of the study area and to conduct the slope stability analysis. The laboratory data were analyzed and interpreted to identify the soil types according to USCS, their role in the landslide occurrences, and analyze the safety factor of the affected and unaffected slope areas by using plaxis 2D and Slide software.

Among known triggering factors of landslide, based on the availability of data, seven factors were used to find out the most causal factors of Chira landslide. The factors used include: Slope aspect, slope angle, curvature and elevation derived from the digital elevation model of 30 m resolution, land use land cover derived from Landsat 8 OLI, soil and Stream distance.

 Finally, corrective actions were offered based on the kind of mass movement and slope stability study results. The study findings and suggestions were given at the end of this work based on the field inquiry, laboratory test results, and software analyses.

The overall works performed in this study was summarized on the following flow chart.
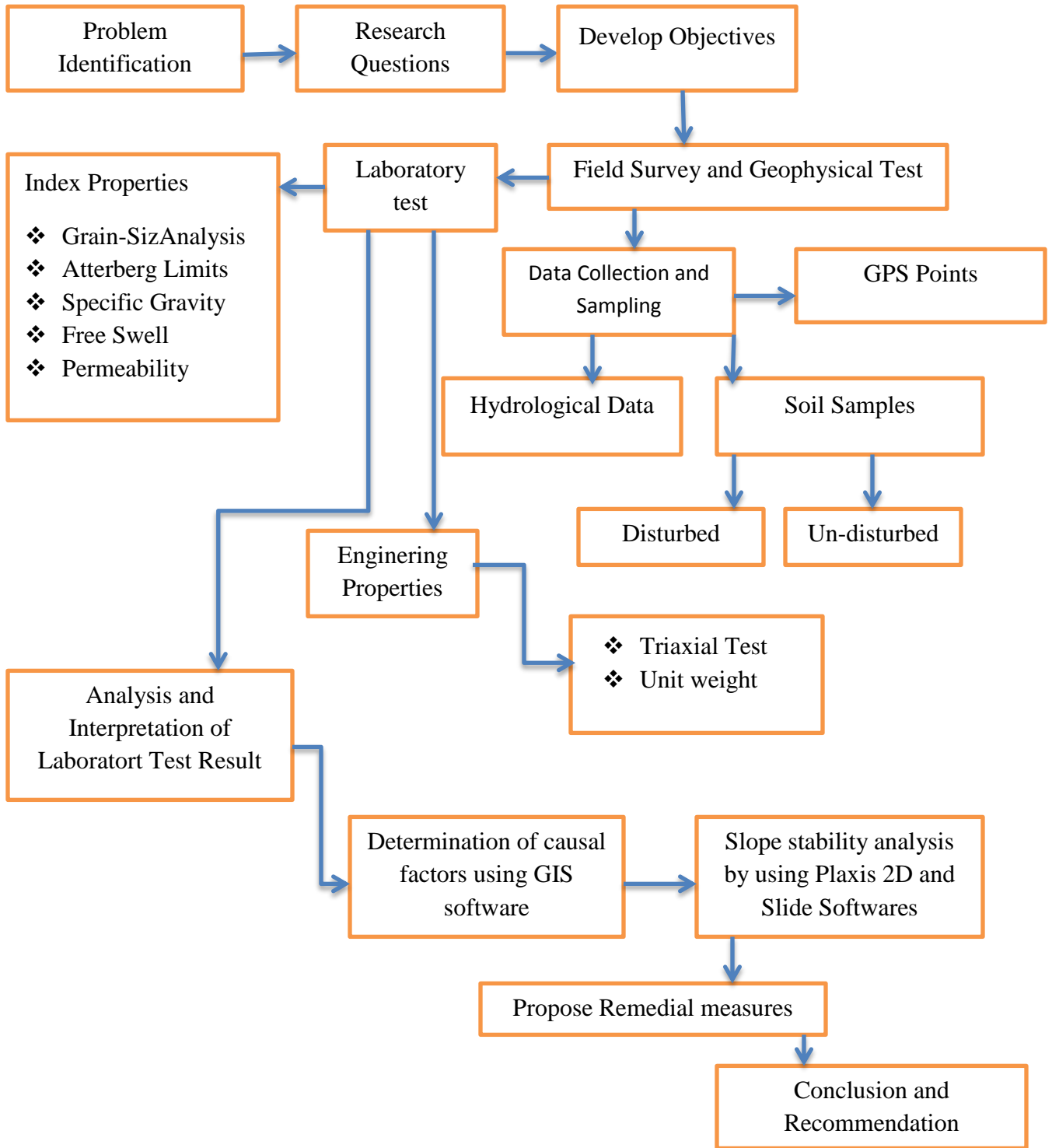
Figure 3.2 Flow Chart Diagram of Research Design

3.4 Study Variables

Independent Variables

In this study, the independent variables are grain size distribution, specific gravity, unit weight, atterberg limits, permeability test, triaxial test, geological sub-surface formation, geometry of the slope, and geomorphological variables.

Dependent Variables

➢ Landslide in the study area.

3.5 Population and Sampling Method

3.5.1 Population

A landslide is a worldwide disaster in which soil mass/rock mass along the slope area moves from an unstable position to a stable position. This research was aim at affected landslide soil and non-affected soil, which is near to affected area as the study population.

3.5.2 Sampling Method

For this study, a purposive sampling technique was used, which is a basic random sample method. This sampling technique was developed based on the information available to the researcher and the researcher's intended or desired outcome.

3.6 Source of Data

The study includes both primary and secondary data. Primary data was collected via laboratory testing, soil samples from the research region, and field tests. Secondary data was gathered from many standards, journals, books, websites, and other sources.

3.7 Data Collection Procedure

One of the most important responsibilities in experimental research is data collecting. The initial stage in data collecting was obtaining consent letters from relevant local administrators in order to define the stated objective for this research. The following stage was a field visit to the research area, where required information regarding the event was gathered from administrative offices and local communities via interviews and pictures of the impacted area. Secondary data, such as meteorological data and the town's periphery, were collected from meteorological stations and the town administration, respectively. Representative soil samples were collected

from five test pits in and around the affected area and brought to the laboratory for further geotechnical investigation. Both disturbed and undisturbed soil samples were collected from five test pits in the landslide impacted area, which contained both affected and non-affected material. In general, main research data was gathered through experiments and site observations. Secondary data was collected from various standards, journals, books, websites, and others to evaluate and assess the issues connected to the study's aims.

3.8 Software's and Instruments Used

This research was performed by using different software and instruments. Softwares such as ArcGIS, Plaxis 2D, Slide, Res2dinvx32, Origin pro 8.5. MS word, and Excel and devices like GPS, Syscal Junior Switch 72, and Mobile Camera were used. ArcGIS was used to delineate the study area, determine causal factors while Plaxi 2D and Slide software's were, numerically analyzes the slope stability against the landslide. Res2dinvx32 was used in the examination of horizontal profile of soil layers depend on different resistivity values. MS Word, Origin pro 8.5, and Excel were used to analyze laboratory and display research data; mobile camera and Garmin GPS were used for documentation and determine the location of landslide affected area respectively. Syscal Junior switch 72 was used to identify the subsurface profile of the soil and groundwater level.

3.9 Field Work

3.9.1 Site Visitation/Reconnaissance

The first task of fieldwork in this research was site visitation. The site was visited to determine the environmental condition of the site, including those factors having contributed to landslide occurrence as well as the damage caused by the mass movement of the study area. During site visitation, many of cracks were visible on subsurface profiles, including ground subsidence, destruction of natural features, and infrastructures like houses, roads, pipelines, and electric power lines were also affected by this problem. As shown in Figure 3.3, a lot of houses become out of function, and during the site visitation, the owners live in rent houses by displacing from their home. But, some people still live in already affected houses especially, those houses found under the toe of the slope. The cracked line of the earth passes through the foundation of residential houses and they live in fear. As local peoples mentioned during an interview; this problem was progressed gradually in the rainy season, and they heard a sound like a spring flow

28

when their homes affected by this phenomenon. Assessing the presence of river and spring at the toe of the slope was also one task during site visitation of the study area. There is a small spring at the toe of the slope in the study area along two sides of the town.

Figure 3.3 Cracks observed on the earth mass and Effects on residential houses.

3.9.2 Geophysical Survey

The geophysical survey procedure involves a desk study and a field investigation (reconnaissance and geophysical surveys).Therefore, fieldwork is set up to sound stations along selected traverse lines to produce a 2-D resistivity image of the subsurface. The 2D Continuous Vertical Electrical Sounding (CVES) geophysical technique employed to delineate the sites and identify the affected site by the landslide of the town. The 2D resistivity imaging survey seeks to carryout continuous vertical electrical sounding along a selected traverse and to produce 2D resistivity model sections of sub-surface geologic layers along with the profile.

The geophysical study was done with the goal of establishing the most favourable position of Landslide in Chira town along multiple lines based on productivity and the preliminary geological, hydro geological, and hydrological models. As a result, more data on the presence and thickness of the subsurface layer was required in order to assess the depth of the Landslide area. As a result, Vertical Electrical Soundings were carried out at certain locations depending on the accessibility of the instrument and its cables, as well as the Survey Specification and Instruments. The latest Instrument siscal junior model with electrode spacing and profiling was employed in this study (2D).

3.9.2.1 Geophysical survey Data Analysis and process

The recorded data was the process of geophysical data from the 2D imaging survey, and the VES survey technique was downloaded at the site from the siscal junior using special siscal Utility software via a communication cable onto a personal computer.

The geophysical survey's findings are based on electrical profiling (Imaging). The apparent resistivity (a) and current electrode separation are factors in the electrical resistivity method. Computer iteration techniques were employed by using software Res2dinvx64 for the Interpretation of apparent resistivity data that produced the computer iterated profiling

3.10 Material Sampling and Preparation for Test

Using purposive and systematic sampling methods, soil samples are taken to determine the geotechnical characteristics of the slope materials using procedures of ASTM standard. Depending on the situations undisturbed and disturbed soil samples were collected from five test pits within the boring depth of 1.5 m to 2.8 m range. For each sampling pit, undisturbed, and

disturbed samples were collected, and taken to the laboratory (JIT Soil Laboratory Test) and ECDSWC to determine index and engineering properties of soils. The disturbed collected samples at different depths were air dried for 3 – 4 days and oven-dried at 105 C° for 16 to 24 Hr. before carrying out laboratory tests. Engineering properties and Natural Moisture Contents were determined immediately after the samples were brought to the laboratory.

Table 3.1 Location, Coordinates, Sampling Depth, and Sampling Types of the Study Area

| Test Pit | Condition of the sample | Location | | | Depth (m) | Slope Number |
		E	N	Elevation (m)		
TP1	Affected	196953	857143	2078	1.5 2.8	S-2
TP2	Affected	195960	857460	2102	2.4	S-1
TP3	Non-Affected	195843	857509	2096	1.5 2.4	S-3
TP4	Affected	195898	857363	2054	2.7	S-1
TP5	Non-Affected	196243	857045	2095	2.0 2.7	-

3.11 Laboratory Tests

Laboratory tests are the main task in the study of Geotechnical conditions. The type of soil, its properties, and strength of a given soil found in a specific area, were determined by laboratory tests. Laboratory tests included in this research were Natural Moisture Content, Specific Gravity, Atterberg Limits, Grain Size Analysis, Free Swell, Permeability Test, and Tri-axial test.

3.11.1 Moisture Content Determination

In this research, following ASTM D2216 testing procedures, the moisture content of eight test samples from the study area was determined in the laboratory. To dry the test samples, an oven drying temperature of l05 ° C was used. To avoid errors, three sets of samples were prepared for each test sample. Finally, the moisture content of the eight samples was determined using standard procedures outlined in ASTM D2216.

3.11.2 Specific Gravity Determination

This test is performed to determine the heaviness of soil compared with water and the test conducted by using a pycnometer following ASTM D 854 test procedures. This test has a significant relation with other tests like hydrometer analysis, phase relationship, and consolidation tests. In this study, eight tests were conducted on disturbed soil samples obtained

from 5 test pits. Oven-dried specific representative samples have been taken. The given sample has been separated and prepared for testing over the No.10 sieve 20 g sample. The sample is then processed using test methods.

3.11.3 Unit Weight Determination

This test was used to determine the density of compacted in-situ soil by taking undisturbed soil samples in accordance with ASTM D2937-00 standard testing procedure, and it's was calculated as the ratio of the mass of soil sample to its volume. The mass of soil in Bulk density determination is moist soil, while in dry density determination, the soil sample used was the dry soil mass. The in-place density of undisturbed soil obtained by moving or drilling a thin-walled cylinder was calculated in these laboratory tests.

3.11.4 Atterberg Limits Determination

This test is performed to determine water contents at which the soil changes from one state to the other. It normally applied to fine-grained soils whose condition is influenced by moisture content fluctuations. This test was carried out following ASTM D 4318 testing procedure, using disturbing samples to determine the Liquid Limit, Plastic Limit, and Plasticity Index of fine-grained soils for their classification. The plasticity or compressibility of the soil samples was also determined by using ASTM standard plasticity chart. The test conducted to determine the soil type for oven-dried samples.

3.11.4.1 Determination of Liquid Limit (LL)

This test was performed on eight samples in according to ASTM D 4318 procedure. It is obtained as the water content at which 25 blows (drops) from a height of 1cm to close along a distance of 13 mm. Since moisture control is difficult for this test, at least four tests for the same soil were conducted for varying moisture content with a variation of the number of blows between 15 and 35.

3.11.4.2 Determination of Plastic Limit (PL)

This test was also performed on plastic soils paste left from liquid limit test by rolling on glass plate until the soils begins to collapse when rolled into threads of a certain size (3 mm). Two trial test was performed and average value was taken in this research on this test.

3.11.4.3 Determination of Plasticity Index (PI)

The Plasticity index was calculated from plastic limit and liquid limit as follows:

PI = LL − PL,

Where

PI- Plasticity Index, LL- Liquid Limit, and PL-Plastic Limit.

3.11.5 Grain-size Analysis

Sieve size analysis and Hydrometer analysis were the two most common tests used for coarse-grain and fine-grain soils respectively. In this study, both of particle size determination methods were performed on eight samples recovered from five test pits of the study area. Since the samples were contain high amount of fine-grained soils; wet sieve method was used in sieve analysis to remove the silt and clay content in the sample by washing the oven-dry sample on 0.075 mm sieve size. During Hydrometer test, Sodium hexamaetaphosphate dispersing agent was used to disperse the sticky particles in fine cohesive soils. Tests were performed on disturbed soil samples for both analyses following the ASTM standard D422-63 and D1140-97 designations.

3.11.6 Free Swell Test

Free swell represented soil expansion and was obtained by dividing the volume difference between the volume of Kerosene and the water into the volume of Kerosene. It's achieved using 10g of dry soil passing sieve No. 40 and pot. It is the indicator of the soil property either its not expansive, moderately expansive and expansive correlating with other index properties. For this study, free swell test performed on five samples.

3.11.7 Permeability Determination

Permeability or Hydraulic conductivity test is performed to determine the capability of the water to flow through soil particles. Various soil particles have different hydraulic conductivity based on the size and shape of soil particles and the viscosity of its water. Permeability is highly dependent on the void ratio of soil particles, and they have direct proportions together. In this study, the Falling Head Method test was run for five soil samples since the dominant soil type of the study area was fine-grained soils, and Falling Head method was applicable for this type of soils. The mold that was used during this test has a volume of 865.71 mm^3.

3.11.8 Unconsolidated Un-drained Tri-axial Test

In a triaxial chamber, the specimen is subjected to confining fluid pressure, and axial load is applied in a manner regulated by strain or stress. Un-drained conditions are achieved in all processes of the test without allowing for any dissipation of pore water pressure. In general, the process does not determine pore water pressures and hence the parameters determined are in terms of overall stresses.

3.12 Determination of Triggering Factors

3.12.1 Rainfall Analysis

Rainfall distribution affects overland flow volume and soil moisture. A 36-year record of rainfall from 1985-2020 was used to analyze the rainfall characteristics in the Chira area. As for any rainfall analysis, the quality of the rainfall record was checked before the analysis. Consequently, 6.8% of the total record for the Chira rainfall station has a missing value. The rainfall data were filled with the multiple imputation (MCMC) technique using the XLSTAT 2021 add-ins plugin Microsoft excel.

3.12.1 Landslide Inventory Mapping

The landslide inventory mapping identifies landslides and compiling the details of the location of the landslide, causing factors, and occurrence (Girma et al., 2015). Inventory mapping forms a basis for landslide hazard evaluation and susceptible mapping techniques. In this regard, the landslide inventory data about the location, type, and number of the landslide, possible causes of the landslide were collected from the study area through direct field investigations. The landslide inventory maps were prepared by collecting Ground Control Points (GCP) for the areas affected by landslide with the aid of Global positioning systems (GPS). The spatial maps of the landslides in the town were created using ArcGIS 10.3. Accordingly, 85 landslide sites of different types, and dimensions were collected and used in landslide mapping works.

3.12.2 Landslide susceptibility Mapping

For landslide hazard mapping, statistical hazard mapping techniques considering various causative factors were used. The procedures used in this study for landslide hazard mapping were developing various factors and their interrelations with the past/historical landslide based

on the statistical model in the GIS environment. Based on the limited data for this study area, the probabilistic models based on frequency and ratio of landslides in different factors were used.

Among known triggering factors of landslide, based on the data availability, seven factors were used for the landslide susceptibility mapping. The factors used include: Slope aspect, slope angle, curvature, and elevation derived from the digital elevation model of 30 m resolution, land use land cover derived from Landsat OLI satellite image by the supervised classification using ERDAS IMAGINE 2015., soil and Stream distance. The digital elevation model of the study area at a resolution of 30 m obtained from the United States Geological Survey (USGS) at https://earthexplorer.usgs.gov/ was used to generate the elevation data. These factors were evaluated on their relative influence on the historical landslides.

3.13 Slope Stability Analysis by using Numerical Method

Slope stability analysis using software is an easy task for engineers when the slope configuration and the soil parameters are known. The slope stability of the study area was analyzed by using Plaxis 2D and Slide, Finite Element and Limit Equilibrium Method based software's respectively. The first step in plaxi software analysis is to set basic parameters like the description of the problem, the type of analysis, the primary type of elements, the basic units, and the size of the draw area.

A plain strain and the 15-node triangular element was selected since it gives more accurate results in slope stability analysis. Boundary conditions were assigned to represent the actual problem accurately. These boundary conditions were constrained the geometric model of the soil in the vertical and horizontal directions. Soil Properties obtained from laboratory test results and lithological information obtained from the geophysical investigation were used in slope stability analysis. Based on those results, soil properties required by the plaxis software were defined for each soil layer. Plaxis describe the numerical behaviour of soils as an stress-strain relationship using constitutive models. Different constitutive models were used in the finite element analysis, such as the Mohr-Columb model, linear elastic model, Soft soil model, Hardening soil model, Soft soil creep model, jointed rock model, and so on. The Mohr-Columb model was used for the slope stability analysis in this study. Soil properties required by the Mohr-Columb model, such as cohesion, angle of internal friction, permeability, Young's modulus, and unit weight of the soil was obtained during laboratory investigation.

After the geometry of soil defined and material properties assigned, meshing was performed on the slope. The Finite element numerical method was based on the discretization of a continuum into finite element, describing the behaviour or actions of each element and reconnecting them to represent the continuum. Different mesh sizes were available in plaxis software, starting from very fine to very coarse global coarseness. Fine mesh size was used for this study since the accuracy of the resulting increase while decreasing the size of the element or increasing the number of nodes.

The execution of the calculations needs a generation of initial stress and pore water pressure distribution. Hence, the initial stress distribution was generated by the k_0 procedure, and the initial pore water pressure was generated by using phreatic level from the global water level. The Factor of safety was performed by using the phi-reduction method procedure. The intensity parameters are successively reduced in the phi-C reduction strategy before structure failure occurs. The Factor of safety keeps on changing until the ultimate state of the system was attained, and the corresponding ΣMSf will be FOS of the slope.

The first step in slide modeling is the project setting where various important modeling and analysis options of the problem i.e. failure direction,units, analysis methods, and groundwater conditions are set. The criterion uses unit weight, cohesion, and angle of internal friction as the input parameter. In the analysis factor of safety and slip surface were evaluated for variation of groundwater conditions using bishop, Jambu, and GLE method. A circular failure surface was used to define the type of slip surface and grid search is used to locate the critical slip surface (slip surface with the lowest safety factor).

Generally,three slopes were selected where two of them are affected slopes while one slopes is un-affected slopes and analyzed using both numerical methods. The total length and depth of slopes used were varies from slope to slopes. The total length and depth used were 100 m and 50 m for slope 1, 50 m and 28 m for slope 2 and 60 m and 25 mfor slope 3 respectively.

CHAPTER 4

RESULT AND DISCUSSION

4.1 Geotechnical Conditions of Study area

4.1.1 Geotechnical Condition of the study area from Laboratory Test Results

4.1.1.1 Natural Moisture Content

Natural moisture content was determined for eight samples immediately after the samples were brought to the laboratory according to ASTM D2216 (Appendix A and Table 4.1). This test was also performed during a triaxial test on five samples, and in both tests, the values of NMC were run in the range of 36.84% – 47.68%. This result is similar with the ranges of clay soils as the observation made by Das (2002), since water content values vary in the range of 30% - 50%. The soil samples were taken during the dry season, and it was expected during rainfall season, the values of NMC would be greater than these values. Therefore, the mass movement of Chira town was highly affected due to high water content, especially during the rainy season.

Table 4.1 Natural Moisture Content of soils of Chira town Landslide

Test Pit Designation	Depth(m)	Moisture Content (%)
TP 1	1.5	43.63
	2.8	47.66
TP 2	2.4	36.84
TP 3	1.5	38.67
	2.4	40.17
TP 4	2.7	42.85
TP 5	2	39.74
	2.7	40.69

The water content of the soil in the research area is directly proportional to depth, as seen in Table 4.1 above. Therefore, as we go deeper the water content of the soil will be greater than what was calculated here.

4.1.1.2 Specific Gravity Determination

This test was performed for eight samples, which are described in Table 4.2 below. The specific gravity of the soils in the study area ranges from 2.67 to 2.80. Based on this test, the soil type of

study area was dominated by clay and silty clay soils. This result agrees with the observations made by Das (2002), since the author state that specific gravity values ranging from 2.67 to 2.90 were assigned to clay and silty clay soils. This number also includes the specific gravity of the study area. As a result, this test indicates that the soil type of the study area is clay and silty clay soils, which are weaker and typically have several planes of weakness, which initiate the occurrence of the Chira town landslide

Table 4.2 Specific Gravity of soils of Chira town Landslide

Test Pit Designation	Depth(m)	Specific Gravity (GS)
TP 1	1.5	2.69
	2.8	2.67
TP 2	2.4	2.70
TP 3	1.5	2.80
	2.4	2.74
TP 4	2.7	2.69
TP 5	2	2.73
	2.7	2.79

Because the Specific gravity (GS) values are more than 2.5, the soils were inorganic, according to the above results.Some soils have Gs values less than the above values, such as 2.3 or less for soils having porous particles, while some soils have GS values greater than three for soils containing heavy chemicals such as iron (Das, 2002). As a result of this test, it can conclude that the soils of the study area do not have heavy porous, which facilitates the permeability of the area, and as the duration of infiltration of water stored in this earth mass increases, the weight of soils increases and pore pressure developed, which is a reason for the occurrence of landslides in the study area, along with other triggering factors.

4.1.1.3 Atterberg Limit Determination

This test was performed on eight samples, as indicated in Appendix A and summerized in Table 4.3. The test results reveal that the LL (percentage) ranges from 67.70 to 71.31, the PL (percentage) ranges from 30.64 to 35.73, and the PI (percentage) goes from 33.60 to 39.47. The values were reduced from top to bottom since the components that impact soil plasticity behavior decrease with depth.

Table 4.3 Atterberg Limit Values of soils of Chira Landslide

Test Pit Designation	Depth (m)	Atterberg Limits			
		LL (%)	PL (%)	PI (%)	LI (%)
TP 1	1.5	71.31	35.16	36.15	0.23
	2.8	70.26	35.73	34.53	0.35
TP 2	2.4	68.45	31.01	37.44	0.16
TP 3	1.5	70.11	30.64	39.47	0.20
	2.4	69.91	35.11	34.80	0.15
TP 4	2.7	67.70	34.10	33.60	0.24
TP 5	2.0	70.77	34.81	35.96	0.14
	2.7	69.37	31.27	38.10	0.25

A decrease in particle size leads to an increase in total surface area and, as a result, an increase in the plasticity index. A soil with a high liquid limit and a low plasticity index indicates that the soil is dominated by clay content, whereas a soil with a low liquid limit and a low plasticity index was seen for silty soils due to the impact of particle sizes. This result support the previous ideas presented by Das (2002), because, clay soils from TP2, TP3, and TP5 contain kaolinite clay minerals based on the percentage of Liquid Limit and Plasticity Index, because the author stated that a soil with LL (percent) between 35-100 and PI (percent) between 20 - 40 is dominated by kaolinite clay minerals. Soils' swelling potential is determined by their Plasticity Index, and they recommended soils with PIs ranging from 20 to 50 percent as having significant swelling potential. Based on this, the soils in the study area were classified as having a high swelling potential. The research area's Liquidity Index values were ranged between 0 and 1, which reflects the state and strength of fine grained soils as plastic state, intermediate strength, and soil deforms like a plastic material.

The Plasticity Chart is a straightforward approach for distinguishing soil types based on Atterberg limit parameters. By plotting the Liquid Limit along the horizontal direction and the Plasticity Index along the vertical direction, the coordinate above or below the A-line, which can be calculated using the equation PI = 0.73 (LL - 20), was determined. Clay soils are those that occur above the A-line, whereas silty soils are those that occur below the A-line. This is because clay content has a high liquid limit and a high plasticity index. The plasticity chart of the study area was plotted on Figure 4.1, which is shown below.
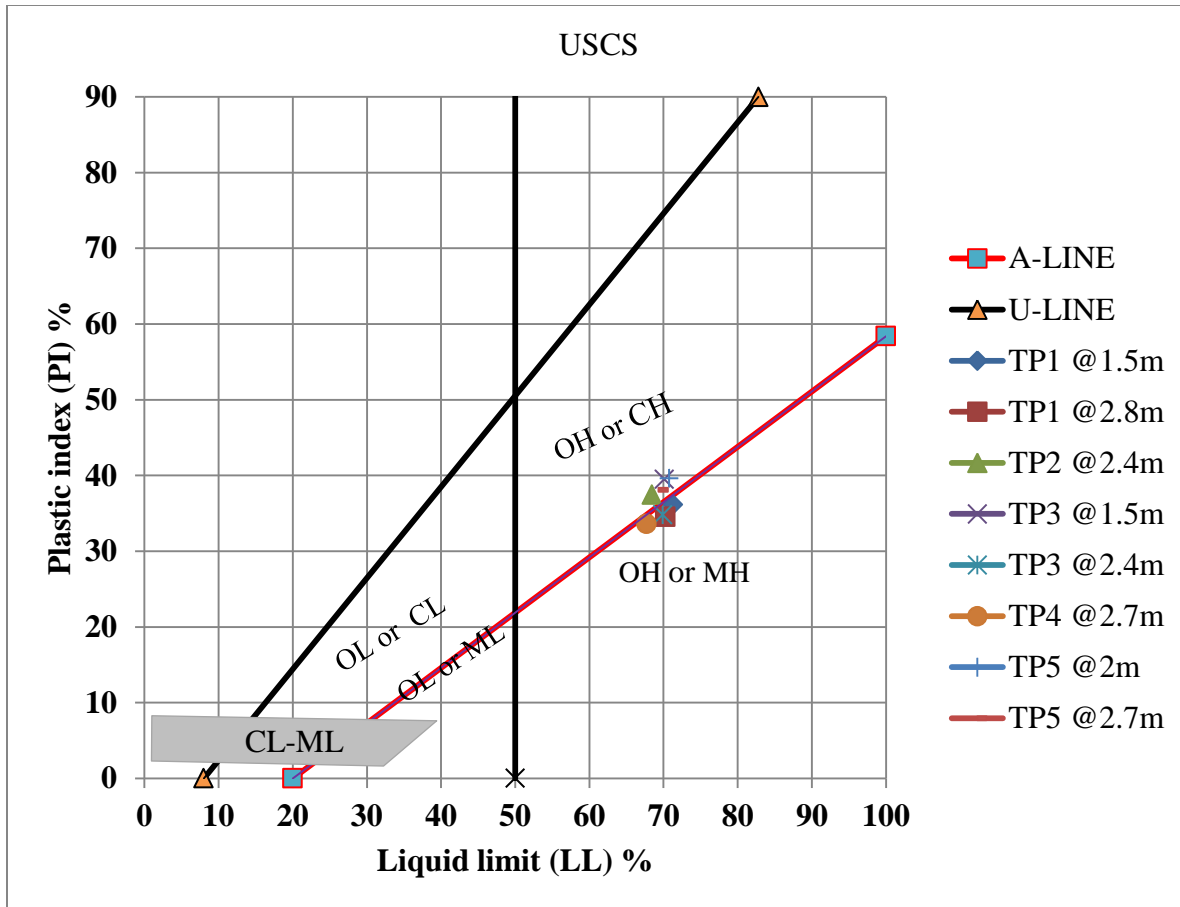
Figure 4.1 Classification of Chira Landslide soils according to USCS classification scheme

According to the classification of soils obtained from five test pits on eight samples according to the USCS scheme, three test pits were clay soils (CH) and two tests were silty soils (MH). As a result, the soils under study have a high probability of losing shear strength when in close contact with water, because the shear strength of fine-grained soils (silt and clay) is primarily determined by inter-particle forces, and this bonding force is easily broken down when exposed to high moisture content.

4.1.1.4 Grain Size Determination

Grain size determination conducted to classify various types of soils that make up soil mass based on their texture. Table 4.4 and Figure 4.2 offer a summary of the test findings and a combined graph of wet sieve and hydrometer analysis, while Appendix A shows the detailed computation.

Table 4.4 Particle Size Distribution of Soils of Chira Town Landslide

Sr. No	Test Pit Designation	Depth (m)	The Percentage amount of Particle Size (%)				%Finer than 0.075mm
			Gravel	Sand	Silt	Clay	
1	TP1	1.50	0.14	1.63	50.19	48.05	98.23
2		2.80	0.00	3.24	48.50	48.26	96.76
3	TP2	2.40	0.12	2.22	47.92	49.74	97.66
4	TP3	1.50	0.88	4.55	30.33	64.54	94.57
5		2.40	0.52	4.80	38.25	56.43	94.68
6	TP4	2.70	1.01	6.31	49.14	43.55	92.68
7	TP5	2.00	0.80	1.08	37.11	61.01	98.12
8		2.70	0.10	1.35	38.28	60.26	98.55

From the above Table 4.4, we can see that more than 92.68% of the soils of the study were dominated by fine-grained soils (silt and clay). As a result, we may conclude that the Chira landslide was greatly affected by material type, because fine-grained soils lose shear strength under high moisture content, causing slope instability.

During the winter season, the high moisture content obtained as a result of heavy rainfall disperses the fine-grained soils and transforms it into a more suitable substance that can flow readily as a liquid. Fine-grained soils were more impacted by saturation because of their structure, grain shape, geological origin, and other factors. The inter-particle forces of soil grains have a greater impact on the shear strength of fine-grained soils.

 As a result, they are prone to losing shear strength under severe rains and high moisture content. Test Pit 2 (TP2), TP3, and TP5 were dominated by clay soils, whereas TP1 and TP4 were dominated by silt soils in the research area's five test pits. When compared to other types of soils, silty and clay soils can simply slide due to moisture content, because fine-grained soils can only achieve their strength through inter-particle forces. Furthermore, clay soils have a poor permeability and can generate pore pressure as groundwater levels rise during the rainy season.
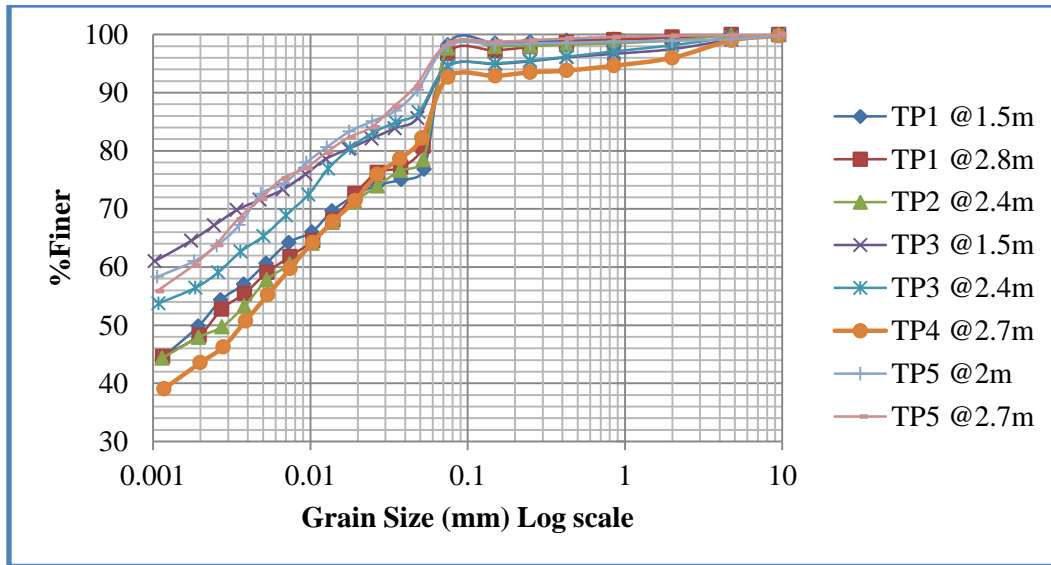
Figure 4.2 Combined Sieve and Hydrometer analysis of Chira Town Landslide Soils

As shown on the above graph (Figure 4.2), for TP1, TP2 and TP3, the graph is relatively steeper than others because of the rapid settlements of the soil particles. Silt soils were high at steeper slopes but clay soils were high at flat slopes.

4.1.1.5 Unit Weight Determination

This test is performed to determine the density of compacted in-situ soil. The dry density and bulk density of soils of the study area range from 1.289 g/cm^3 to 1.481 g/cm^3 and 1.844 g/cm^3 to 2.024 g/cm^3, respectively. The summary of results was shown in Table 4.5 shown below.

Table 4.5 Unit weight determination of soils of Chira Landslide

Pit Designation	Bulk Density (g/cm^3)	Unit Weight (kn/m^3)	Dry Density (g/cm^3)	Dry Unit Weight(kn/m^3)	Saturated unit Weight(kn/m^3)
TP1	1.94	19.01	1.32	12.92	17.98
TP2	2.02	19.86	1.48	14.53	18.96
TP3	1.94	19.06	1.38	13.56	18.42
TP4	1.84	18.09	1.29	12.65	17.76
TP5	1.98	19.40	1.41	13.82	18.68

Based on the observations made by Das (2002) the soils of Chira town are classified as silty soils based on the dry unit weight and void ratio of the study area. Das stated that soils having a void ratio of minimum of 0.4 and maximum 1as well as the dry unit weight of minimum

13KN/M^3, and maximum 19KN/M^3 were categorized silty sand soils in which most the soils of Chira town was falls in this range.

4.1.1.6 Free Swell Determination

Free swell represented soil expansion and was obtained by dividing the volume difference between the volume of Kerosene and water into the volume of kerosene. The free swell values obtained from five test pits of soils of the study area vary between 25.00% and 41.67%. The free well values of the study area show that the soils did not have expansiveness properties, and it can be considered as a low degree of expansion soils since it has free swell values of less than 50%.

Table 4.6 Free swell values of soils of Chira Landslide

Designation	Depth (m)	The volume of sample in Kerosene (ml)	The volume of sample in Water (ml)	Free swell (%)
TP1	2.8	12	15	25.00
TP2	2.4	12	16	33.33
TP3	2.4	11	15	36.36
TP4	2.7	11	14	27.27
TP5	2.7	12	17	41.67

4.1.1.7 Permeability Test Determination

Permeability, also known hydraulic conductivity (K), is the property of soil to pass any liquid like water through its mass. Permeability of soil is highly affecting the engineering properties of soil. Coarse grained soils are categorized under highly permeable soils while fine grained soils was categorized under poor to impervious materials. Various soil particles have different hydraulic conductivity based on their particle size, shape, the void ratio, water properties, soil structure, and specific surface area of the particles. Permeability is highly dependent on the void ratio of soil particles, and they have direct proportions together.

 In this study, the Falling Head Method test conducted for five soil samples since the dominant soil type of the study area is fine-grained soils, and the Falling Head method was applicable for this type of soil. The coefficient of permeability obtained from this test result reveals that the soil of study area was catagorized under clay and silt soils because the result ranges between 6.23E-05 and 9.95E-07.

Summary of determination of permeability test is in Table 4.7 below and detail presentation of the test was given on Appendix A.

Table 4.7 Permeability Coefficient of Chira Landslide Soils

Test No	Test Pit Designation	Depth (m)	Coefficient of permeability K(cm/sec)
1	TP 1	2.8	2.68E-06
2	TP2	2.4	9.48E-07
3	TP3	2.4	3.49E-07
4	TP4	2.7	6.23E-05
5	TP5	2.7	9.95E-07

As shown in Table 4.7 above, the coefficient of permeability of soil of the study area is very small value. Hence, the high water content in relation with low permeability behaviour of soil develops positive pore pressure, which can significantly disperse soil particles; this tends to decrease the shear strength of soil which can initiate landslide occurrence.

4.1.1.8 Triaxial (UU) Test Determination

A Triaxial UU test is conducted to determine the un-drained shear strength of saturated cohesive soil. Soil parameters such as unit weight, elastic modulus, cohesion, and angle of internal friction was obtained from this test. For this research, triaxial tests were conducted at Ethiopian Construction Design & Supervision Works Corporation Laboratory on Five samples. From this test, shear strength parameters were determined and used in slope stability analysis. Summary of test results for Triaxial UU test was shown in Table 4.8 given below, and a detail presentation of the test was attached at the Appendix A.

Table 4.8 Summary of Triaxial UU test result of Cira Landslide Soils

No:-	Test Type	Standard Method	Soil Test Results				
			TP1 @2.4m	TP2 @2.4m	TP3 @2.4m	TP4 @2.7m	TP5 @2.7m
1	Triaxial Test	ASTM D 2850					
	C (Kpa)		58.81	68.06	87.42	26.07	153.28
	Ø(Degree)		18.45	22.56	17.25	25.65	8.02

Elastic Modulus Determination from Triaxial Test

Elastic modulus used for slope stability analysis determined from the stress-strain curve that was obtained from the triaxial test. The slope of the linear line on the stress-strain curve was used as the Elastic Modulus of the soils (Figure 4.3, a &c). For this study, the Elastic modulus obtained from the triaxial test was run in the range of 7,836 – 12,124 Kn/m^2 (Figure 4.3, b & d).

a.

b.

c.

d.
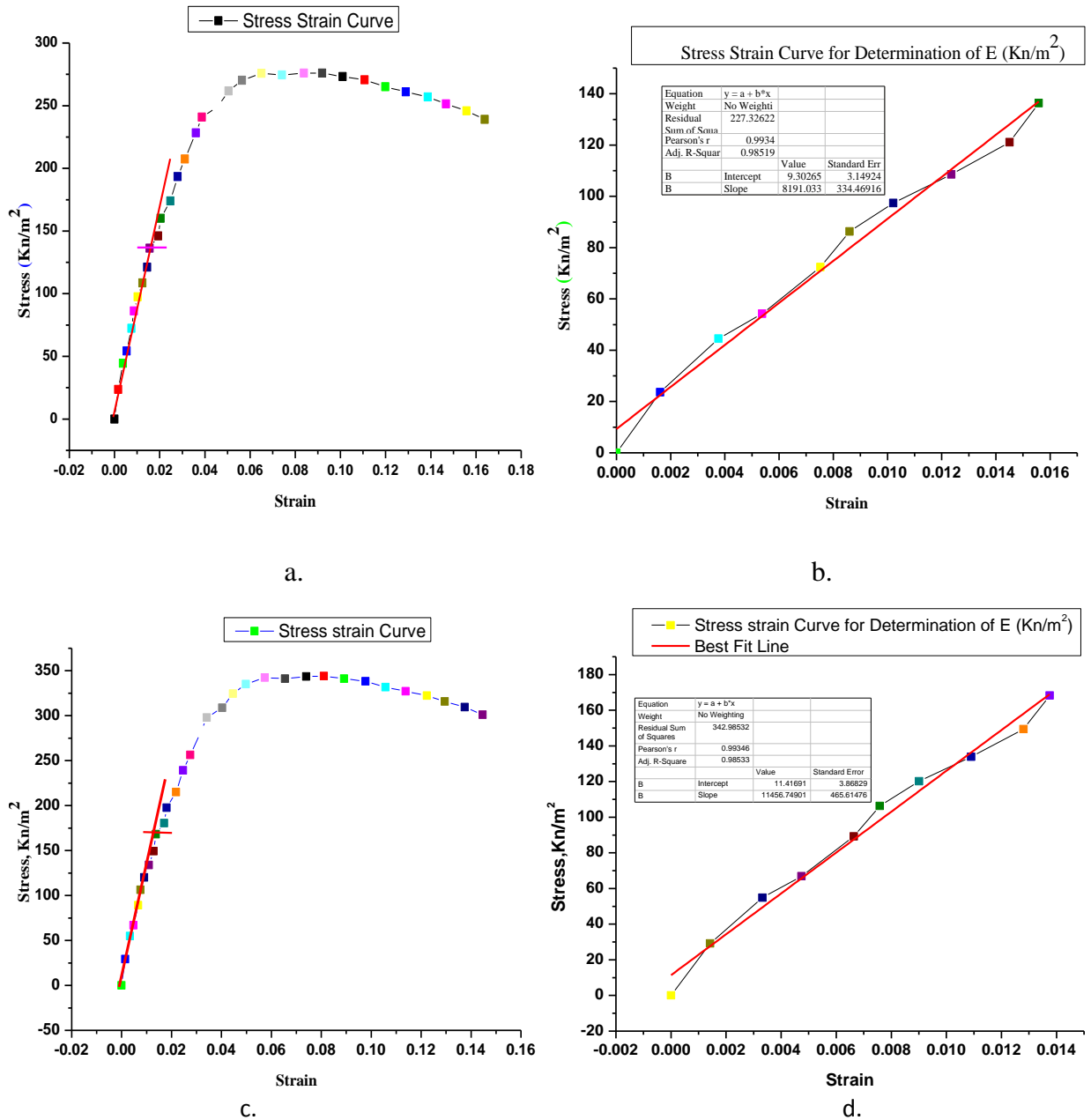
Figure 4.3 Elastic Modulus determinations from stress-strain curve of triaxial test

4.2 Geophysical Test Results.

Electrical resistivity results were conducted on different locations of the towns along affected slopes, and the output of the investigation was discussed below. The subsurface 2D resistivity sections illustrate heterogeneous structures both horizontally and vertically. It is observed that there are low to high resistivity zones in all vertical profile sections. Low resistivity materials within the bodies of landslide are designated with clayey, silty materials, and moisture contents.

Figure 4.4 shows a profiling image of various layers of geological settings with different electrical resistivity values. The profile helps to identify the lateral and depth of Subsurface Lithology/layer formation. At the center of sliding mass, it is observed that the profile having a relatively massive resistivity of about 448 Ωm, indicating the massive basaltic tertiary volcanic rock, which is overlaid by the very low resistivity value of less than 10 Ωm, is indicating the sticky clay soil. This soil is highly characterized by very low hydraulic conductivity result in the significant cause for the increment of pore pressure and weight of soil mass over massive basaltic tertiary volcanic rock. These phenomena decrease the shear strength of soil causes mass movement that consequences landslide.
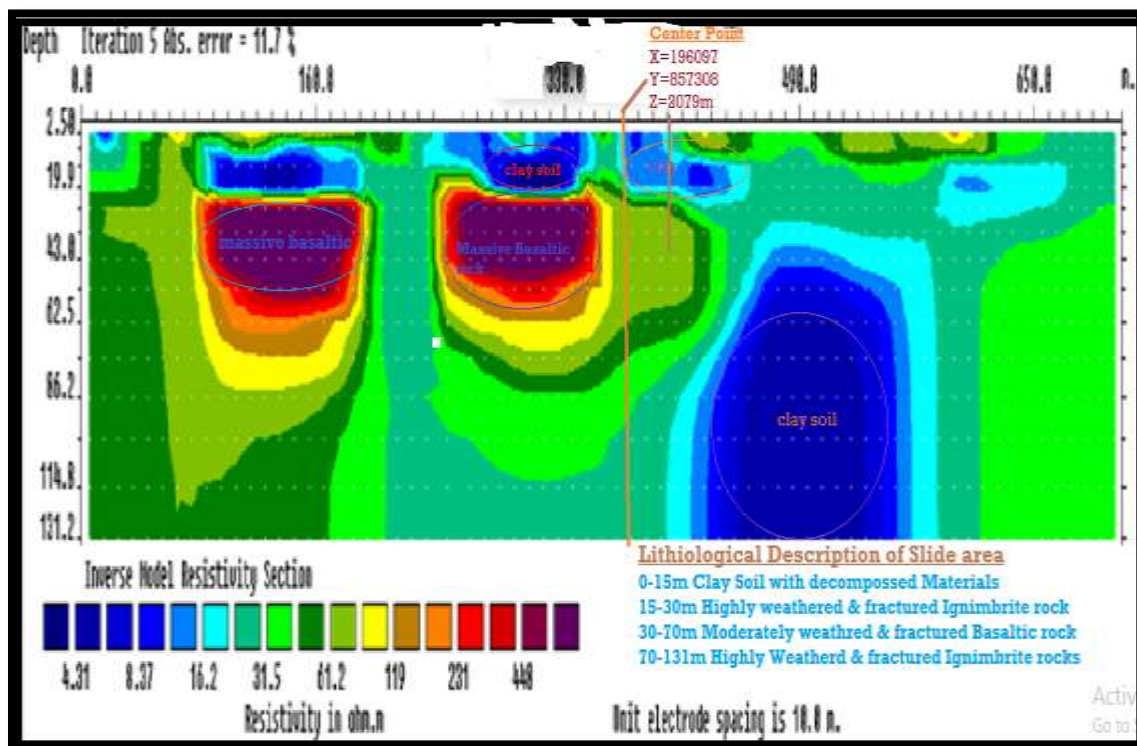
Figure 4.4 Muje Ber site Electrical Profiling 1

46

Figure 4.5 shows a profiling image of various layers of geological settings with different electrical resistivity values. The stratification comprises the different geological formations such as highly weathered and fractured ignimbrite rock, thick clay soil, and highly weathered ignimbrite with clay soil. Profile having relatively massive resistivity of about 111 Ωm, indicating the moderately tertiary volcanic rock (Ignimbrite) overlaid by the very low resistivity value of less than 10 Ωm is meaning the sticky clay soil. This formation eases for development of pore water pressure.
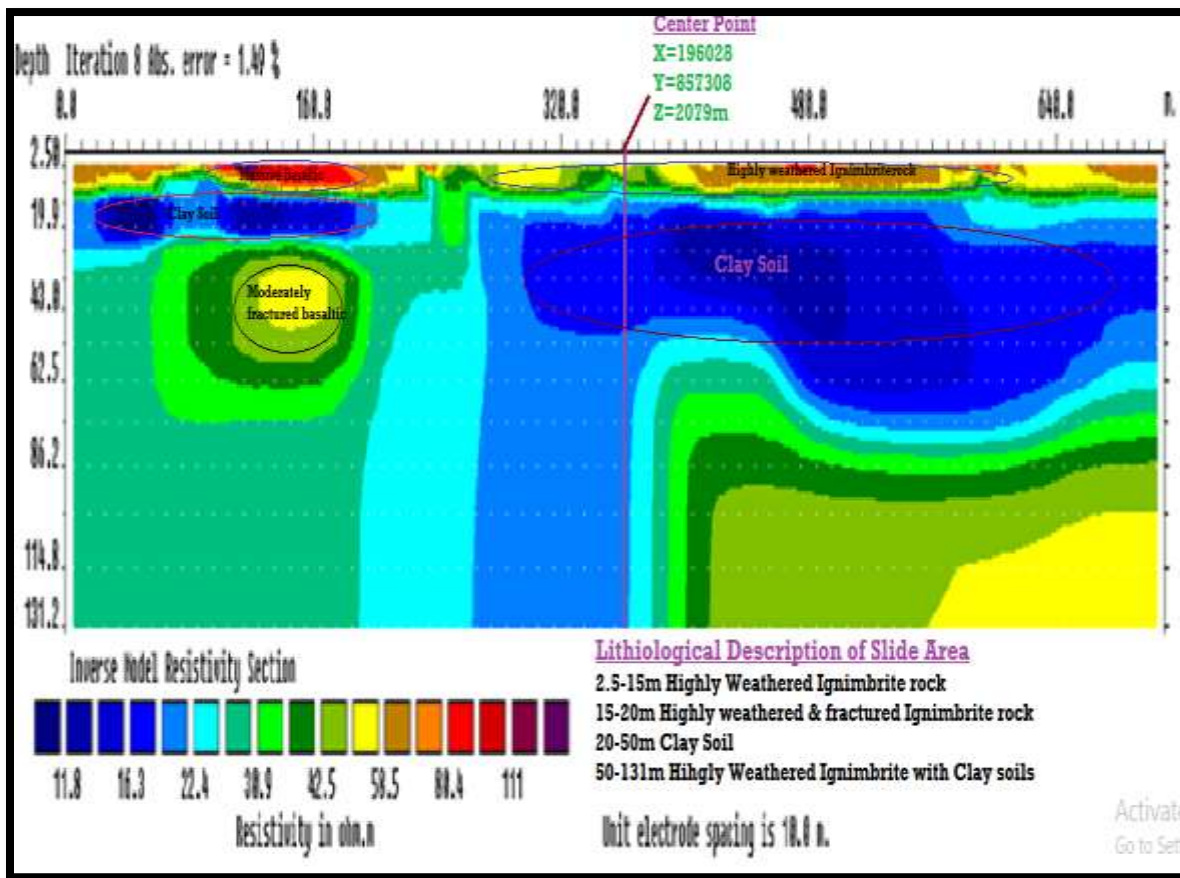
Figure 4.5 Muje Ber site Electrical Profiling 2

Figure 4.6 shows lateral and depth of subsurface lithological characteristics. The lithology is composed of moderately weathered and fractured ignimbrite, highly decomposed ignimbrite with clay soil, and slightly weathered ignimbrite rock. These weathered and fractured formations used as the line of stream flow. Both the right and left-hand side of the ground is divided in different layer based on the capacity of its electrical resistivity which indicates the formation of each

47

layer. The multi-layers indicate the existence unconfined aquifer with multi fracture, which is a trigger for the formation of sliding.
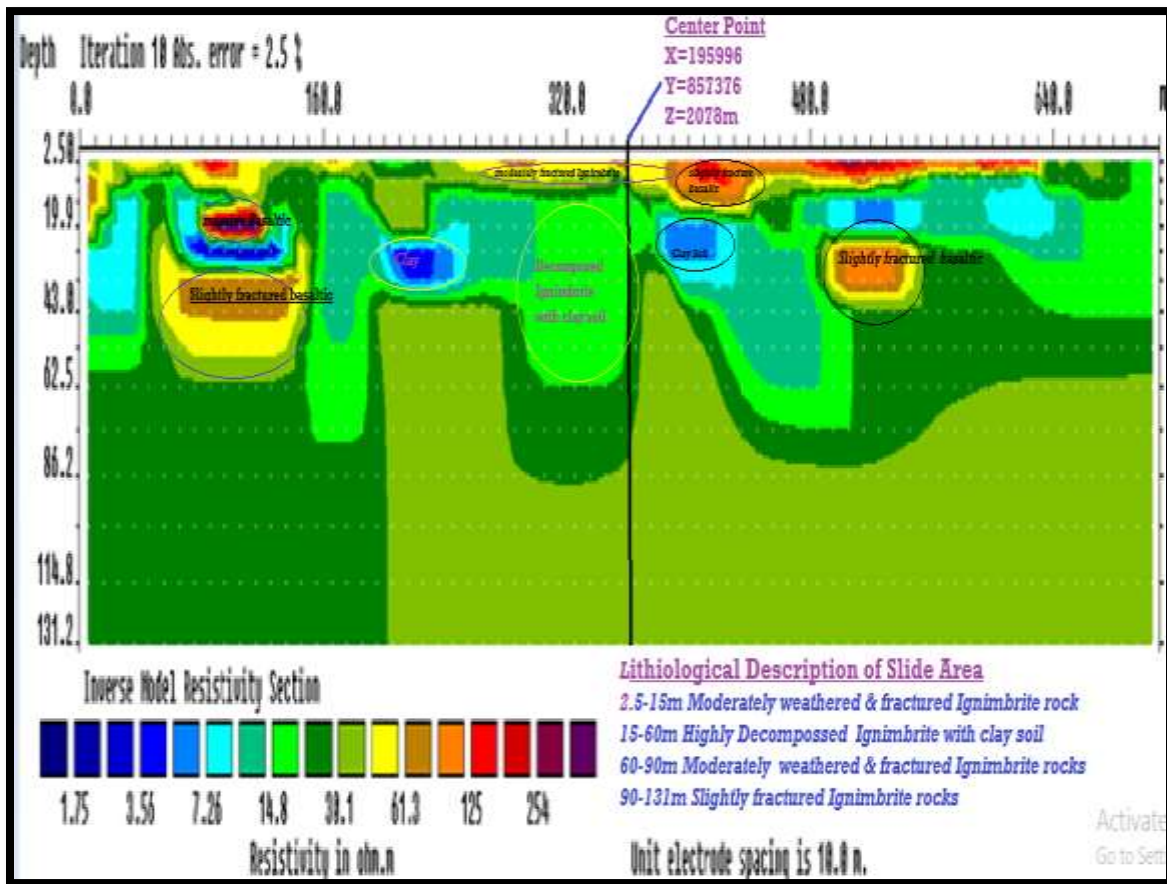
Figure 4.6 Muje Ber site Electrical Profiling 3

Figure 4.7 depicts various lithological formations along the center of the sliding mass. According to the profiling image, having a relatively Slightly fractured resistivity of about 134 Ωm indicates a slightly fractured tertiary volcanic rock that is underlain by a very low resistivity value of less than 10 Ωm, indicates a sticky clay soil. It has been observed that the subsurface is made up of various stratified formations. At the third layer, which is about seven meters thick, clay soil is overlaid by highly fractured, weathered basaltic rock and slightly fractured basaltic rock. If surface water flows in or groundwater rises and saturates the formation, fractured formations over clay formation make it highly susceptible to sliding. It facilitates the development of pore water pressure in the clay layer.
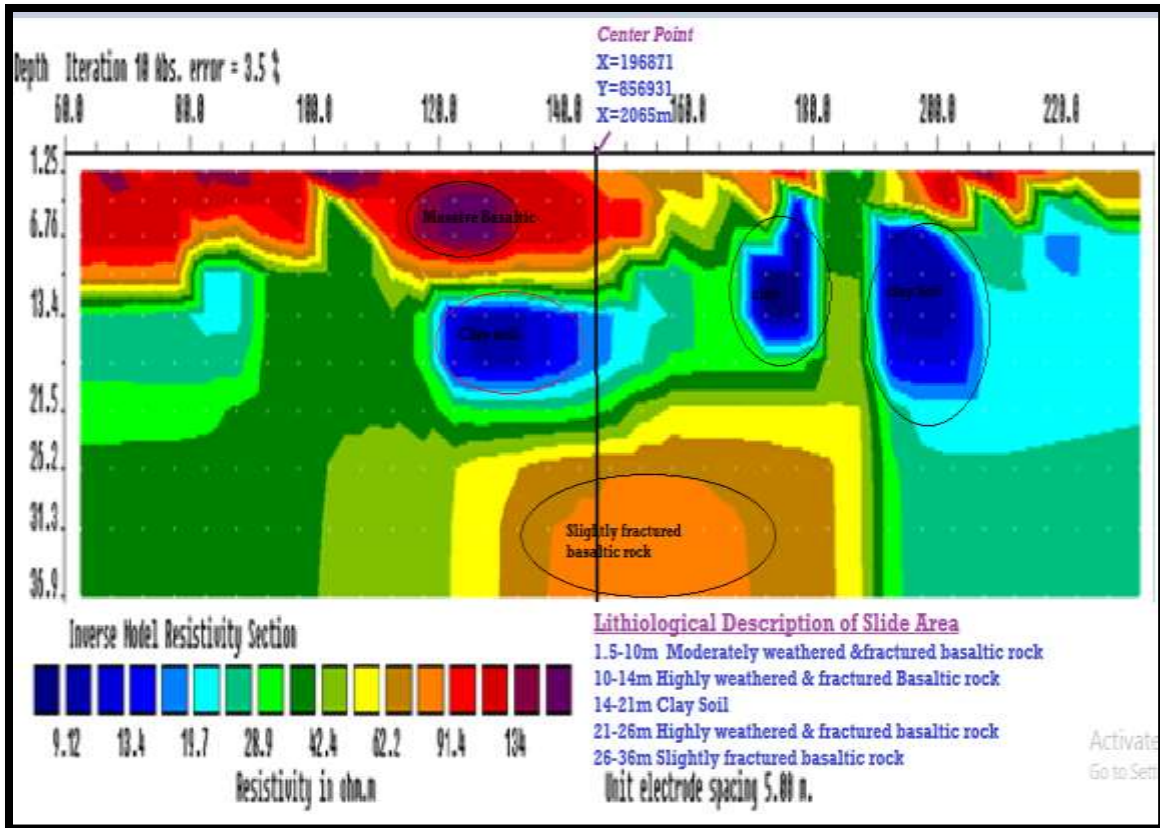
Figure 4.7 At the back Agriculture Office site Electrical Profiling

4.3 Causes and Triggering Factors of Landslides in Chira Town

Based on site visitation, laboratory test results, assessments of landslide causal factors by using GIS software, and stability analysis by using Plaxis 2D and slide softwares; the following causal factors was find out for occurrences of Chira town landslide.

4.3.1 Rainfall Analysis

The annual analysis of Chira rainfall shows the amount of rainfall is increased over the area from 2014, with the maximum annual rainfall record in 2016 as shown in Figure 4.8. As the information obtained from local peoples during site visitation, the extent of cracks observed on ground surface was increased gradually after the heavy rainfall that, the area obtained in 2016. The shear strength of soils become decline due to this high rainfall intensity and initiates the occurrence of landslide in Chira town. The average mean annual rainfall of Chira was 1955.4 mm with a maximum and minimum rainfall of 2967.8 and 1414.1 mm, respectively. This affirms that the preceding recent rainfall records can be the possible cause of landslide activities.

49

Summary of rainfall in chira town was presented in Figure 4.8 shown below.
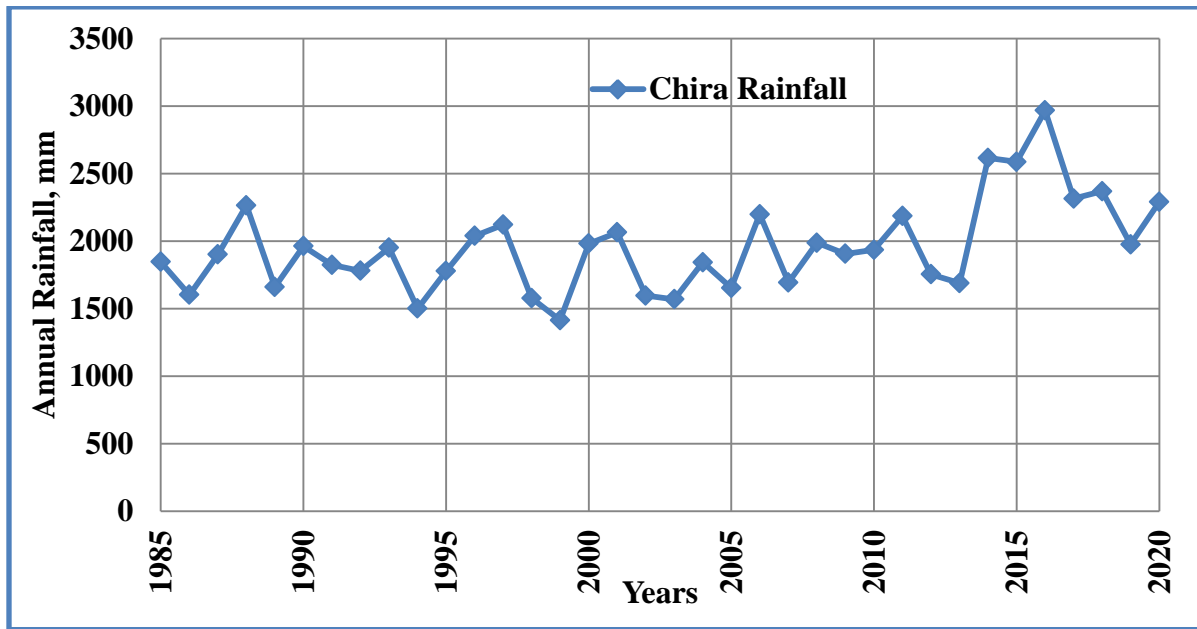
Figure 4.8 Annual rainfalls Analysis of Chira Rainfall

The Monthly Analysis of Chira Rainfall shows the area will get rainfall throughout the year, with a small rainfall in January, February, and December. In contrast, the main rainfall seasons of the area were May, June, July, August, and September, with the highest rainfall records in June, July, and August.
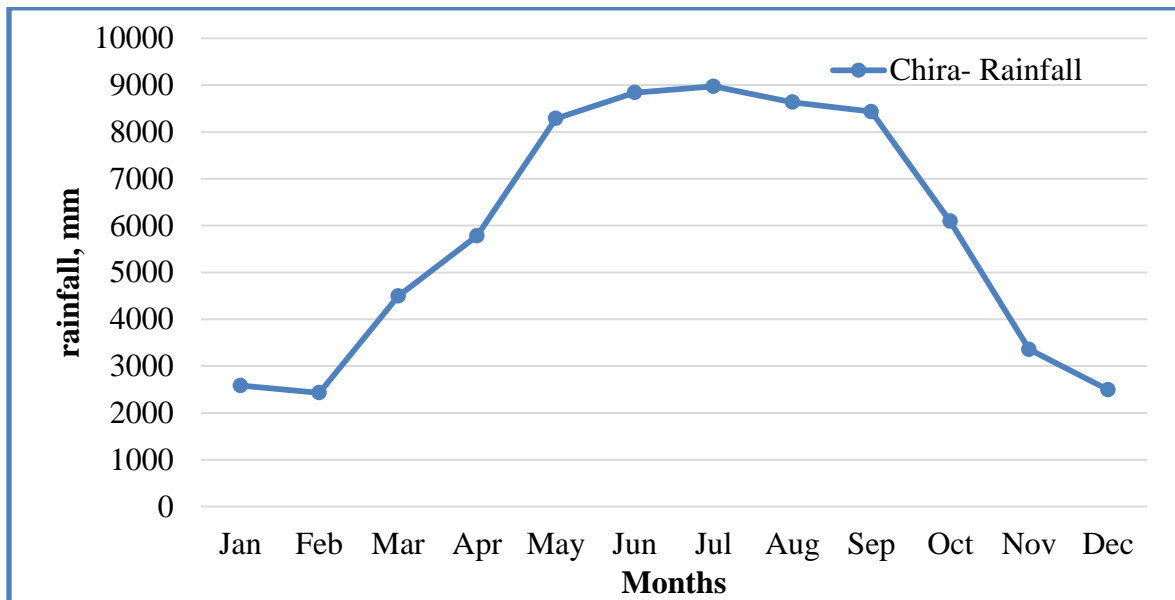
Figure 4.9 Monthly Rainfall Analyses

4.3.2 Slope Aspect

Aspect derived from DEM was classified into ten classes, as shown in Figure 4.10.The distribution of past landslides using the training points reveals that the maximum landslide occurred on slopes which are inclined towards the South (32.4%) followed by the Northeast (19.1%) and southwest (17.6%) direction. This is due to the fact that weathering is very high in the south direction and decrease the shear strength of the soils. The amount of sun light with in aday was large on afternoon. In Ethiopia, the south direction is the most susceptible direction for sun light and it takes from 11:00 Am to 6:00 Am. The intensity of the sun light also very high during this time. This is the main reaon, why the weathrering is high and landslide was occurred along this drection.

4.3.3 Curvature

In this study, curvature was grouped into three classes. The, negative values (< -0.05), flat (-0.05 - 0.05) and positive value (> 0.05). The landslide effect was high at flat curvature and the occurrence of landslide decreases for convex and concave slopes. But, the concave slopes also have high probability of landslide susceptibility since water concentrate at the lowe ends. In convex slope the runoff disperse equally and it has a low probabiliy for landslide occurrances.

4.3.4 Elevation

Elevation was classified into seven classes for the landslide hazard analysis, as shown in Figure 4.10. From the results, most of the landslide have occurred in elevations of 2077-2107 (45.6%) followed by 2048-2077 (38.2%). The study area has complex geographical topography. Some parts of the area is flat where as some parts have high elevation. This variation in elavation cause the tendency of runoff to affect the shear strenth of the soil.

4.3.5 Land use/land Cover

For lan duse/land cover, the study area was classified into four land use/land cover classes, Urban and built up, agricultural land, grassland and forest land. The distribution of the past landslide shows that landslide has occurred within all land use/land cover classes. However, the severity of the landslide has occurred in Urban and built-up lands, as shown in Figure 4.10. This is due to the fact that the activities done due to urban development like deforestation, additional loads incrase the driving force and decrease the stability of slopes in the study area.
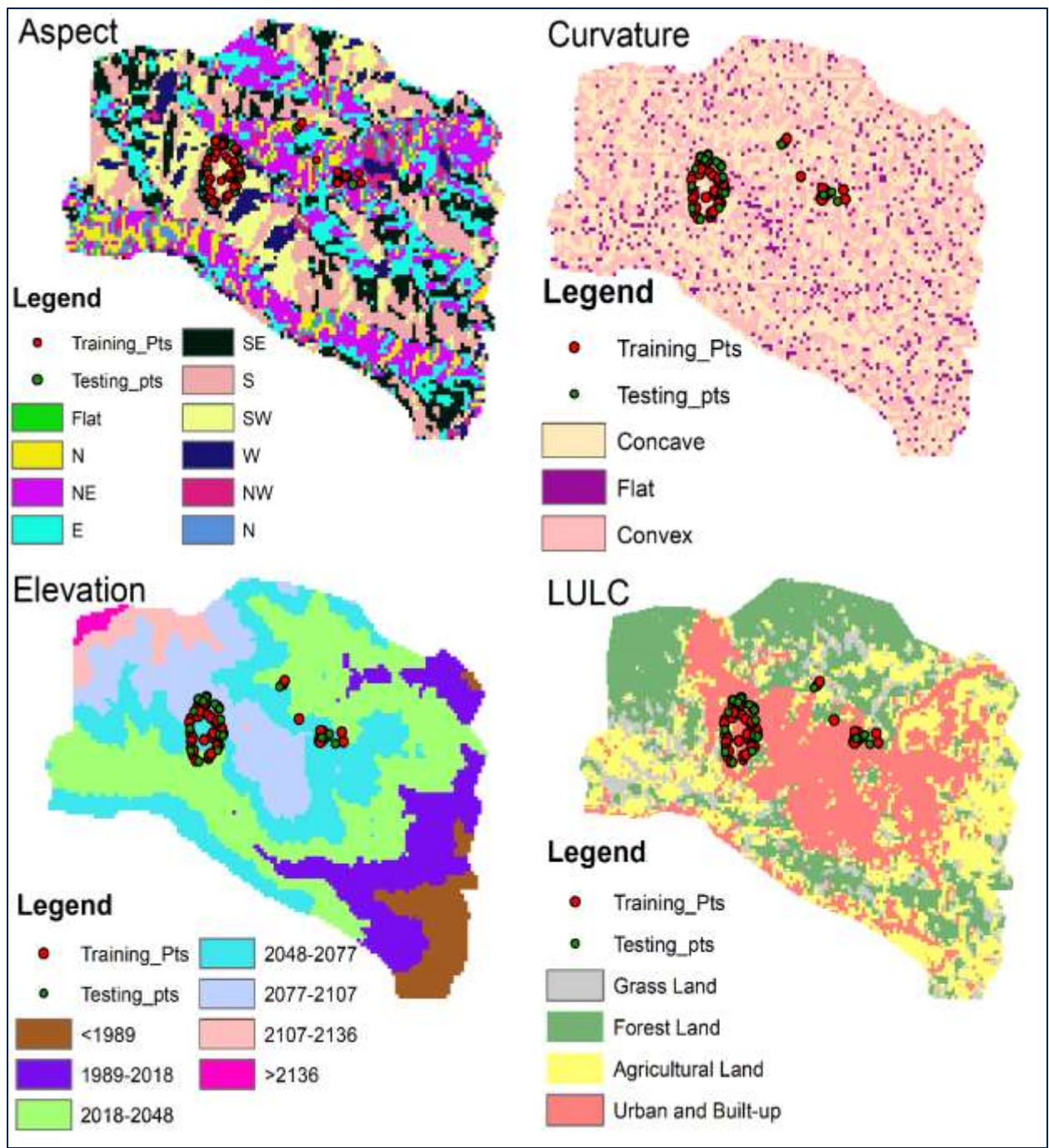
Figure 4.10 Aspect, curvature, elevation, and land use/land cover factors

4.3.6 Slope Angle

An increment in shear stress and the tangential component of the weight of the mass increases while the perpendicular component decreases with a steeper slope (Acharya and Lee, 2019). When the increase in shear stress is more than the resisting force, the slope mass will acquire a tendency to slide. DEM was used to extract the slope data in ArcGIS 10.3. The maximum slope angle was 27° with a minimum slope angle of 0° in flat areas. For this study, the slope was categorized into five classes; (0-5°), (5-12°), (12-20°), (20-25°), and (> 25°) as shown in Figure 4.11. The distribution of the past landslide shows the maximum landslide has occurred in slope ranges of 5-12 degrees (60.3%), followed by the slope range of < 5 degrees (23.5%).

4.3.7 Soil

The study area was grouped into three soil classes: Luvisols, vertisols, and Nitosols. The dominant soil in the area was luvisols, followed by nitosols. The type of soils obtained from this analysis consider only the organic parts of the soil. Luvisols are highly weathered with a subsurface accumulation of clay and are characterized by low nutrient retention and erosion hazards. The past landslide was dominantly occurred in the luvisol classes of soil, as shown in Figure 4.11. This is because of the tendency of water to percolate throgh subsurface of the ground in luvisol is very high and the highly accumulated clay soils under this soils produce the posetive pore pressure and cause landslide.

4.3.8 Stream Distance

Normally, a river network is an outcome of long-time interaction between the geological structures, topography, and slope under the influence of water (Hamza and Raghuvanshi, 2016). Considering the slope and elevation, distance to streams in the study area was derived based on Euclidean distance. Accordingly, stream distances were grouped in to five classes: < 57, 57 - 115, 115 - 180, 180 - 260, > 260 (Figure 4.11). Landslide is very high in-stream distance of between < 57 and 180 - 260. This is because, the existence of a river at the toe of the slopes and distance of the slopes from the river is a matter rather than the steepness of the slopes in this study area. Because, at the toe of the slope, the bank erosion and river incision have a great impact on the stability of slopes', that can initiate the mass movement of the study area.
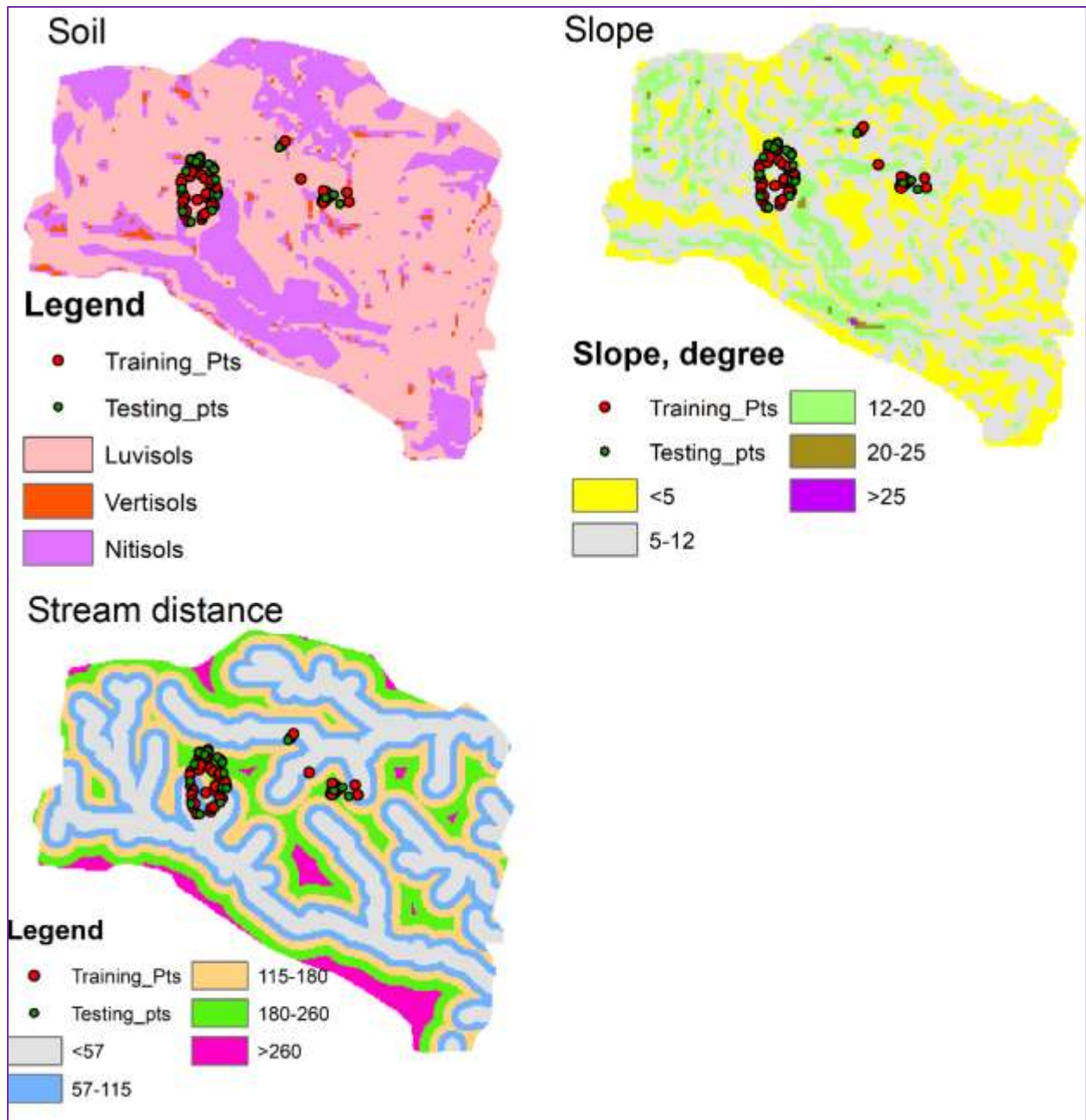
Figure 4.11 Slope, soil, and stream distance factors

4.3.9 Groundwater Condition and Elevation Difference

Groundwater condition is varied due to rainfall variation and elevation difference. It has occurred as a result either of water infiltration in the ground or a decrease in the aquifer during the dry season. The runoff that flows from a higher elevation and stored into lower elevation was also increases the groundwater. As shown in Figure 4.12, the runoff that comes from points "A" and "B" will infiltrate into the soil and be stored at point "C" that can increase the groundwater

condition at this point. An increase in Groundwater will increase the weight of the earth mass, decrease the shear strength of the weak layer, which results in increasing driving force over the resisting forces and facilitate the occurrence of the landslide. Groundwater level of chira town was varied between 5-16 m in different location of the town. This groundwater fluctuation cause fluctuation of pore water pressure which has an adverse effect on the stability of earth mass. Hence, the drying and wetting behavior of weather conditions corporate with elevation difference on the slope of study area result in groundwater fluctuation and considered as one of triggering factors for chira town landslide.
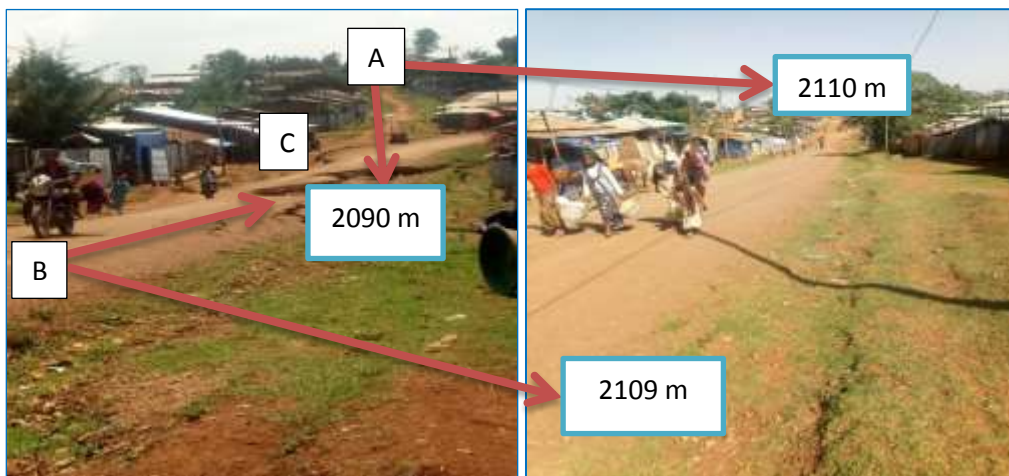
Figure 4.12 Effect of elevation difference on Pore pressure development

4.3.10 Human Activities

Chira town was found in 2007 before 14 years ago. As shown on the Land use land cover above, urban development is very high in this study area, and during this period, a lot of infrastructures such as houses and roads were constructed. The expansion of populations in this newly established town is rapidly increased, and a lot of natural environment was degraded. Excavation for roads, deforestation for construction of houses, a lot of dynamic forces, milling machine in the town, such as traffic loads were considered as triggering factors of the study area. Compaction during roads construction has a significant effect on increasing the density of underlayer soil and decreasing the permeability of that soil, which can result in the rising of the positive pore pressures.

4.3.11 Lithology of Earth Mass

There are different layers in earth mass. This variation of layers under the earth, starting from the surface, is called the lithology of earth mass. The study area's detailed lithological formation was investigated by using geophysical tests on the field (Figure 4.4 - 4.7), and the result varies from soft clay soils to hard bedrocks. There are very soft clay soils and highly weathered ignimbrite rocks in a great depth, which can lose their shear strength in moisture conditions and affected the landslide. Therefore, the presence of weak zone (highly to moderately weathered and fractured rock) and clay soil with large thickness were the main causes for landslide occurrence in the study area.

4.3.12 Slope Materials

Several properties are found in different soil types. The particle size and their formation, the shear strength parameters, their ability to pass water through their voids were significantly affected the soil properties. From laboratory test and geophysical test results, the soil types of the study area were categorized under fine-grained soils, which are mainly classified as silt of highly plastic (MH) and clay of highly plastic (CH) soil type according to USCS scheme. But, from geophysical test results, clay content also covers large areas of subsurface stratification. These soils are characterized as swell when wet and shrink in dry weather conditions and commonly have multiple planes of weakness, which initiate the occurrence of landslide. Soil particles which have a high amount of fine-grained soils can simply lose their strength after saturated with water. The weathered/fractured rocks found under the fine-grained soils have high permeability coefficient, while the overburdened clay materials have a very low coefficient of permeability. The discontinuities found in weathered rocks increase the permeability of materials. In contrast, the absorbed water that were found in fine-grain soils reduce the pores that was used to the passage water through the soil and decrease the permeability of fine-grained soils. The permeability variations between the two materials were creating pore pressures and initiate the occurrence of landslide in the study area. Hence, the soil type of Chira Town was the cause of the landslide that occurred in the study area.

4.4 Landslide susceptibility map

Using collected past landslide points, FR, RF, and prediction rate (PR) of all factors were calculated. The detailed analysis of the factor classes with their corresponding FR, RF, and PR

presented in Table 4.9. FR values normalized into the 0 - 1 values from FR for a better comparison of the factor classes and landslide susceptibility index (LSI) whereas PR values used to provide the weightage of the factors influencing the LSI (Acharya and Lee, 2019).

Generally, the highest RF value shows the highest probability of the landslide occurrence in the corresponding classes (Acharya and Lee, 2019). In this regard, the highest probability of landslide occurrence is in the south slope aspect followed by North-east direction. Similarly, flat and concave curvature has much compared to the other classes.

The slope angle of 12 - 20 degree and elevation ranges of 2077 - 2107 m has the highest probability of landslide occurrence. The study clearly shows that the highest slope and elevation not associated with the highest probability of landslide occurrence. The expansion of urban and built-up has the highest RF value, indicating the highest probability of landslide is associated with the expansion of urban expansion.

Table 4.9 Frequency Ratio, Relative frequency, and prediction rate of each class within each factor in the study area.

Factors	Class	Class pixels (%)	Landslide Pixels (%)	FR	RF	RFmax	RFmin	Rfmax-Rfmin	PR
	Flat	0.79	0	0.00	0.00				
	North	6.69	0	0.00	0.00				
	Northeast	17.74	0	0.00	0.00				
	East	14.21	16	1.13	0.10				
	Southeast	15.66	10	0.64	0.05				
Aspect	South	20.15	10	0.50	0.04	0.33	0.00	0.33	1.33
	Southwest	12.63	36	2.85	0.25				
	West	5.40	20	3.71	0.33				
	Northwest	3.25	2	0.61	0.05				
	North	3.49	6	1.72	0.15				
	Sum	100.00	100	11.15	1.00				
	< 5	27.87	22	0.79	0.26				
	5 - 12	57.35	62	1.08	0.36				
Slope(degree)	12 - 20	14.39	16	1.11	0.37	0.37	0.00	0.37	1.49
	20 - 25	0.36	0	0.00	0.00				
	> 25	0.03	0	0.00	0.00				
	Sum	100.00	100	2.98	1.00				
	< 1989	6.57	0	0.00	0.00				
Elevation	1989 - 2018	15.08	0	0.00	0.00	0.54	0.00	0.54	2.16
	2018 - 2048	33.86	16	0.47	0.10				

Factor	Class								
	2048 - 2077	24.93	44	1.77	0.36				
	2077 - 2107	15.20	40	2.63	0.54				
	2107 - 2136	3.63	0	0.00	0.00				
	> 2136	0.73	0	0.00	0.00				
	Sum	100.00	100	4.87	1.00				
Land use	Grassland	11.05	7.55	0.68	0.19				
	Forestland	27.98	13.21	0.47	0.13				
	Agriculture land	29.10	1.89	0.06	0.02	0.67	0.02	0.65	2.59
	urban and built-up	31.87	77.36	2.43	0.67				
	Sum	100.00	100	3.65	1.00				
Curveture	Concave	45.57	50	1.10	0.43				
	Flat	8.87	4	0.45	0.18	0.43	0.18	0.25	1.00
	Convex	45.56	46	1.01	0.39				
	Sum	100.00	100	2.56	1.00				
Distance to stream	< 57	30.32	26	0.86	0.18				
	57 - 115	25.05	12	0.48	0.10				
	115 - 180	24.13	22	0.91	0.19	0.53	0.00	0.53	2.12
	180 - 260	15.70	40	2.55	0.53				
	> 260	4.80	0	0.00	0.00				
		100.00	100	4.80	1.00				
Soil	Luvisols	65.41	86	1.31	0.75				
	Vertisols	1.97	0	0.00	0.00				
	Nitosols	32.62	14	0.43	0.25	0.75	0.00	0.75	3.02
		100.00	100	1.74	1.00				

The prediction rate of all factors reveals that the highest landslide occurrence was associated with soil factor followed by land use land cover factor. This shows that the most driving factors of the landslide in the study area were soil and land use land cover activities. When these are added with high rainfall intensity, the magnitude of the landslide intensifies. In this study, curvature was the least affecting factor of the past landslide, as shown in Figure 4.13.
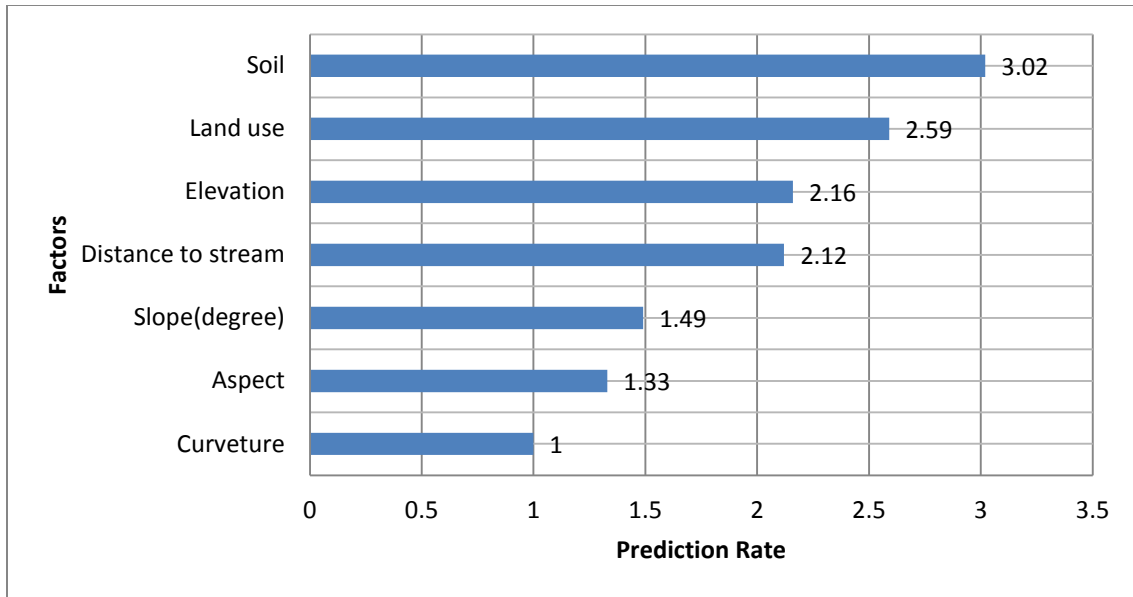
Figure 4.13 The prediction rates of the LSI factors

From the prediction rate shown on the above chart, the type of soil was the main triggering factor among selected factors, and it accounts for around 22.03%, followed by land-use land cover and elevation by 18.89% and 15.75%, respectively. The percentage contribution of the selected factors based on the prediction rate given above summarized in chart shown in Figure 4.14.
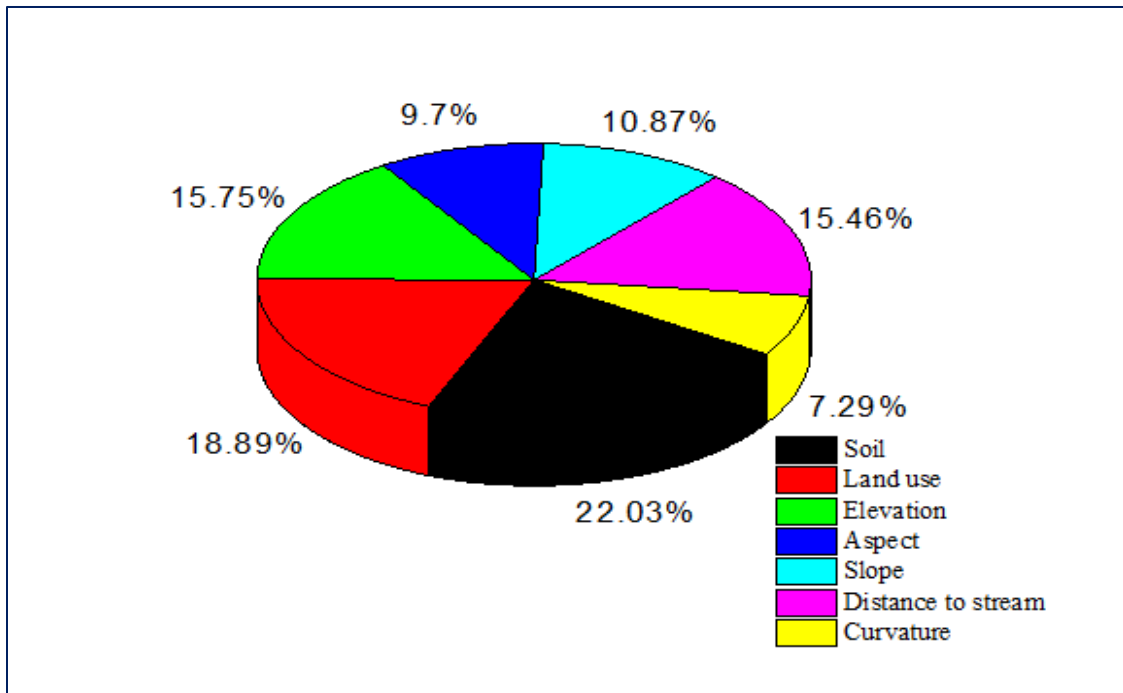
Figure 4.14 Percentage contribution of causal factors depend on prediction rate.

The LSI analysis shows that the LSI of the study area varies from 7.7 (the most vulnerable area) to 0.75 (the least vulnerable area). The index classified into five discrete susceptible classes with very high, high, moderate, low, and very low severity, as presented in Figure 4.15 given below.
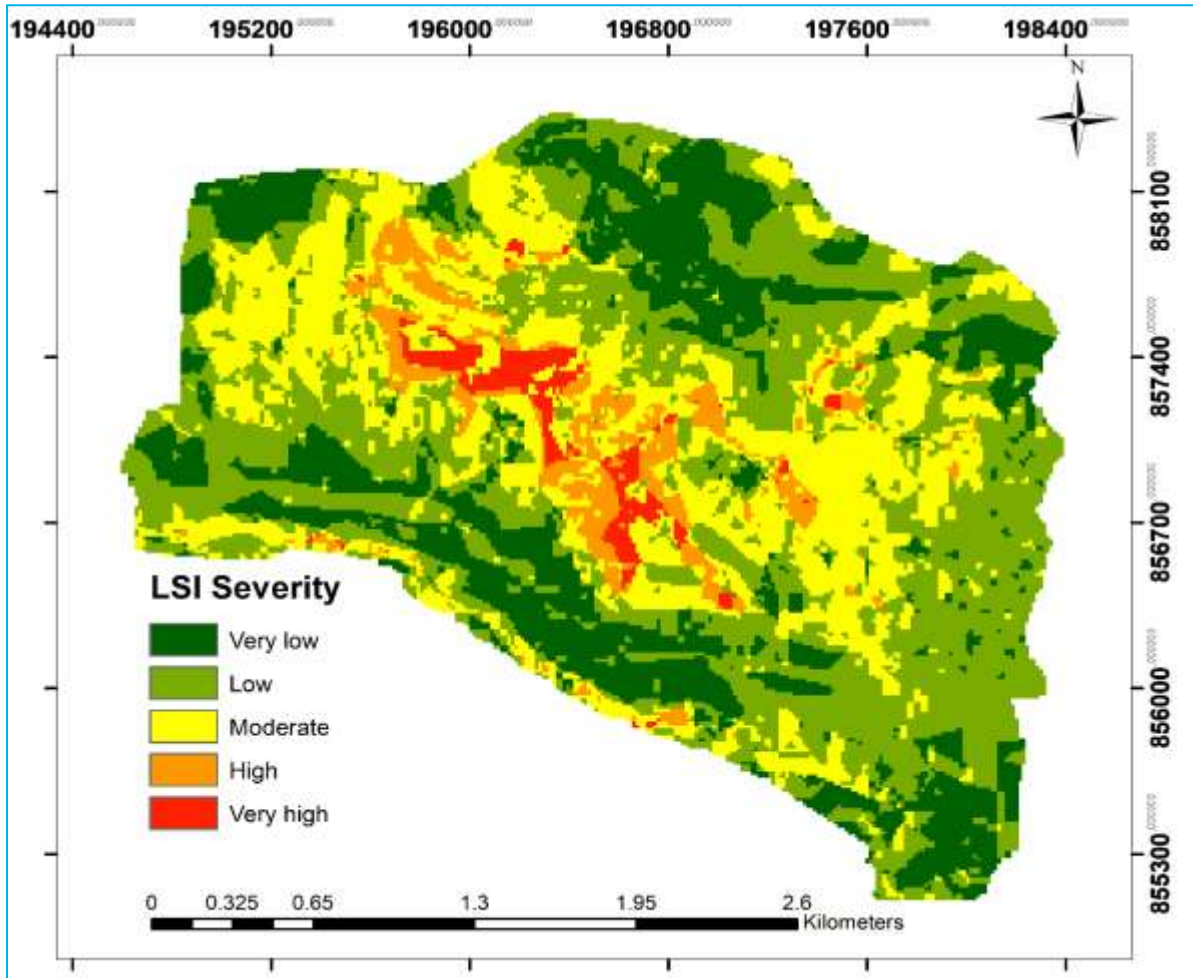
Figure 4.15 LSI map of the study area

The LSI map shown on the Figure 4.15 above indicate that there is most vulnerable areas to a landslide in the center of the town and there is low to very low vulnerable areas to the landslide around the border of the town. This is due to the fact that the areas occupy more population and consider more activities that can facilitate the triggering factors cause the landslide at the center of the town. The low vulnerability of LSI around the border of the town is because of less population and the soil slopes around this area gets strength from the tree roots, and obtain their stability against the mass movement in this area.

4.5 Consequence of Chira Landslide

The landslide effect on the study area, as information obtained from field observations, local peoples, and municipality offices evaluated. Even though no loss of human life due to landslides was reported in the study area, a huge impact was observed. The effects of landslides in this study area were both direct and indirect effects. As shown below, many houses in the study area become out of function due to this phenomenon. A lot of families live in rental houses after the occurrence of this landslide. In addition to this, roads, pipelines, and electricity power lines were blocked and interrupted in this study area. The natural environment has become out of function in most of the affected areas due to the mass movement of Chira town.

Figure 4.16 Some Photos on Consequences of Chira Town Landslide

4.6 Slope Stability Analysis Results

4.6.1 Stability Analysis using Plaxis 2D Software

In this study, slopes from affected and un-affected sites of the study area were analyzed. Two slopes along the affected area and one slope along un-affected area were analysed. For all slopes, different condition of the groundwater table (GWT) was used. The GWT of the study area was determined during site investigation from hand-dug wells. In most areas, the groundwater level was varied between 5-10 m, while there is a case in which there is no water table existed in some wells up to 13 m, especially at the place near to buffer zone. The GWT was used at great depth for dry condition cases, at 5-10 m depth for partially saturated conditions, and at surface level for fully saturated conditions. A summary of the slope stability analysis for different slopes in different GWT level conditions was given in Table 4.10 given below.

Table 4.10 Summary of slope stability results using plaxis 2D software

Slope	Site Condition	GWT Condition	FS	Deformation (m)
S-1	Affected Area	Dry Condition	1.34	$341.03*10^{-3}$
		Partially Saturated @10 m BGL	0.90	1.62
		Partially Saturated @5 m BGL	0.66	1.82
S-2	Affected Area	Dry Condition	1.95	$144.53*10^{-3}$
		Partially Saturated @5 m BGL	1.27	$279.29*10^{-3}$
		Partially Saturated @2 m BGL	1.10	$952.03*10^{-3}$
		Partially Saturated @1 m BGL	0.98	2.87
S-3	Un-affected area	Dry Condition	3.18	$62.85*10^{-3}$
		Partially Saturated	2.52	$87.10*10^{-3}$
		Saturated Condition	1.83	$176.58*10^{-3}$

BGL-Below Ground Level

As shown in Table 4.10 above, as the groundwater table level increase from great depth to surface condition, the stability of slopes becomes decreased. This fact is valid for all slopes, including unaffected slopes. This is due to the fact that, increasing moisture content increasing the driving force and decrease the shear strength of soil particles, and decrease in factor of safety of slopes. Like factor safety the deformation was also decreased when grounwater level increases from great depth to ground surface level. The deformation in affected area were very high in saturated state and this show us that the stability of study area was highly associated with rainfall.
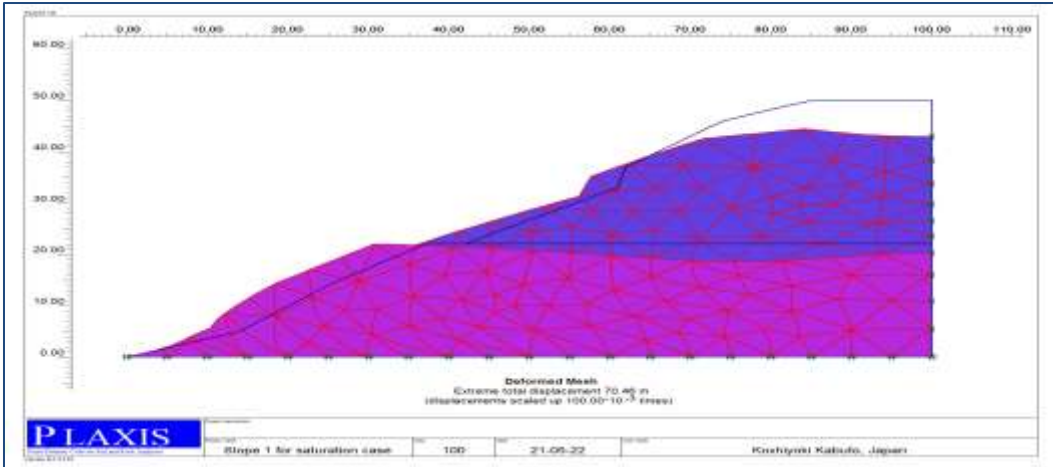
Figure 4.17 Total deformation meshes when GWT at 10 m below ground level
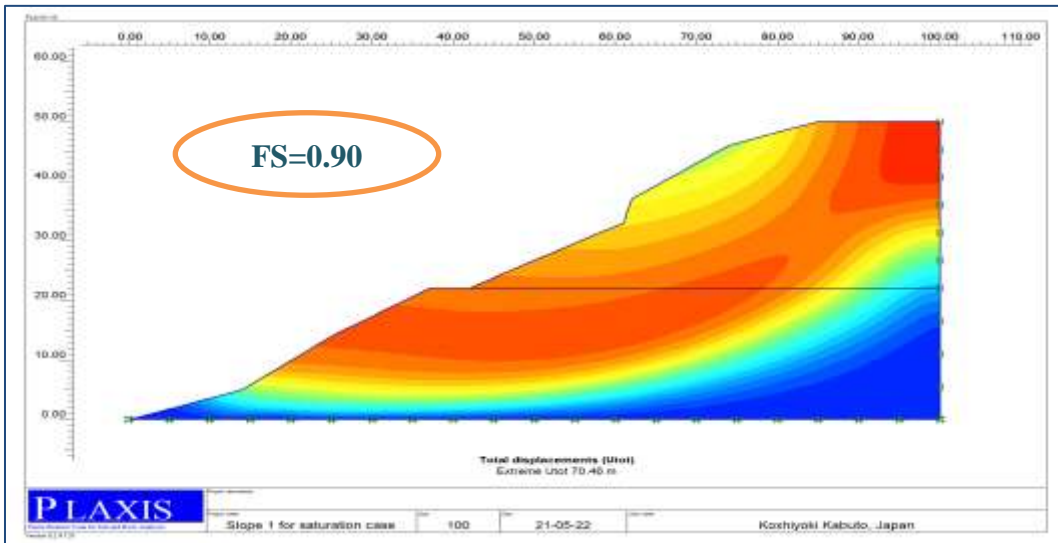
Figure 4.18 Total displacements when GWT at 10 m below ground level
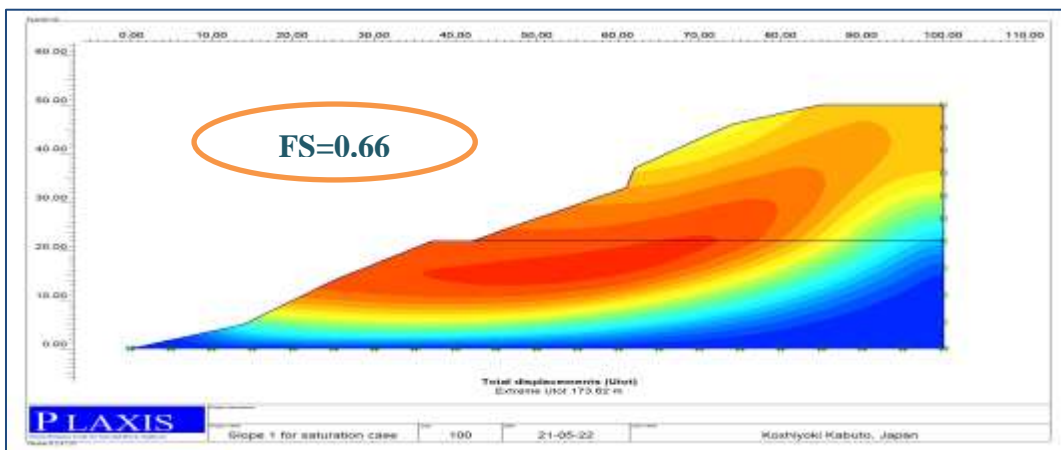
Figure 1Total displacements when GWT at 5 m below ground level
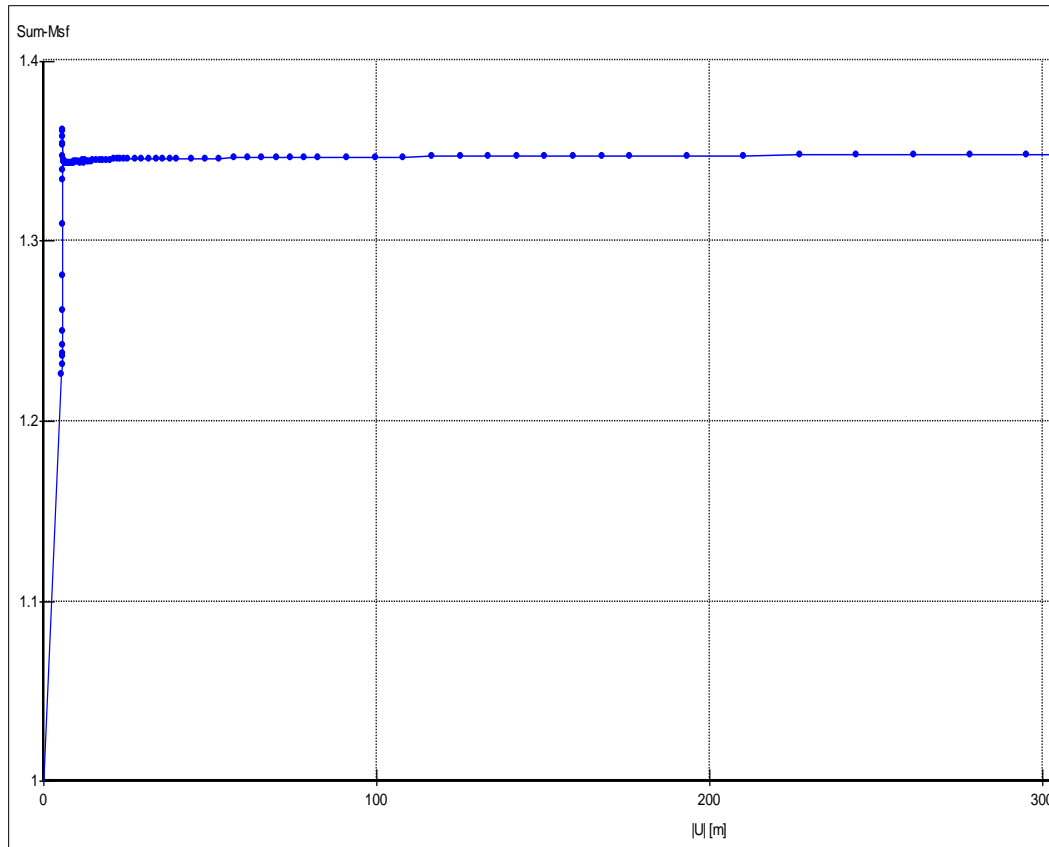
Figure 4.20 Safety Factor for Slope 1 affected in dry condition

The factor of safety of slope one, as shown on the plaxis output presented above, was under the unstable condition. Except for dry condition, the numerical values of safety factor were less than 1. This is an indication that increasing the water content increase the weight of the soil mass and decreases the shear strength of the soil which initiates the occurrence of the landslides. The factor safety was 1.34, 0.90, and 0.66 for dry, partially saturated at 10 m and 5 m below ground surface, respectively. The slope stability decreased by 32.94% and 26.55% when the groundwater table raised from great depth to 10 m below ground level and from 10 m to 5 m below ground level respectively. The more increment of groundwater level up to 5 m has decreased the FS by 50.74% from the stability obtained in dry condition.The deformation analysis for slope one also show that the increase of grounwater level increase the deformation in all aspects. The deformation was increased from 0.34 m to 1.82 m by 81.26% from dry condition to when groundwater table at 5 m respectively.
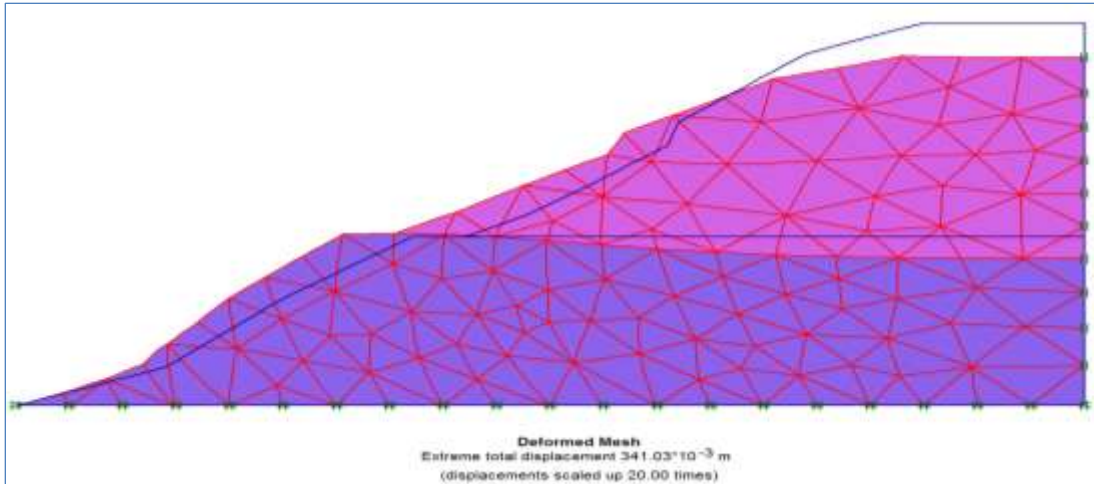
Figure 4.21 Deformation analysis for slope 1 in dry condition
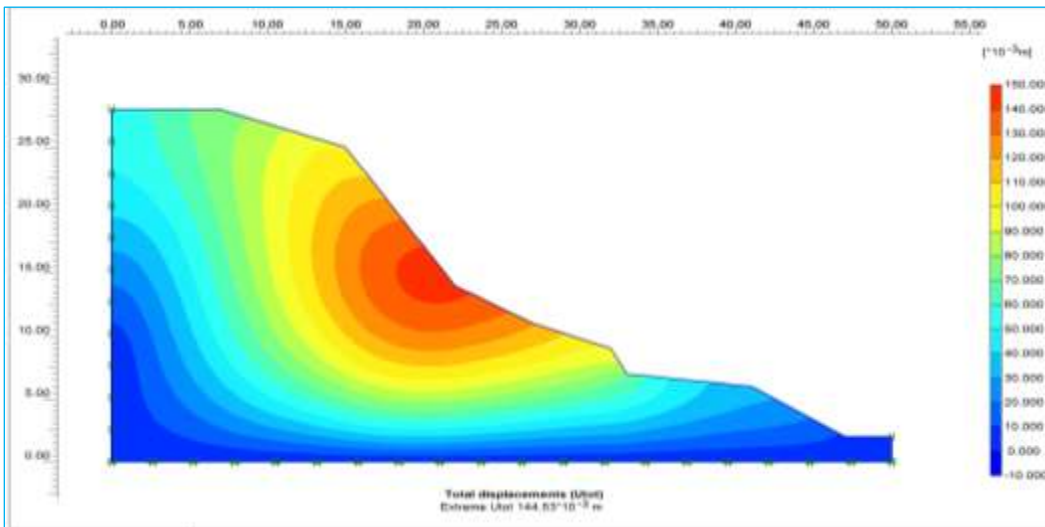
Figure 4.22 Deformation of slope 2 in dry condition
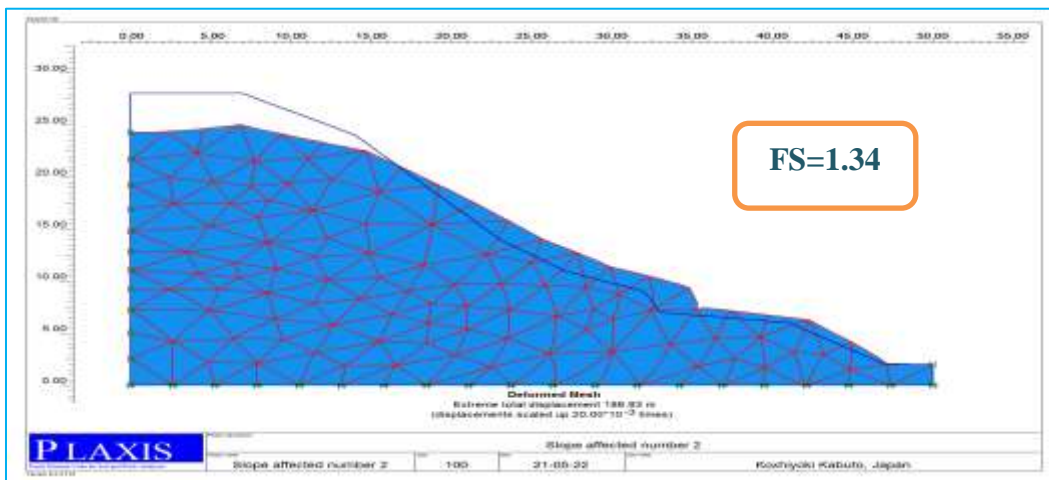
Figure 4.23 Deformed mesh of affected slope 2 when GWT at 5 m below ground surface
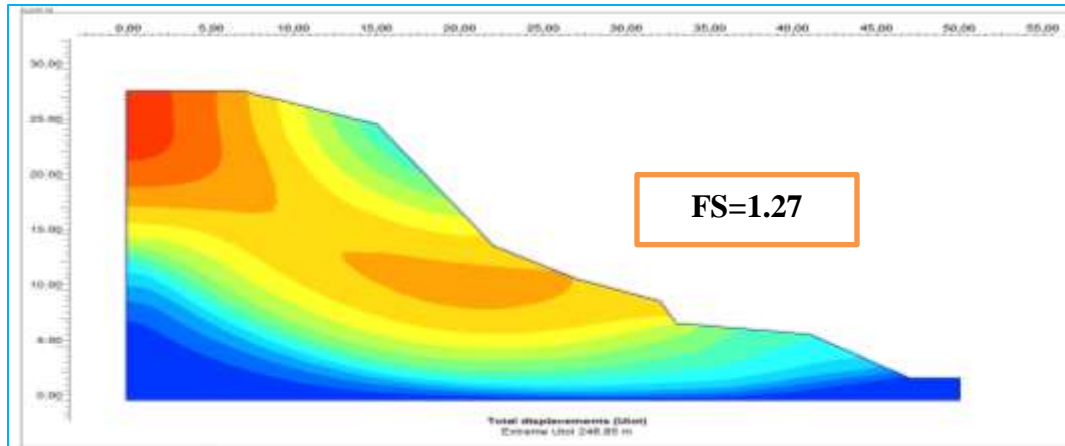
Figure 4.24 Total displacement of affected slope 2 when GWT at 5 m below ground surface

As shown in Figures 4.24 above, the factor of safety of the slopes decreased as the groundwater table level increased. The safety factor has been reduced from 1.95 to 1.27 in dry condition and when GWT at 5 m, respectively. The FS was decreased by 32.92% when the groundwater level raised from great depth to 5 m below ground surface. Similarly, an additional increment in the level of the groundwater in this slope decreases the safety factor. The safety factor due to additional increments of the GWT from great depth to 2 m and 1 m below ground surface was decreased the numerical values of factor of safety by 43.52% and 48.80% respectively.

The deformation analysis for slope 2 reveals that the additional groundwater level from dry condition to partially saturated at 2 m level increases the deformation from 144.53 mm to 95.2 mm by 84.82%.

The slope condition of the unaffected case occurred in very gentle slopes. The slope was located at the border of the town to the west direction and it was almost covered by vegetation due to less population and fewer activities done on this slope. In addition to this, as shown in Figure 4.12 given above, the elevation difference between the affected slope, and slopes located near (un-affected slope) was also have a significant effect. The unaffected slope was located above the affected slope, and moisture moves and stored in affected slopes to increase the pore pressure.

66
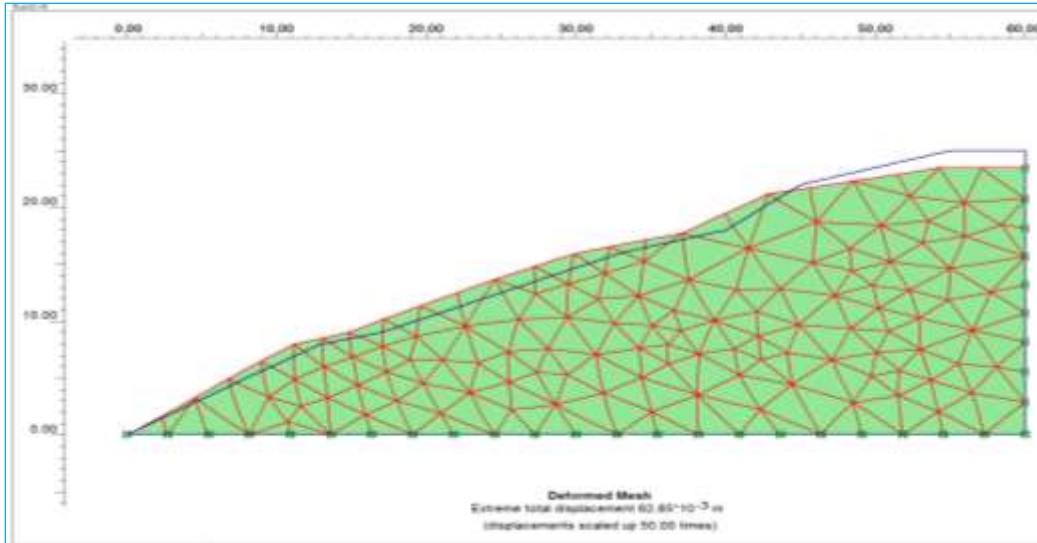
Figure 4.25 Total deformed mesh of unaffected slope for dry condition Condition.

The slope was marginally stable in a saturated conditions and stable for other conditions. Since the area was prone to landslide; much attention should be taken on this slope for future use. Even if the slopes were not failed, the increment of groundwater level in these slopes also decreased the numerical values of the factor of safety.

The FS was decreased from 3.18 in dry condition to 2.52 in partially saturated conditions and further decline to 1.83 in saturated condition. The stability of the slope decreased by 42.39% due to increments in moisture content from dry to saturated condition.
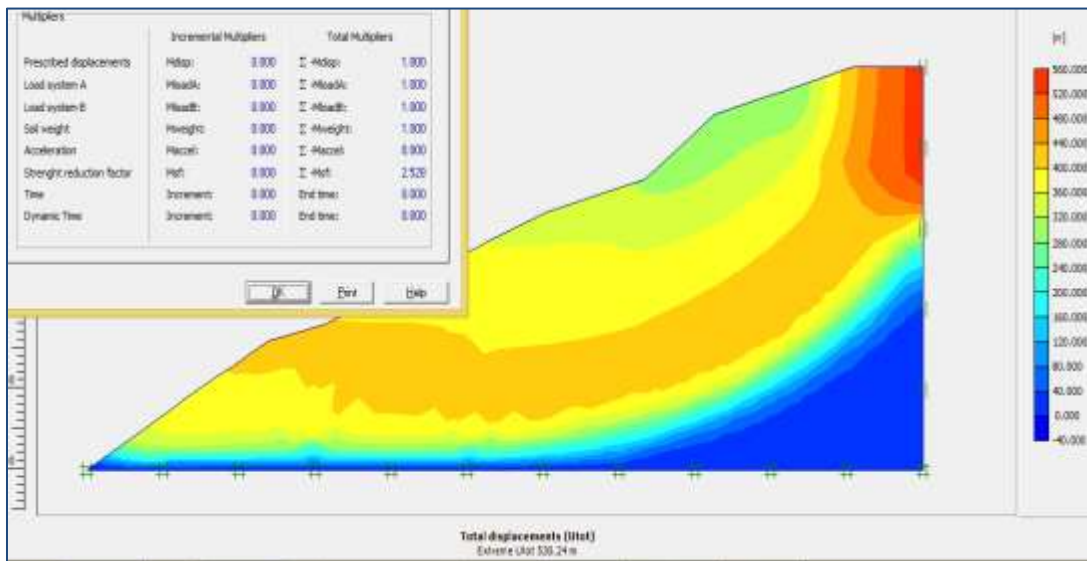
Figure 2Total displacement on slope 3 unaffected for partially saturated condition

The deformation analysis on slope 3 reveals that, the slope was sensative to failure in an increase of moisture content Like the affected slope, the un-affected slope was also sensative to failure in saturated condition. Both factor safety and deformation was affected for variation of grounwater level and addition of surcharge load. Therefore, this slope will have a high probability to failure when construction activities and human settlement become increase.

4.6.2 Stability Analysis Using Slide Software

Among most known LEM analysis approaches, three of them were chosen in this study to analysis stability of the slope in different condtions. Bishop, GLE, and Janbu approaches were chosen in Slide software. The slide software gives us the result of factor of safety and depth of slip surface using method of slice. In this study, the slope analyzed in plaxis software were analyzed for different grounwater conditions.

Table 1Summary of Slope stability results from Slide software

Slope	GWT Condition	Bishop	GLE	Janbu
	Great Depth	1.42	1.48	1.35
S-1	GWT at 10 m	0.98	0.99	0.91
	GWT at 5 m	0.82	0.83	0.77
	GWT at 2 m	0.73	0.73	0.67
	Great Depth	2.06	2.05	1.93
	GWT at 5 m	1.47	1.47	1.39
S-2	GWT at 2 m	1.28	1.28	1.19
	GWT at 1 m	1.23	1.23	1.13
	GWT at Surface	1.18	1.18	1.07
	Great Depth	3.37	3.37	3.17
S-3	GWT at 5 m	2.66	2.66	2.52
	GWT at Surface	2.16	2.16	2.02

As shown in Table 4.11 above, the FS values is different for different groundwater condition. For Slope 1, the minimum FS was decreased for GWT raised from dry condition to 2 m below ground surface by 48.52%, 49.93%, and 47.95% in Bishop, GLE, and Janbumethod respectively. The slide software gives higher values than plaxis software's. All the FS values obtained in dry condition was greater than one. While the FS was reduced in further increases of groundwater level. This results reveals that the mass movement of study area was intiated by rainfall as the result presented during plaxis analysis.
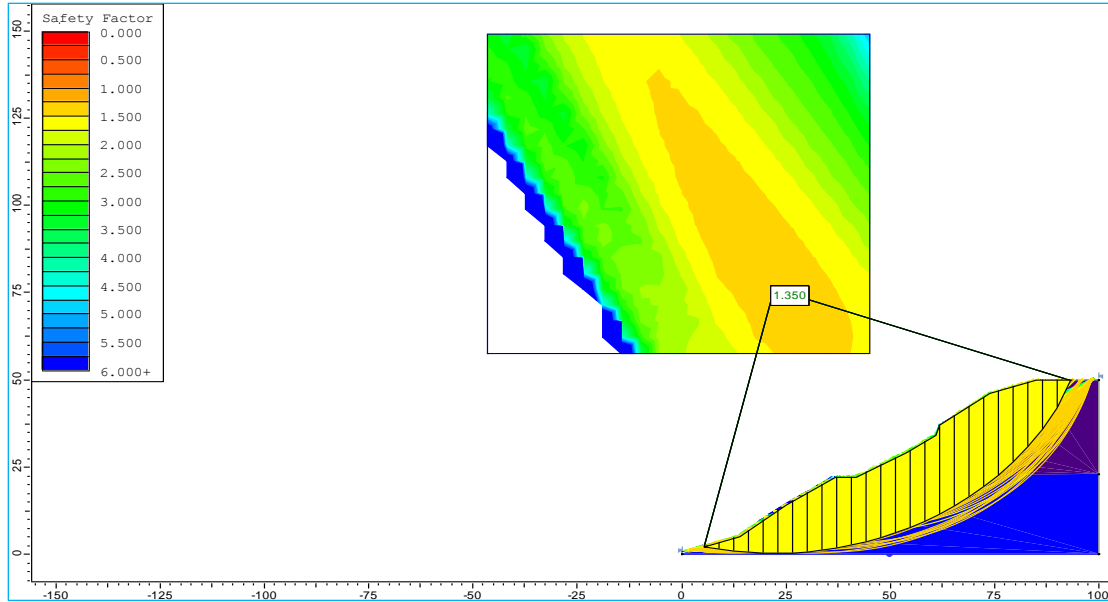
Figure 4.27 Factor of safety of Slope 1 in dry condition

The result from slide software reveals that the FS for slope 2 was decreased when GWT level raised from dry condition to fully saturated condition by 42.72%, 42.50%, and 44.38% in Bishop, GLE, and Janbu methods respectively.
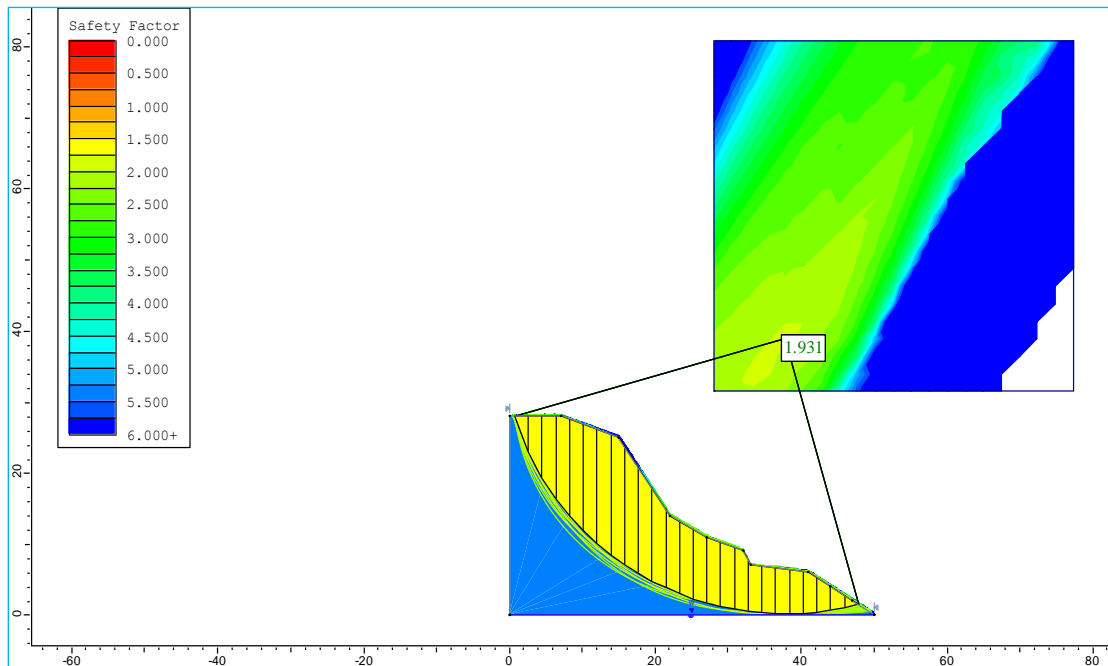
Figure 4.28 Factor of safety of Slope 2 in dry condition

Like the FS obtained from FEM analysis, the FS calculated in LEM for slope 3 was runs between 2.02 to 3.37 for different conditions. Even if the FS of this slope decreased while incresing the

groundwater level, it was stable slope. The decline of numerical values of FS with addition of GWT level indicating that the slope will not be longer stable if proper management not given since the area was landslide susceptible prone areas. For slope 3 the FS decreased from dry condition to fully saturated condition by 35.94%, 35.94%, and 36.18% in Bishop, GLE, and Janbu methods respectively.
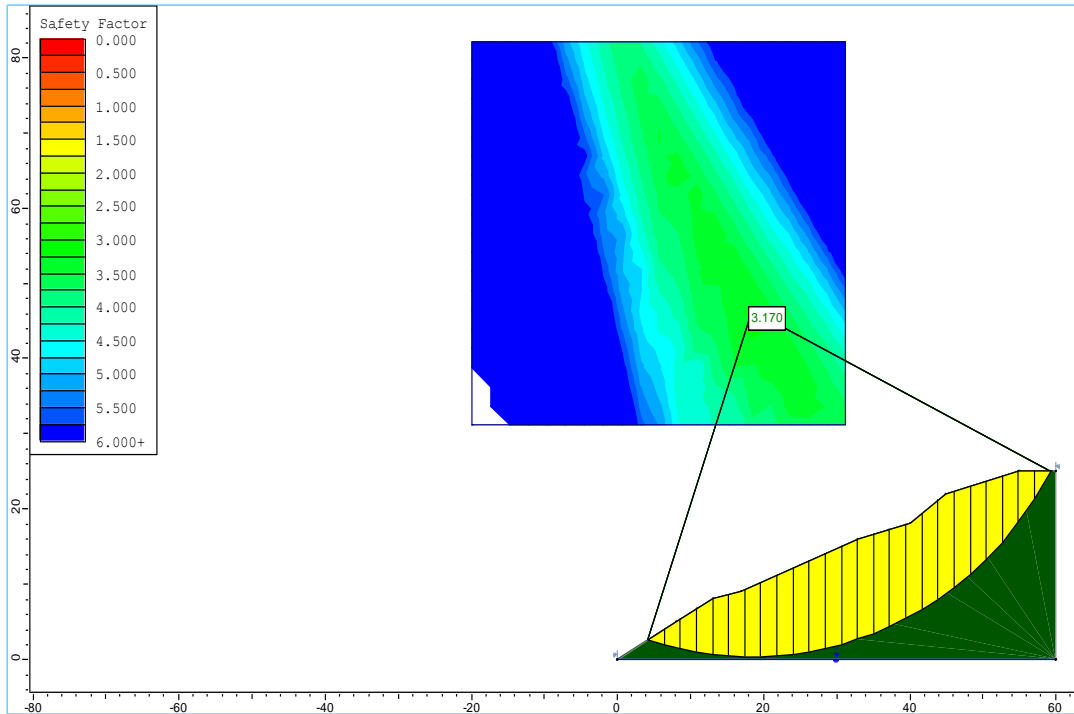
Figure 4.29 Factor of safety of Slope 3 in dry condition

In slope stability analysis FS greater than one are considered as safe slope and FS lessthan one taken as unstable slope. However, FS values greaterthan one can also taken as unsafe slope especially FS between 1 upto 1.5. In every calculation whether by using numerical method or conventional method there is uncertainities from material investigation, the use of boundary conditions, the methods of analysis, and numerical approximation and they can influence the analysis results. Therefore, all the FS obtained from both Plaxis Software and Slide Software's in this study consider the desired stable safety factor 1.5.

The FS obtained from LE analysis was overstimated when compared with FE analysis.The LE (Bishop method) overstimate the FS from 5% - 20% over FE analysis in dry conditions and partially saturated conditions respectively. However, the Janbu method approximately calculate the FS equal with FS calculated from FE methods in Plaxis software's.In saturated conditions due

to LE analysis gives inaccurate compution of stresses and may have resulted with such like FS values differences. Krishna in (2006) compare the values of FS obtained from LE analysis and FE nalysis and conclude that, the FS obtained from LE (M-PH) overstimated from (5-10)% in dry and fully saturated conditions. Hence, this study also agrees with his findings.

4.7 Numerical Validation

In this study, the result obtained from software's (Plaxis 2D and Slide) were validated with the various literatures. The paper published by (Zhang *et al.*, 2013) in Canadian Geotechnical Survey was used for validation of numerical values of this study with other result of investigators. The model and soil properties used to validate this work was originally used by Fredlund and Krahn (1977) and followed by Zhang, (1988). The first authors used 2D while the second author extended to 3D. Since then, various investigators used for validating their works as shown in Table C1 under Appendix C. In this study, the slope geometry with the same material properties was modeled by using plaxis 2D and Slide software's. and the computed FS by both software's were compared with the result of other investigators. Hence, the FS computed in this study shows a good agreement when compared with the result obtained from various investigators. The summary of computed FS in this study and by different investigators was shown in the Figure shown below and the detail presentation of analysis was shown on Appendix C.
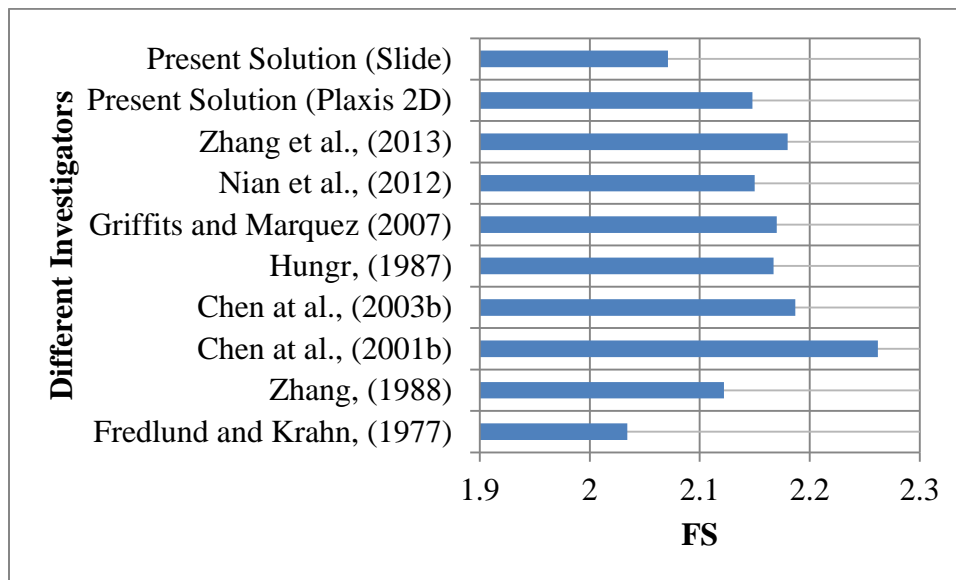
Figure 4.30 Comparision of FS for the same slope with different investigators for Validation

4.8 Proposed Remedial Measures

Based on the site visitation, laboratory test results, and numerical analysis of the slope, the following remedial measures are proposed to prevent or minimize the effects of landslide in the study area.

4.8.1 Design of Surface Drainage

Rainfall is one of the triggering factors of landslides in the study area. Due to rainfall, the groundwater fluctuates and destabilizes the slope as well as decrease the internal strength of earth mass in the study area. As shown on stability analysis (Table 4.10), the numerical value of the factor of safety were decreased as the groundwater level increased and vice versa. Hence, providing appropriate surface drainage used to collect the runoff from the study area and decrease the amount of water seeps in to the sub-surface, thus increase the stability of the slopes. The surface drainage has a low weight and does not increase the driving force of the study area. Therefore, surface drainage is an economic proposed remedial measure for Chira landslide.

4.8.2 Vegetation

Planting Vetiver grass in Chira town is considered as propsed remedial measures. It can penetrate upto 3 m and used as soil reinforcement, which can improve the sher strenth of the soils along the affected slope. In addition to this, vetiver grass has less weight when compared with other vegetations and it cannot increase the driving force if it would used as a soil reinforcement, or as erosion retention material on the slope. Hence, this vegetation can be used as one of mechanisms in which chira town landslide would be safeguard from future faillure.

4.8.2 Land use Management

Based on the site visitation and analysis of landslide causal factors using GIS, expansion of urbanization in Chira town was one of major triggering factors. The slope stability analysis and landslide susceptability Index (Figure,) also reveals that the slopes found at the border of the town, where there is less activities and less human settlement exist was stable slopes. Therefore, appropriate land use management is recommended in the study area to keep this slopes safe as it is now for future. Unless appropriate landuse management applied on this area, all the areas of town have a high probability to be affected more by landslide.

CHAPTER 5

CONCLUSION AND RECOMMENDATION

5.1 CONCLUSION

This study was conducted in Chira town, south-western Ethiopia. During site investigation, it is observed that a large area of Chira town affected by a landslide and cause a lot of damages on infrastructures and natural environment. Hence, the main aim of this study was to indentify the soil type, causal factors, stability condition, and propose remedial measures of landslide of study area. Based on the site visitation, field study, laboratory test results, and stability analysis, the following conclusion was forwarded as a finding of this study. The geophysical test result of the study area showed that there is slightly to a highly fractured volcanic rock, which is overlaid by fine-grained silty and clay soils. Therefore, based on this investigation, the geological sub-surface formation of Chira town has a significant effect on the occurrence of the landslide in this area.

Based on the laboratory test results, all the properties of soils were coincide with the properties of fine-grained soils (Silt and Clay). From grain size analysis test results, above 92.68% of soil types were dominated by fine-grained soils, which have high plasticity and are easily affected during saturation state. The plasticity chart obtained from Atterberg limits tests indicates that the soils from three test pits were falls in highly plastic clays (CH) and the soils from two test pits were falling in highly silt (MH) soils. The type of soil obtained in this study was caharacterized by low permeability. Hence, the difference in permeability of overburdened materials and fractured volcanic rocks at the interface produces the positive pore pressure and initiate the occurrence of landslide in the study area. Based on this study, Soils that are weaker and usually have multiple planes of weakness, characterized by high compressibility and high swelling potential, which deforms like a plastic material were dominated in the study area and they can easily initiate the occurrence of landslide when they saturated and loose their shear strength.

Based on statical biverate frequecny ratio, seven causal factors were analyzed using GIS software. As a result, the prediction rate of causal factors reveals that the soil type, land use, elevation, distance to stream, slope, aspect, and curvature have triggered the occurrence of Chira landslide by 22.03%, 18.89%, 15.75%, 15.46%, 10.87%, 9.7%, and 7.5% respectively. Based

on the site visitation, information gathered from local peoples, and slope stability analysis, the heavy rainfall, which increases the groundwater moisture, was considered as the triggering factors that initiate the landslide of the study area.

The stability analysis of slope was performed by using both Plaxis 2D (FEM) and Slide (LEM) softwares. The numerical values of FS obtained from both methods on three slope show that, for an increase of groundwater table, the FS was decreased. This reveals that the rainfall obtained in the study area was one of the major triggering factors cause the landslide. Therefore, an additional activities like infrastructures may cause additional mass movements in the study area and care should be taken on those slopes. The FS obtained from LE analysis is slightly higher when compared with FE analysis.

Based on the site visitation, laboratory test results, and result of FS of the slope of the study area, surface drainage was a proposed remedial measure to minimize the effects of the landslide of the study area.

Therefore, the soil type of Chira town obtained from laboratory test result and the geophysical test result were clay and silt soils, and they are susceptabile in the occurrence of landslide during heavy rainfall. The high rainfall intensity , soil type, landuse landcover, aspect, elevation, distance from stream, slope angle, and lithological formation are the main causal factors in the occurrence of Chira landslide. The stability condition of the study area was runs from marginally stable to unstable in affected area, and marginally stable to stable condition in unaffected area. To minimize the effect of landslide of Chira town, surface drainage, planting vetiver vegetation, and landuse management were the most proposed remedial measures.

5.2 RECOMMENDATION

Landslide is a damaging phenomenon that can occur in every corner of the world, and engineers give attention to study this problematic situation across the globe. This study also gives its finding for the landslide of the study area. In addition to this, based on this study, the following recommendation was forwarded for other researchers:-

➢ Investigation on the effect of traffic load and other dynamic loads on the stability of slopes of study area.

➢ In-depth investigation on the relationship of rainfall and landslide of south-western Ethiopia

➢ Detail Investigation on the effect of subsurface formation on Chira town landslide

REFERENCES

Abderrahmane, T. H. and Abdelmadjid, B. (2016) 'Assessment of Slope Stability by Continuum and Discontinuum Methods', *Researchgate.Net*, 10(4), pp. 543–548. Available at: https://www.researchgate.net/publication/301689759.

Abebe, B., Dramis, F., Fubelli, G., Mohhammed, U., Asrat, A., (2010) 'Landslides in the Ethiopian highlands and the Rift margins', *Journal of African Earth Sciences*, 56(4–5), pp. 131–138. DOI: 10.1016/j.jafrearsci.2009.06.006.

Acharya, T. D. and Lee, D. H. (2019) 'Landslide Susceptibility Mapping using Relative Frequency and Predictor Rate along Araniko Highway', *KSCE Journal of Civil Engineering*, 23(2), pp. 763–776. doi: 10.1007/s12205-018-0156-x.

Azeze, A. W. (2020) 'Assessments of Geotechnical Condition of Landslide Sites and Slope Stability Analysis Using Limit Equilibrium Method around Gundwin Town Area, Northwestern Ethiopia'. DOI: 10.21203/rs.3.rs-20574/v1.

Broothaerts, N., Kissi, E., Poesen, J., Van Rompae, A., Getahun, K., Van Ranst, E., Diels, J., (2012) 'Spatial patterns, causes and consequences of landslides in the Gilgel Gibe catchment, SW Ethiopia', *Catena*, 97, pp. 127–136. DOI: 10.1016/j.catena.2012.05.011.

BUDHU, M. (2011) *SOIL MECHANICS AND FOUNDATIONS*.

Choi, K. Y. and Cheung, R. W. M. (2013) 'Landslide disaster prevention and mitigation through works in Hong Kong', *Journal of Rock Mechanics and Geotechnical Engineering*, 5(5), pp. 354–365. DOI: 10.1016/j.jrmge.2013.07.007.

Coutinho, R. Q., Silva, M.M., Santos, A. N., Lacererda, W. A., (2019) 'Geotechnical Characterization and Failure Mechanism of Landslide in Granite Residual Soil', *Journal of Geotechnical and Geoenvironmental Engineering*, 145(8), p. 05019004. DOI: 10.1061/(asce)gt.1943-5606.0002052.

Das (2002) *Soil Mechanics*.

Duan, G., Chen, D. and Niu, R. (2019) 'Forecasting groundwater level for soil landslide based on

a dynamic model and landslide evolution pattern', *Water (Switzerland)*, 11(10). DOI: 10.3390/w11102163.

Fisseha, S. and Mewa, G. (2016) 'Road failure caused by landslide in north Ethiopia: A case study from Dedebit - Adi-Remets road segment', *Journal of African Earth Sciences*, 118, pp. 65–74. DOI: 10.1016/j.jafrearsci.2016.02.022.

Forbes, K. and Broadhead, J. (2013) 'I3245E.Pdf'. Available at: http://www.fao.org/docrep/016/ba0126e/ba0126e00.htm%5Cnhttp://www.fao.org/docrep/016/ba0126e/ba0126e00.pdf.

Gaurina-Medjimurec, N. (2014) *Handbook of research on advancements in environmental engineering*, *Handbook of Research on Advancements in Environmental Engineering*. DOI: 10.4018/978-1-4666-7336-6.

Geertsema, M. and Highland, L. M. (2011) 'Landslides: Human Health Effects', *Encyclopedia of Environmental Health*, (December), pp. 380–395. DOI: 10.1016/B978-0-444-52272-6.00550-X.

Geertsema, M., Highland, L. and Vaugeouis, L. (2009) 'Environmental impact of landslides', *Landslides - Disaster Risk Reduction*, (1), pp. 589–607. DOI: 10.1007/978-3-540-69970-5_31.

Girma, F., Raghuvanshi, T. K., Ayenew, T., Hailamariam, T., (2015) 'Landslide hazard zonation in Ada Berga District, Central Ethiopia – A GIS based statistical Approach', *J.ournal of Geomatics*, 90(1), pp. 25–38.

Hamza, T. and Raghuvanshi, T. K. (2016) 'GIS based landslide hazard evaluation and zonation – A case from Jeldu District, Central Ethiopia', *Journal of King Saud University - Science*. DOI: 10.1016/j.jksus.2016.05.002.

Hearn, G. J. (2019) 'Slope hazards on the ethiopian road network', *Quarterly Journal of Engineering Geology and Hydrogeology*, 52(3), pp. 295–311. DOI: 10.1144/qjegh2018-058.

Highland, L. M. and Bobrowsky, P. (2008) 'The landslide Handbook - A guide to understanding landslides', *US Geological Survey Circular*, (1325), pp. 1–147. DOI: 10.3133/cir1325.

Hulagabali, A., Gudissa, D. and Ararsa, W. (2008) 'Analysis of Landslide near Ambo City,

Ethiopia, East Africa', *International Research Journal of Engineering and Technology*, 513, pp. 513–517. Available at: www.irjet.net.

J.Crozier, T. G. and M. (2004) 'Part 1 Conceptual Models in Approaching', in.

Jacob, A., Thomas, A. A., G Nath, A., MP, A., (2018) 'Slope Stability Analysis Using Plaxis 2D', *International Research Journal of Engineering and Technology*, pp. 3666–3668.

Kabeta, W. F. and Teshager, D. K. (2020) 'Assessments of Geotechnical Conditions and Slope Stability Analysis : Case Study in Gedo town , Ethiopia', 6(3), pp. 1250–1258.

Liu, J., Yang, Ch., Gan, J., Liu, Y., Wei, Liu., Xie, Q., (2017) 'Stability Analysis of Road Embankment Slope Subjected to Rainfall Considering Runoff-Unsaturated Seepage and Unsaturated Fluid–Solid Coupling', *International Journal of Civil Engineering*, 15(6), pp. 865–876. DOI: 10.1007/s40999-017-0194-7.

Lollino, G., Manconi, A., Clague, J., Shan, W., Chiarle, M., (2015) 'Engineering geology for society and territory – Volume 2: Landslide processes', *Engineering Geology for Society and Territory - Volume 2: Landslide Processes*, (July 2020), pp. 1–2177. DOI: 10.1007/978-3-319-09057-3.

Marwa Mostafa, Amr Radwan, and M. B. (2016) 'Application of electrical resistivity in site investigation', (December 2015).

McColl, S. T. (2015) *Landslide Causes and Triggers*, *Landslide Hazards, Risks, and Disasters*. Elsevier Inc. DOI: 10.1016/B978-0-12-396452-6.00002-1.

Mia, M., Sultana, N. and Paul, A. (2016) 'Studies on the Causes, Impacts and Mitigation Strategies of Landslide in Chittagong city, Bangladesh', *Journal of Environmental Science and Natural Resources*, 8(2), pp. 1–5. DOI: 10.3329/jesnr.v8i2.26854.

Mr. Digvijay P. Salunkhe., Ms. Rupa N. Bartake., Ms. Poja. R. Kathavale., Chvan, G., (2017) 'An Overview on Methods for Slope Stability Analysis', *International Journal of Engineering Research and*, V6(03), pp. 528–535. DOI: 10.17577/ijertv6is030496.

Nelson, S. A. (2013) 'Slope Stability, Triggering Events, Mass Movement Hazards', *EENS 3050*

Natural Disasters Tulane University, pp. 1–17.

OCHA, N. (2020) 'Ethiopia: 2020 kiremt weather outlook, Floods Update No.3 as Of 18 August 2020 .', (3), pp. 1–5.

Patra, P. and Devi, R. (2018) 'Assessment, prevention and mitigation of landslide hazard in the Lesser Himalaya of Himachal Pradesh', *Environmental & Socio-economic Studies*, 3(3), pp. 1–11. DOI: 10.1515/environ-2015-0062.

Popescu, M. E. and Sasahara, K. (2009) 'Engineering measures for landslide disaster mitigation', *Landslides - Disaster Risk Reduction*, pp. 609–631. DOI: 10.1007/978-3-540-69970-5_32.

Senouci, O. (2020) 'Mining : A Key Human Cause of Landslides', *International Research Journal of Engineering and Technology (IRJET)*, 07(04), pp. 6604–6606.

Serdarevic, A. and Babic, F. (2019) 'Landslide Causes and Corrective Measures – Case Study of the Sarajevo Canton', 9(2), pp. 51–57. DOI: 10.5923/j.jce.20190902.02.

Shano, L., Raghuvanshi, T. K. and Meten, M. (2020) 'Landslide susceptibility evaluation and hazard zonation techniques – a review', *Geoenvironmental Disasters*, 7(1). DOI: 10.1186/s40677-020-00152-0.

Sharma, A. and Ram, S. (2014) 'A Review on Effects of Deforestation on Landslide: Hill Areas', *IJSRD -International Journal for Scientific Research & Development|*, 2(07online), pp. 2321–613. Available at: www.ijsrd.com.

Sharma, A., Ram, S. and Arabia, W. A. (2014) 'Deforestation and its Effect on Landslides', 2(10), pp. 102–118.

Silalahi, F. E. S., Pamela., Arifanti, Y., Hidayat. F., (2019) 'Landslide susceptibility assessment using frequency ratio model in Bogor, West Java, Indonesia', *Geoscience Letters*, 6(1). DOI: 10.1186/s40562-019-0140-4.

Tsige, D., Quezon, P. E. T. and Woldearegay, K. (2017) 'Geotechnical Conditions and Stability Analysis of Landslide Prone Area: A Case Study in Bonga Town, South-Western Ethiopia', 8(4).

Walker, L. R. and Shiels, A. B. (2013) 'Chapter 4 Biological consequences for Landslide

Ecology', *Landslide Ecology*, pp. 46–82.

Wang, G. and Sassa, K. (2003) 'Pore-pressure generation and movement of rainfall-induced landslides: Effects of grain size and fine-particle content', *Engineering Geology*, 69(1–2), pp. 109–125. DOI: 10.1016/S0013-7952(02)00268-5.

Winter, M. G*.,* Shearer, B., Palmer, D., Peeling, D., Harmer, C., Sharpe., (2016) 'The Economic Impact of Landslides and Floods on the Road Network', *Procedia Engineering*, 143(Ictg), pp. 1425–1434. DOI: 10.1016/j.proeng.2016.06.168.

Woldearegay, K. (2013) 'Review of the occurrences and influencing factors of landslides in the highlands of Ethiopia: With implications for infrastructural development', *Momona Ethiopian Journal of Science*, 5(1), p. 3. DOI: 10.4314/mejs.v5i1.85329.

Yifru, B. A. and Ayehu, F. M. (2017) 'Prediction of Groundwater Level Fluctuation towards Rainfall Induced Landslide: Case of Blue Nile Gorge, Central Ethiopia', *Open Journal of Modern Hydrology*, 07(04), pp. 274–297. DOI: 10.4236/ojmh.2017.74016.

Zhang, Y., Chen, G., Zheng, L., Li, Y., Zhuang, X., (2013) 'Effects of geometries on three-dimensional slope stability Abstract ':, pp. 1–44.

Zumpano, V., Piano, L., Malek, Z., Micu, M., Aucelli, P.P.C., Rosskof, C. M., Balteanu, D., Parise, M., (2018) 'Economic Losses for Rural Land Value Due to Landslides Economic Losses for Rural Land Value Due to Landslides', (July). DOI: 10.3389/feart.2018.00097.

Appendix A. Labooratory Test Results

A1. Natural Moisture Content Determination Results

Sample Description: Clay and Silt

Standard Test Method: ASTM D 2216 Standard Method

Table A1.1Datasheet for natural moisture content determination for Test Pit 1@1.5m

Depth of Sample	1.5m	1.5m	1.5m
Container Number	IIA	G2	A3
Mass of Can (g)	16.01	17.04	17.54
Mass of Wet soil + Can (g)	63.92	63.06	60.81
Mass of Dry soil + Can (g)	49.32	48.96	47.82
Mass of Water (g)	14.6	14.1	12.99
Mass of Dry Soil (g)	33.31	31.92	30.28
Moisture content	43.83	44.17	42.90
Average Moisture content	43.63		

Table A1.2 Datasheet for natural moisture content determination for Test Pit 1@2.8m

Depth of Sample	2.8m	2.8m	2.8m
Container Number	A36	G3	4-Z
Mass of Can (g)	17.73	16.46	23.4
Mass of Wet soil + Can (g)	61.44	41.76	52.3
Mass of Dry soil + Can (g)	47.42	33.51	43.01
Mass of Water (g)	14.02	8.25	9.29
Mass of Dry Soil (g)	29.69	17.05	19.61
Moisture content	47.22	48.39	47.37
Average Moisture content	47.66		

Table A1.3 Datasheet for natural moisture content determination for Test Pit 2@2.4m

Depth of Sample	2.4m	2.4m	2.4m
Container Number	FT2	B3	4-G
Mass of Can (g)	17.67	17.44	18.5
Mass of Wet soil + Can (g)	54.17	63.22	60.54
Mass of Dry soil + Can (g)	44.22	51.01	49.26
Mass of Water (g)	9.95	12.21	11.28
Mass of Dry Soil (g)	26.55	33.57	30.76
Moisture content	37.48	36.37	36.67
Average Moisture content	36.84		

Table A1.4 Datasheet for natural moisture content determination for Test Pit 3@1.5m

Depth of Sample	1.5m	1.5m	1.5m
Container Number	RW	S2	W11
Mass of Can (g)	17.21	16.54	5.87
Mass of Wet soil + Can (g)	63.16	58.34	63.54
Mass of Dry soil + Can (g)	50.05	46.81	47.66
Mass of Water (g)	13.11	11.53	15.88
Mass of Dry Soil (g)	32.84	30.27	41.79
Moisture content	39.92	38.09	38.00
Average Moisture content	38.67		

Table A1.5 Datasheet for natural moisture content determination for Test Pit 3@2.4m

Depth of Sample	2.4m	2.4m	2.4m
Container Number	P5	D3	A4
Mass of Can (g)	17.22	18.64	17.42
Mass of Wet soil + Can (g)	53.02	74.92	51.62
Mass of Dry soil + Can (g)	42.85	58.62	41.84
Mass of Water (g)	10.17	16.3	9.78
Mass of Dry Soil (g)	25.63	39.98	24.42
Moisture content	39.68	40.77	40.05
Average Moisture content	40.17		

Table A1.6 Datasheet for natural moisture content determination for Test Pit 4@2.7m

Depth of Sample	2.7m	2.7m	2.7m
Container Number	C-12	G21	IC
Mass of Can (g)	16.36	19.92	19.33
Mass of Wet soil + Can (g)	50.23	57.83	52.18
Mass of Dry soil + Can (g)	40.15	46.47	42.24
Mass of Water (g)	10.08	11.36	9.94
Mass of Dry Soil (g)	23.79	26.55	22.91
Moisture content	42.37	42.79	43.39
Average Moisture content	42.85		

Table A1.7 Datasheet for natural moisture content determination for Test Pit 5@2m

Depth of Sample	2.0m	2.0m	2.0m
Container Number	G3T2	A6-3	B-12
Mass of Can (g)	18.01	17.12	16.6
Mass of Wet soil + Can (g)	52.04	58.35	52.18
Mass of Dry soil + Can (g)	42.47	46.37	42.17
Mass of Water (g)	9.57	11.98	10.01
Mass of Dry Soil (g)	24.46	29.25	25.57
Moisture content	39.13	40.96	39.15
Average Moisture content	39.74		

Table A1.8 Datasheet for natural moisture content determination for Test Pit 5@2.7m

Depth of Sample	2.7m	2.7m	2.7m
Container Number	SSB	29X	P4-C
Mass of Can (g)	18.03	17.47	17.29
Mass of Wet soil + Can (g)	85.3	63.63	50.94
Mass of Dry soil + Can (g)	65.72	50.43	41.16
Mass of Water (g)	19.58	13.2	9.78
Mass of Dry Soil (g)	47.69	32.96	23.87
Moisture content	41.06	40.05	40.97
Average Moisture content	40.69		

A2.Specific Gravity Determination Results

Project Name:Chira Town Landslide

Depth: 1.5-2.8m

Sample Description: Clay and Silt

Standard Test Method: ASTM D 854-00 Standard Method

Table A2.1 Datasheet for specifiv gravity determination for Test Pit 1@1.5m

Sample depth		1.5 m	1.5m	1.5m
Pycnometer Code		A11	M2T	D45
Mass of Pycnometer, Mp		22.52	27.17	27.47
Mass of Pycnometer + Soil, Mps		42.52	47.17	47.47
Mass of Pycnometer + Soil + Water, Mpws		130.64	132.15	133.54
Mass of Pycnometer + Water, Mpw @ Ti		118	119.54	120.83
The water temprature, Ti		26	26	26
Temperature of contents of Pycnometer When Mpws was taken, Tx		23	23	23
Mass of Dry Soil, Ms		20	20	20
Density of water at Ti,	ρ_W @ Ti	0.99681	0.99681	0.99681
Density of water at Tx	ρ_W @ Tx	0.99757	0.99757	0.99757
Mpw (@Tx)=[ρW @ Tx]		118.0728	119..6104	120.9012
Conversion factor, K		0.9993	0.9993	0.9993
Specific Gravity, @ 20°C		2.69	2.68	2.72
			2.69	

Table A2.2 Datasheet for specifiv gravity determination for Test Pit 1@2.8m

Sample depth		2.8 m	2.8m	2.8m
Pycnometer Code		A03	T2	G07
Mass of Pycnometer, Mp		27.00	25.47	27.04
Mass of Pycnometer + Soil, Mps		47	45.47	47.04
Mass of Pycnometer + Soil + Water, Mpws		133.92	130.18	134.21
Mass of Pycnometer + Water, Mpw @ Ti		121.48	117.71	121.69
The water temprature, Ti		26	26	25
Temperature of contents of Pycnometer When Mpws was taken, Tx		27	28	27
Mass of Dry Soil, Ms		20	20	20
Density of water at Ti,	ρ_W @ Ti	0.99681	0.99681	0.99681
Density of water at Tx	ρ_W @ Tx	0.99654	0.99626	0.99654
Mpw (@Tx)=[ρW @ Tx]		121.4544	117.6591	121.6644
Conversion factor, K		0.9983	0.998	0.9983
Specific Gravity, @ 20°C		2.65	2.67	2.68
			2.67	

Table A2.3 Datasheet for specifiv gravity determination for Test Pit 2@2.4m

Sample depth		2.4 m	2.4m	2.4m
, Mp Pycnometer Code		G07	A03	T2
Mass of Pycnometer		27.04	27.00	25.47
Mass of Pycnometer + Soil, Mps		47.04	47	45.47
Mass of Pycnometer + Soil + Water, Mpws		133.13	134.15	133.55
Mass of Pycnometer + Water, Mpw @ Ti		120.59	121.48	120.89
The water temprature, Ti		26	26	26
Temperature of contents of Pycnometer When Mpws was taken, Tx		24	24	24
Mass of Dry Soil, Ms		20	20	20
Density of water at Ti,	ρ_W @ Ti	0.99681	0.99681	0.99681
Density of water at Tx	ρ_W @ Tx	0.99732	0.99732	0.99732
Mpw (@Tx)=[ρW @ Tx]		120.5878	121.5283	120.9388
Conversion factor, K		0.9991	0.9991	0.9991
Specific Gravity, @ 20°C		2.68	2.71	2.70
			2.70	

Table B4 Datasheet for specifiv gravity determination for Test Pit 3@1.5m

Sample depth		1.5 m	1.5m	1.5m
Mass of Pycnometer, Mp		22.52	27.47	27.17
Mass of Pycnometer + Soil, Mps		42.52	47.47	47.17
Mass of Pycnometer + Soil + Water, Mpws		132.03	131.95	133.45
Mass of Pycnometer + Water, Mpw @ Ti		119.1	119.05	120.54
The water temprature, Ti		26	26	26
Temperature of contents of Pycnometer When Mpws was taken, Tx		24	24	24
Mass of Dry Soil, Ms		20	20	20
Density of water at Ti,	ρ_W @ Ti	0.99681	0.99681	0.99681
Density of water at Tx	ρ_W @ Tx	0.99732	0.99732	0.99732
Mpw (@Tx)=[ρW @ Tx]		119.1494	119.0969	120.5878
Conversion factor, K		0.9991	0.9991	0.9991
Specific Gravity, @ 20°C		2.81	2.80	2.80
			2.80	

Table B5 Datasheet for specifiv gravity determination for Test Pit 3@2.4m

Sample depth		2.4 m	2.4m	2.4m
Mass of Pycnometer, Mp		27.17	22.52	27.47
Mass of Pycnometer + Soil, Mps		47.17	42.52	47.47
Mass of Pycnometer + Soil + Water, Mpws		130.58	133.61	133.18
Mass of Pycnometer + Water, Mpw @ Ti		118	120.83	120.54
The water temprature, Ti		26	26	26
Temperature of contents of Pycnometer When Mpws was taken, Tx		28	28	28
Mass of Dry Soil, Ms		20	20	20
Density of water at Ti,	ρ_W @ Ti	0.99681	0.99681	0.99681
Density of water at Tx	ρ_W @ Tx	0.99626	0.99626	0.99626
Mpw (@Tx)=[ρW @ Tx]		117.9499	125.773	123.487
Conversion factor, K		0.9986	0.9986	0.9986
Specific Gravity, @ 20°C		2.71	2.79	2.73
			2.74	

Table B6 Datasheet for specifiv gravity determination for Test Pit 4@2.7m

Sample depth		2.7 m	2.7m	2.7m
Mass of Pycnometer, Mp		27.00	25.47	27.04
Mass of Pycnometer + Soil, Mps		47.00	45.47	47.04
Mass of Pycnometer + Soil + Water, Mpws		133.93	130.32	134.22
Mass of Pycnometer + Water, Mpw @ Ti		121.48	117.71	121.69
The water temprature, Ti		26	26	26
Temperature of contents of Pycnometer When Mpws was taken, Tx		28	28	28
Mass of Dry Soil, Ms		20	20	20
Density of water at Ti,	ρ_W @ Ti	0.99681	0.99681	0.99681
Density of water at Tx	ρ_W @ Tx	0.99626	0.99626	0.99626
Mpw (@Tx)=[ρ_W @ Tx]		121.4279	117.6591	121.6378
Conversion factor, K		0.9986	0.9986	0.9986
Specific Gravity, @ 20°C		2.66	2.72	2.69
			2.69	

Table B7 Datasheet for specifiv gravity determination for Test Pit 5@2m

Sample depth		2 m	2m	2m
Mass of Pycnometer, Mp		27.00	25.47	27.04
Mass of Pycnometer + Soil, Mps		47	45.47	47.04
Mass of Pycnometer + Soil + Water, Mpws		133.85	130.64	134.38
Mass of Pycnometer + Water, Mpw @ Ti		121.13	117.91	121.69
The water temprature, Ti		26	26	26
Temperature of contents of Pycnometer When Mpws was taken, Tx		25	25	25
Mass of Dry Soil, Ms		20	20	20
Density of water at Ti,	ρ_W @ Ti	0.99681	0.99681	0.99681
Density of water at Tx	ρ_W @ Tx	0.99707	0.99707	0.99707
Mpw (@Tx)=[ρ_W @ Tx]		121.1546	117.9341	121.7147
Conversion factor, K		0.9988	0.9988	0.9988
Specific Gravity, @ 20°C		2.73	2.74	2.72
			2.73	

Table B8 Datasheet for specifiv gravity determination for Test Pit 5@2.7m

Sample depth		2.7 m	2.7m	2.7m
Mass of Pycnometer, Mp		27.17	22.52	27.47
Mass of Pycnometer + Soil, Mps		47.17	42.52	47.47
Mass of Pycnometer + Soil + Water, Mpws		134.35	130.87	133.63
Mass of Pycnometer + Water, Mpw @ Ti		121.54	118.00	120.83
The water temprature, Ti		26	26	25
Temperature of contents of Pycnometer When Mpws was taken, Tx		27	27	27
Mass of Dry Soil, Ms		20	20	20
Density of water at Ti,	ρ_W @ Ti	0.99681	0.99681	0.99681
Density of water at Tx	ρ_W @ Tx	0.99654	0.99654	0.99654
Mpw (@Tx)=[ρ_W @ Tx]		123.5139	117.9741	125.8034
Conversion factor, K		0.9983	0.9983	0.9983
Specific Gravity, @ 20°C		2.79	2.81	2.78
			2.79	

A3. Sieve Size Analysis Results

A3.1. Wet Seive Analysis Results

Project Name:Chira Town Landslide

Depth: 1.5-2.8m

Sample Description: Clay and Silt

Standard Test Method: ASTM D 854-00 Standard Method

A3.2. Hydrometer Analysis Results

Sample Description: Clay and Silt

Depth: 1.5-2.8m

Standard Test Method: ASTM D 854-00 Standard Method

Dispersing Agent: Sodium Metahexaphosphate

Hydrometer Number: 152H

Table A3.1.1 Datasheet for wet seive analysis for test Pit 1 at 1.5 and 2.8m

	SS, (mm)	MR, (g)	% R	% CR	% P		SS, (mm)	MR, (g)	% R	% CR	% P
Test Pit 1 @ 1.5m	9.5	0.5	0.1	0.1	99.9	Test Pit 1 @ 2.8m	9.5	0	0	0	100
	4.75	0.2	0.04	0.14	99.86		4.75	0	0	0	100
	2	2.1	0.42	0.56	99.44		2	2.3	0.46	0.46	99.54
	0.85	1.29	0.25	0.82	99.18		0.85	2.1	0.42	0.88	99.12
	0.425	0.95	0.19	1.01	98.99		0.425	2.5	0.5	1.38	98.62
	0.25	1.19	0.24	1.25	98.75		0.25	3.6	0.72	2.1	97.9
	0.15	1.23	0.25	1.49	98.51		0.15	3.2	0.64	2.74	97.26
	0.075	1.38	0.28	1.77	98.23		0.075	2.5	0.5	3.24	96.76
	Pan	491.1	98.23	100	0		Pan	483.8	96.76	100	0

SS= Sieve Size, MR= Mass Retained, %R= Percentage of Retained, %CR= Cumulative Percentage of Retained, %P= Percentage of Pass, g= gram, No. =Numb

Table A3.1.2 Datasheet for wet seive analysis for test Pit 2 at 2.4m and test pit 3 at1.5m

	SS, (mm)	MR, (g)	% R	% CR	% P		SS, (mm)	MR, (g)	% R	% CR	% P
Test Pit 2 @ 2.4m	9.5	0	0	0	100	Test Pit 3 @1.5m	9.5	0	0	0	100
	4.75	0.6	0.12	0.12	99.88		4.75	4.4	0.88	0.88	99.12
	2	4.5	0.9	1.02	98.98		2	8.1	1.62	2.5	97.5
	0.85	2.5	0.5	1.52	98.48		0.85	4.1	0.82	3.32	96.68
	0.425	1.1	0.22	1.74	98.26		0.425	3.0	0.6	3.92	96.08
	0.25	1.1	0.22	1.96	98.04		0.25	3.4	0.68	4.6	95.4
	0.15	0.3	0.06	2.02	97.98		0.15	2.3	0.46	5.06	94.94
	0.075	1.6	0.32	2.34	97.66		0.075	1.87	0.374	5.43	94.57
	Pan	488.3	97.66	100	0		Pan	472.83	94.566	100	0

SS= Sieve Size, MR= Mass Retained, %R= Percentage of Retained, %CR= Cumulative Percentage of Retained, %P= Percentage of Pass, g= gram, No. =Number

Table A3.1.3 Datasheet for wet seive analysis for test Pit 3 at 2.4m and test pit 4 at 2.7 m

	SS, (mm)	MR, (g)	% R	% CR	% P		SS, (mm)	MR, (g)	% R	% CR	% P
Test Pit 3 @2.4m	9.5	0	0	0	100	Test Pit 4 @ 2.7m	9.5	1.09	0.218	0.218	99.782
	4.75	2.6	0.52	0.52	99.48		4.75	3.96	0.792	1.01	98.99
	2	6.6	1.32	1.84	98.16		2	14.96	2.992	4.00	96
	0.85	5.3	1.06	2.9	97.1		0.85	6.76	1.352	5.35	94.65
	0.425	4.6	0.92	3.82	96.18		0.425	4.18	0.836	6.19	93.81
	0.25	3.2	0.64	4.46	95.54		0.25	1.56	0.312	6.50	93.50
	0.15	2.5	0.5	4.96	95.04		0.15	2.96	0.592	7.09	92.91
	0.075	1.8	0.36	5.32	94.68		0.075	1.11	0.222	7.32	92.68
	Pan		94.68	100	0		Pan	463.42	92.68	100	0

SS= Sieve Size, MR= Mass Retained, %R= Percentage of Retained, %CR= Cumulative Percentage of Retained, %P= Percentage of Pass, g= gram, No. =Number

Table A3.1.4 Datasheet for wet seive analysis for test Pit 5 at 2 and 2.7 m.

	SS, (mm)	MR, (g)	% R	% CR	% P		SS, (mm)	MR, (g)	% R	% CR	% P
Test Pit 5 @2m	9.5	1.0	0.2	0.2	99.8	Test Pit 5 @ 2.7m	9.5	0	0	0	100
	4.75	3.0	0.6	0.8	99.2		4.75	0.5	0.1	0.1	99.9
	2	1.40	0.28	1.08	98.92		2	0.5	0.1	0.2	99.8
	0.85	0.70	0.14	1.22	98.78		0.85	1.1	0.22	0.42	99.58
	0.425	1.0	0.2	1.42	98.58		0.425	1.3	0.26	0.68	99.32
	0.25	0.6	0.12	1.54	98.46		0.25	1.5	0.3	0.98	99.02
	0.15	0.6	0.12	1.66	98.34		0.15	1.25	0.25	1.23	98.77
	0.075	1.1	0.22	1.88	98.12		0.075	1.11	0.22	1.45	98.55
	Pan	490.6	98.12	100	0		Pan	492.74	98.55	100	0

SS= Sieve Size, MR= Mass Retained, %R= Percentage of Retained, %CR= Cumulative Percentage of Retained, %P= Percentage of Pass, g= gram, No. =Number

A3.2. Data sheet for Hydrometer Analysis
Sample Description: Clay and Silt
Depth: 1.5-2.8 m

Standard Test Method: ASTM D 854-00 Standard Method

Dispersing Agent: Sodium Metahexaphosphate

Hydrometer Number: 152H

Specific Gravity: 2.69

Table A3.2.1Datasheet for Hydrometer analysis for Test Pit 1 at 1.5 m.

Time (minutes)	HR	T(°C)	CHR		Cf (a)	EDR (L)	K	DSP (mm)	% P
			R'	R"					
0.5	48	23	49	42.7	0.991	8.3	0.01301	0.053	76.84
1	47	23	48	41.7	0.991	8.4	0.01301	0.038	75.04
2	46.5	23	47.5	41.2	0.991	8.5	0.01301	0.027	74.14
4	45.5	23	46.5	40.2	0.991	8.7	0.01301	0.019	72.34
8	44	23	45	38.7	0.991	8.9	0.01301	0.014	69.64
15	42	23	43	36.7	0.991	9.2	0.01301	0.010	66.04
30	41	23	42	35.7	0.991	9.4	0.01301	0.007	64.24
60	39	23	40	33.7	0.991	9.7	0.01301	0.005	60.64
120	37	23	38	31.7	0.991	10.1	0.01301	0.004	57.04
240	35	23	36	30.2	0.991	10.4	0.01301	0.003	53.44
480	32	23	33	27.7	0.991	10.9	0.01301	0.002	48.05
1440	29.5	23	30.5	24.7	0.991	11.3	0.01301	0.001	43.55

HR = Hydrometer reading, T = Temperature, CHR = Corrected hydrometer reading, Cf = Corrected factor, EDR = Effective depth reading, DSP = Diameter of soil particle and % P = percentage of fine.

Sample Description: Clay and Silt
Depth: 1.5-2.8 m

Standard Test Method: ASTM D 854-00 Standard Method

Dispersing Agent: Sodium Metahexaphosphate

Hydrometer Number: 152H

Specific Gravity: 2.67

Table A3.2.2 Datasheet for Hydrometer analysis for Test Pit 1 at 2.8 m.

Time (minutes)	HR	T(°C)	CHR		Cf (a)	EDR (L)	K	DSP (mm)	% P
			R'	R"					
0.5	50	23	51	44.7	0.995	7.9	0.01309	0.052	80.79
1	48	23	49	42.7	0.995	8.3	0.01309	0.038	77.18
2	47.5	23	48.5	42.2	0.995	8.3	0.01309	0.027	76.28
4	45.5	23	46.5	40.2	0.995	8.7	0.01309	0.019	72.66
8	43	23	44	37.7	0.995	9.1	0.01309	0.014	68.14
15	41	23	42	35.7	0.995	9.4	0.01309	0.010	64.53
30	39.5	23	40.5	34.2	0.995	9.7	0.01309	0.007	61.82
60	38	23	39	32.7	0.995	9.9	0.01309	0.005	59.10
120	36	23	37	30.7	0.995	10.2	0.01309	0.004	55.49
240	34.5	23	35.5	29.2	0.995	10.5	0.01309	0.003	52.78
480	32	23	33	26.7	0.995	10.9	0.01309	0.002	48.26
1440	30	23	31	24.7	0.995	11.2	0.01309	0.001	44.64

HR = Hydrometer reading, T = Temperature, CHR = Corrected hydrometer reading, Cf = Corrected factor, EDR = Effective depth reading, DSP = Diameter of soil particle and % P = percentage of fine.

Sample Description: Clay and Silt
Depth: 1.5-2.8 m

Standard Test Method: ASTM D 854-00 Standard Method

Dispersing Agent: Sodium Metahexaphosphate

Hydrometer Number: 152H

Specific Gravity: 2.70

Table A3.2.3 Datasheet for Hydrometer analysis for Test Pit 2 at 2.4 m.

Time (minutes)	HR	T(°C)	CHR		Cf (a)	EDR (L)	K	DSP (mm)	% P
			R'	R"					
0.5	49	23	50	43.7	0.989	8.1	0.01297	0.053	78.46
1	48	23	49	42.7	0.989	8.3	0.01297	0.038	76.67
2	46.5	23	47.5	41.2	0.989	8.5	0.01297	0.027	73.98
4	45	23	46	39.7	0.989	8.8	0.01297	0.019	71.28
8	43	23	44	37.7	0.989	9.1	0.01297	0.014	67.69
15	41	23	42	35.7	0.989	9.4	0.01297	0.010	64.10
30	39	23	40	33.7	0.989	9.7	0.01297	0.007	60.51
60	37.5	23	38.5	32.2	0.989	10.0	0.01297	0.005	57.82
120	35	23	36	29.7	0.989	10.4	0.01297	0.004	53.33
240	34	23	35	28.7	0.989	10.6	0.01297	0.003	51.53
480	33	23	34	27.7	0.989	10.7	0.01297	0.002	49.74
1440	30	23	31	24.7	0.989	11.2	0.01297	0.001	44.35

HR = Hydrometer reading, T = Temperature, CHR = Corrected hydrometer reading, Cf = Corrected factor, EDR = Effective depth reading, DSP = Diameter of soil particle and % P = percentage of fine.

Sample Description: Clay and Silt
Depth: 1.5-2.8 m

Standard Test Method: ASTM D 854-00 Standard Method

Dispersing Agent: Sodium Metahexaphosphate

Hydrometer Number: 152H

Specific Gravity: 2.80

Table A3.2.4 Datasheet for Hydrometer analysis for Test Pit 3 at 1.5 m.

Time (minutes)	HR	T(°C)	CHR		Cf (a)	EDR (L)	K	DSP (mm)	% P
			R'	R"					
0.5	54	23	55	48.7	0.968	7.3	0.01261	0.048	85.64
1	53	23	54	47.7	0.968	7.4	0.01261	0.034	83.88
2	52	23	53	46.7	0.968	7.6	0.01261	0.025	82.13
4	51	23	52	45.7	0.968	7.8	0.01261	0.018	80.37
8	50	23	51	44.7	0.968	7.9	0.01261	0.013	78.61
15	48.5	23	49.5	43.2	0.968	8.2	0.01261	0.009	75.97
30	47	23	48	41.7	0.968	8.4	0.01261	0.007	73.33
60	46	23	47	40.7	0.968	8.6	0.01261	0.005	71.57
120	45	23	46	39.7	0.968	8.8	0.01261	0.003	69.82
240	43.5	23	44.5	38.2	0.968	9.0	0.01261	0.002	67.18
480	42	23	43	36.7	0.968	9.2	0.01261	0.002	64.54
1440	40	23	41	34.7	0.968	9.6	0.01261	0.001	61.02

HR = Hydrometer reading, T = Temperature, CHR = Corrected hydrometer reading, Cf = Corrected factor, EDR = Effective depth reading, DSP = Diameter of soil particle and % P = percentage of fine.

Sample Description: Clay and Silt
Depth: 1.5-2.8 m

Standard Test Method: ASTM D 854-00 Standard Method

Dispersing Agent: Sodium Metahexaphosphate

Hydrometer Number: 152H

Specific Gravity: 2.74

Table A3.2.5 Datasheet for Hydrometer analysis for Test Pit 3 at 2.4 m.

Time (minutes)	HR	T(°C)	CHR		Cf (a)	EDR (L)	K	DSP (mm)	% P
			R'	R"					
0.5	54	23	55	48.7	0.980	7.3	0.012826	0.049	86.70
1	53	23	54	47.7	0.980	7.4	0.012826	0.035	84.92
2	52	23	53	46.7	0.980	7.6	0.012826	0.025	83.14
4	50.5	23	51.5	45.2	0.980	7.8	0.012826	0.018	80.47
8	48.5	23	49.5	43.2	0.980	8.2	0.012826	0.013	76.91
15	46	23	47	40.7	0.980	8.6	0.012826	0.010	72.46
30	44	23	45	38.7	0.980	8.9	0.012826	0.007	68.90
60	42	23	43	36.7	0.980	9.2	0.012826	0.005	65.33
120	40.5	23	41.5	35.2	0.980	9.5	0.012826	0.004	62.66
240	38.5	23	39.5	33.2	0.980	9.8	0.012826	0.003	59.10
480	37	23	38	31.7	0.980	10.1	0.012826	0.002	56.43
1440	35.5	23	36.5	30.2	0.980	10.3	0.012826	0.001	53.76

HR = Hydrometer reading, T = Temperature, CHR = Corrected hydrometer reading, Cf = Corrected factor, EDR = Effective depth reading, DSP = Diameter of soil particle and % P = percentage of fine.

Sample Description: Clay and Silt
Depth: 1.5-2.8 m

Standard Test Method: ASTM D 854-00 Standard Method

Dispersing Agent: Sodium Metahexaphosphate

Hydrometer Number: 152H

Specific Gravity: 2.69

Table A3.2.6 Datasheet for Hydrometer analysis for Test Pit 4 at 2.7 m.

Time (minutes)	HR	T(°C)	CHR		Cf (a)	EDR (L)	K	DSP (mm)	% P
			R'	R"					
0.5	51	23	52	45.7	0.991	7.8	0.01301	0.051	82.24
1	49	23	50	43.7	0.991	8.1	0.01301	0.037	78.64
2	47.5	23	48.5	42.2	0.991	8.3	0.01301	0.027	75.94
4	45	23	46	39.7	0.991	8.8	0.01301	0.019	71.44
8	43	23	44	37.7	0.991	9.1	0.01301	0.014	67.84
15	41	23	42	35.7	0.991	9.4	0.01301	0.010	64.24
30	38.5	23	39.5	33.2	0.991	9.8	0.01301	0.007	59.74
60	36	23	37	30.7	0.991	10.2	0.01301	0.005	55.24
120	33.5	23	34.5	28.2	0.991	10.6	0.01301	0.004	50.74
240	31	23	32	25.7	0.991	11.0	0.01301	0.003	46.25
480	29.5	23	30.5	24.2	0.991	11.3	0.01301	0.002	43.55
1440	27	23	28	21.7	0.991	11.7	0.01301	0.001	39.05

HR = Hydrometer reading, T = Temperature, CHR = Corrected hydrometer reading, Cf = Corrected factor, EDR = Effective depth reading, DSP = Diameter of soil particle and % P = percentage of fine.

Sample Description: Clay and Silt
Depth: 1.5-2.8 m

Standard Test Method: ASTM D 854-00 Standard Method

Dispersing Agent: Sodium Metahexaphosphate

Hydrometer Number: 152H

Specific Gravity: 2.73

Table A3.2.7 Datasheet for Hydrometer analysis for Test Pit 5 at 2 m

Time (minutes)	HR	T(°C)	CHR		Cf (a)	EDR (L)	K	DSP (mm)	% P
			R'	R"					
0.5	56	23	57	50.7	0.982	6.9	0.01286	0.048	90.45
1	54	23	55	48.7	0.982	7.3	0.01286	0.035	86.88
2	53	23	54	47.7	0.982	7.4	0.01286	0.025	85.10
4	52	23	53	46.7	0.982	7.6	0.01286	0.018	83.31
8	50.5	23	51.5	45.2	0.982	7.8	0.01286	0.013	80.64
15	49	23	50	43.7	0.982	8.1	0.01286	0.009	77.96
30	47	23	48	41.7	0.982	8.4	0.01286	0.007	74.39
60	46	23	47	40.7	0.982	8.6	0.01286	0.005	72.61
120	43	23	44	37.7	0.982	9.1	0.01286	0.004	67.26
240	41	23	42	35.7	0.982	9.4	0.01286	0.003	63.69
480	39.5	23	40.5	34.2	0.982	9.7	0.01286	0.002	61.01
1440	38	23	39	32.7	0.982	9.9	0.01286	0.001	58.34

HR = Hydrometer reading, T = Temperature, CHR = Corrected hydrometer reading, Cf = Corrected factor, EDR = Effective depth reading, DSP = Diameter of soil particle and % P = percentage of fine.

Sample Description: Clay and Silt
Depth: 1.5-2.8 m

Standard Test Method: ASTM D 854-00 Standard Method

Dispersing Agent: Sodium Metahexaphosphate

Hydrometer Number: 152H

Specific Gravity: 2.79

Table A3.2.8 Datasheet for Hydrometer analysis for Test Pit 5 at 2.7 m.

Time (minutes)	HR	T(°C)	CHR		Cf (a)	EDR (L)	K	DSP (mm)	% P
			R'	R"					
0.5	57	23	58	51.7	0.970	6.8	0.01265	0.047	91.10
1	55	23	56	49.7	0.970	7.1	0.01265	0.034	87.58
2	53	23	54	47.7	0.970	7.4	0.01265	0.024	84.05
4	52	23	53	46.7	0.970	7.6	0.01265	0.017	82.29
8	50.5	23	51.5	45.2	0.970	7.8	0.01265	0.013	79.65
15	49	23	50	43.7	0.970	8.1	0.01265	0.009	77.00
30	48	23	49	42.7	0.970	8.3	0.01265	0.007	75.24
60	46	23	47	40.7	0.970	8.6	0.01265	0.005	71.72
120	44	23	45	38.7	0.970	8.9	0.01265	0.003	68.19
240	41.5	23	42.5	36.2	0.970	9.3	0.01265	0.002	63.79
480	39.5	23	40.5	34.2	0.970	9.7	0.01265	0.002	60.26
1440	37	23	38	31.7	0.970	10.1	0.01265	0.001	55.86

HR = Hydrometer reading, T = Temperature, CHR = Corrected hydrometer reading, Cf = Corrected factor, EDR = Effective depth reading, DSP = Diameter of soil particle and % P = percentage of fine.

A4. Atterberg Limit Test Results

Project Name: Cira Town Landslide

Sample Depth= 1.5 to 2.8 m

Table A4.1 Datasheet for Atterberg Limit Analysis For TP1 at 1.5 m

Determination	Liquid Limit					Plastic Limit		
Trial Number	1	2	3	4		1	2	3
Can Code	6-3	K4	M1	G7		B10	113	R1
Wt. of Can, W_C (G)	17.13	17.86	17.24	17.44		9.61	6.48	5.82
Wt. of Wet Soil + Can, W_{wsc} (G)	42.46	40.80	41.06	39.83		16.42	13.97	12.97
Wt. of Dry Soil + Can, W_{dsc} (G)	32.11	31.28	31.08	30.35		14.64	12.01	11.13
Wt. of Water, W_w (G)	10.35	9.55	9.98	9.48		1.78	1.96	1.84
Wt. of Dry Soil, W_d (G)	14.98	13.42	13.84	12.91		5.03	5.53	5.31
No. Blows	33	28	23	18				
Moisture Content, W_c (%)	69.10	70.94	72.11	73.43		35.39	35.44	34.65
LL= W_c at 25 Blows and PL= Average of PL at Trial 1, 2, 3 and 4	LL= 71.31%					PL= 35.16 %		
	PI=LL-PL= 23.26							

Liquid Limit Determination

y = -0.2838x + 78.629

Water Content (%) vs Number of Blows
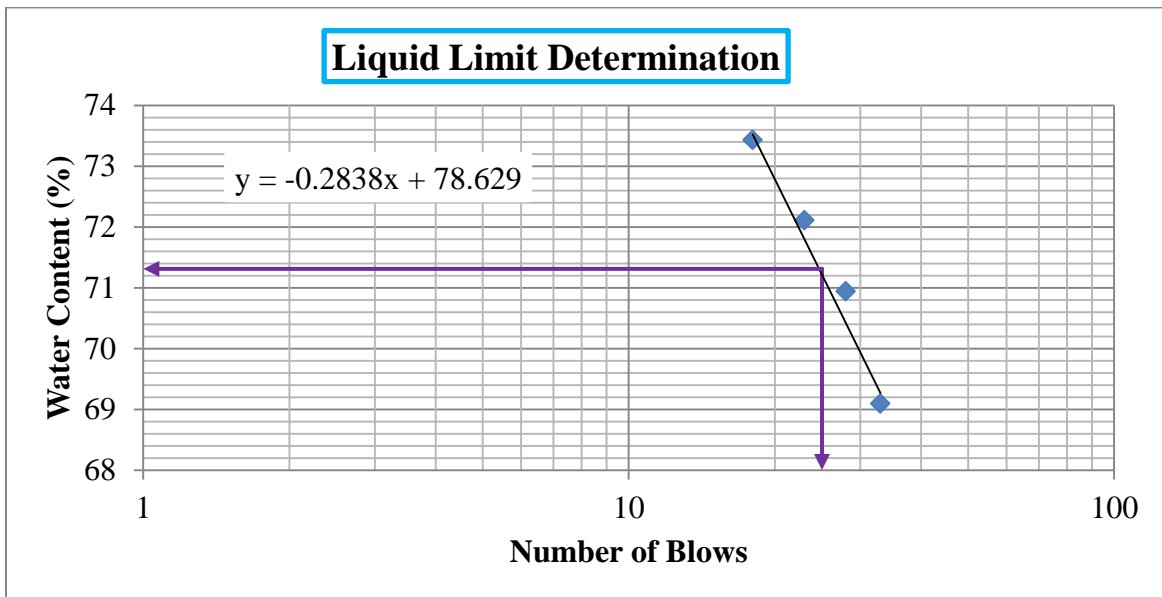
Table A4.2 Datasheet for Atterberg Limit Analysis For TP1 at 2.8 m

Determination	Liquid Limit					Plastic Limit		
Trial Number	1	2	3	4		1	2	3
Can Code	2-3	A12	M1	H		5TH	4E	4F
Wt. of Can, W_C (G)	5.55	16.12	17.24	19.32		28.12	27.95	27.77
Wt. of Wet Soil + Can, W_{wsc} (G)	30.47	37.80	38.67	39.27		34.19	35.66	35.16
Wt. of Dry Soil + Can, W_{dsc} (G)	20.40	28.91	29.77	30.90		32.58	33.62	33.24
Wt. of Water, W_w (G)	10.07	8.89	8.90	8.37		1.61	2.04	1.92
Wt. of Dry Soil, W_d (G)	14.85	12.79	12.53	11.58		4.46	5.67	5.47
No. Blows	32	27	22	20				
Moisture Content, W_c (%)	67.81	69.51	71.03	72.28		36.10	35.98	35.10
LL= W_c at 25 Blows and PL= Average of PL at Trial 1, 2, and 3	LL= 70.26%					PL= 35.73%		
	PI= LL-PL = 21.07							

Liquid Limit Determination

$y = -0.4896x + 83.03$

Water Content (%) vs. Number of Blows

101
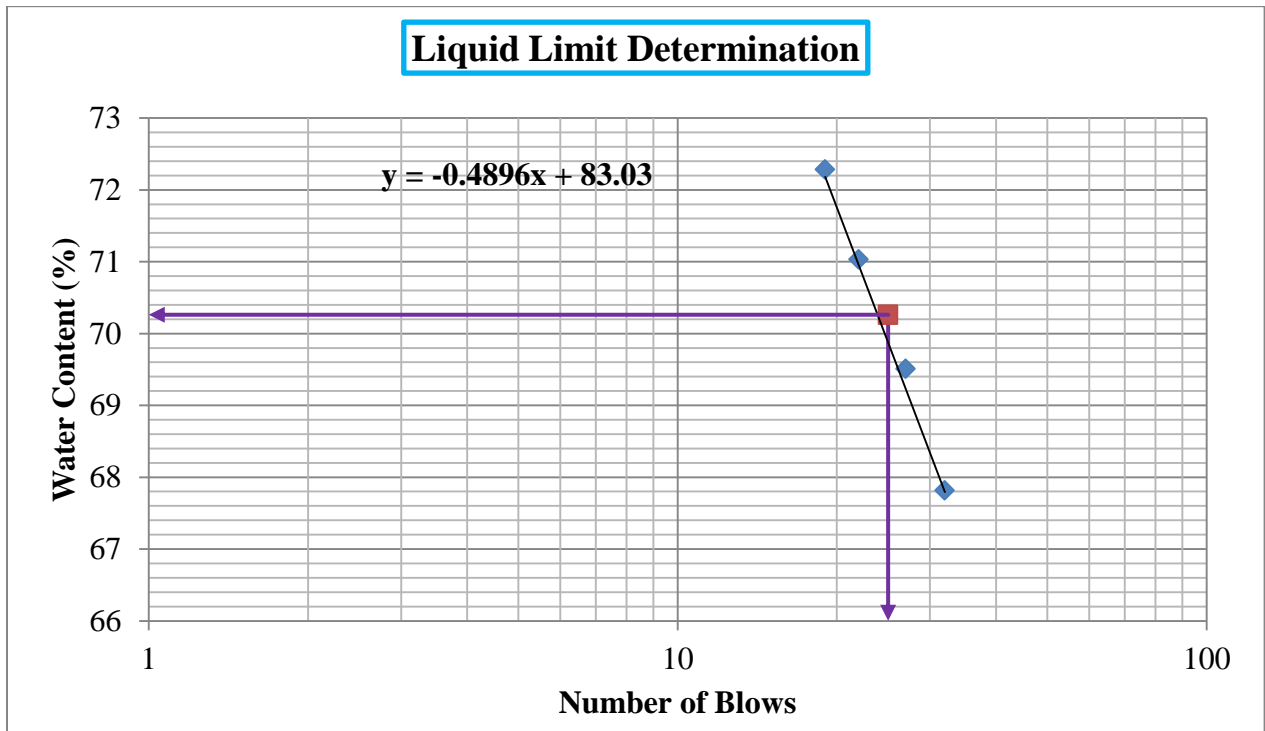
Table A4.3 Datasheet for Atterberg Limit Analysis For TP2 at 2.4 m

Determination	Liquid Limit				Plastic Limit		
Trial Number	1	2	3	4	1	2	3
Can Code	6-3	GST2	S88	5HY	4E	4A	5TH
Wt. of Can, W_C (G)	17.13	17.38	17.23	27.80	27.97	15.12	28.11
Wt. of Wet Soil + Can, W_{wsc} (G)	28.15	30.36	32.54	41.40	33.26	23.12	34.99
Wt. of Dry Soil + Can, W_{dsc} (G)	23.75	25.10	26.29	35.80	31.98	21.19	33.43
Wt. of Water, W_w (G)	4.40	5.26	6.25	5.6	1.28	1.93	1.56
Wt. of Dry Soil, W_d (G)	6.62	7.72	9.06	8.00	4.01	6.07	5.32
No. Blows	33	26	22	20			
Moisture Content, W_c (%)	66.47	68.13	68.98	70.00	31.92	31.80	29.32
LL= W_c at 25 Blows and PL= Average of PL at Trial 1, 2, and 3	LL= 68.45 %				PL= 31.01%		
PI=LL-PL= 19.67							

Liquid Limit Determination

$y = -0.2294x + 74.182$

Water Content (%) vs Number of Blows
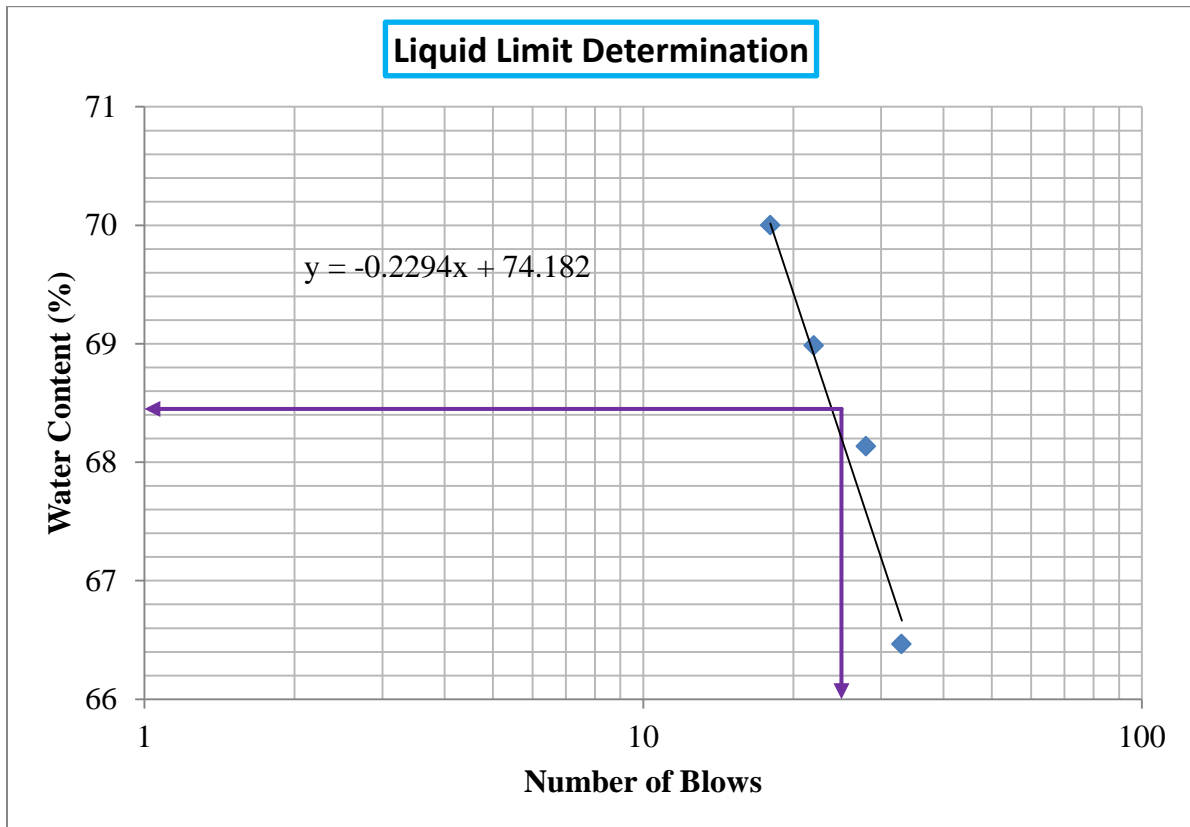
Table A4.4 Datasheet for Atterberg Limit Analysis For TP3 at 1.5 m

Determination	Liquid Limit					Plastic Limit		
Trial Number	1	2	3	4		1	2	3
Can Code	4F	4G	G3	5HD		4D	1B	O
Wt. of Can, W_C (G)	27.77	18.49	17.67	18.23		25.64	17.90	15.35
Wt. of Wet Soil + Can, W_{wsc} (G)	42.40	34.74	35.14	32.40		43.00	28.00	26.00
Wt. of Dry Soil + Can, W_{dsc} (G)	36.63	28.13	27.90	26.45		38.88	25.68	23.48
Wt. of Water, W_w (G)	5.77	6.61	7.24	5.95		4.12	2.32	2.52
Wt. of Dry Soil, W_d (G)	8.86	9.64	10.23	8.22		13.24	7.78	8.13
No. Blows	34	27	24	20				
Moisture Content, W_c (%)	65.12	68.57	70.77	72.38		31.12	29.82	31.00
LL= W_c at 25 Blows and PL= Average of PL at Trial 1, 2, 3and 4	LL= 70.11%					PL= 30.64%		
PI=LL-PL= 26.43								

Liquid Limit Determination

$y = -0.5128x + 82.929$

Water Content (%) vs Number of Blows
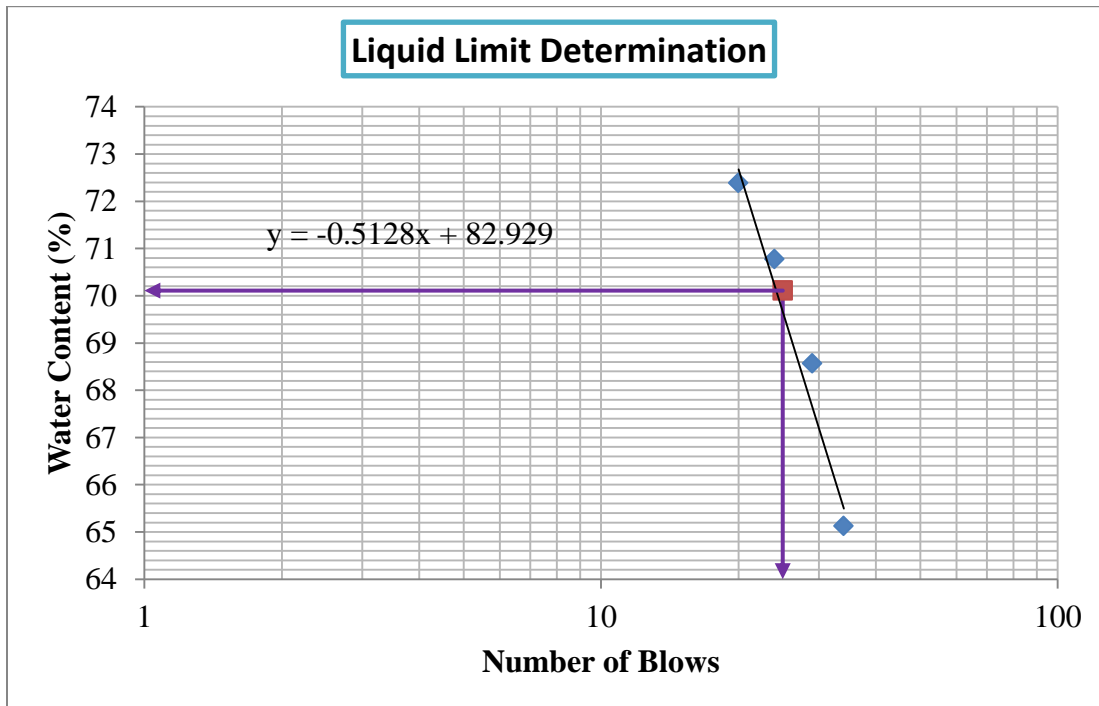
Table A4.5 Datasheet for Atterberg Limit Analysis For TP3 at 2.4 m

Determination	Liquid Limit					Plastic Limit		
Trial Number	1	2	3	4		1	2	3
Can Code	A2-3	F2	T4	G 7		13	B12	P1
Wt. of Can, W_C (G)	5.53	5.87	6.24	17.44		6.52	16.60	5.85
Wt. of Wet Soil + Can, W_{wsc} (G)	17.92	16.24	17.46	30.91		13.32	25.39	13.86
Wt. of Dry Soil + Can, W_{dsc} (G)	12.92	12.01	12.81	25.48		11.51	23.15	11.79
Wt. of Water, W_w (G)	5	4.23	4.65	5.64		1.81	2.24	2.07
Wt. of Dry Soil, W_d (G)	7.39	6.14	6.57	7.83		4.99	6.55	5.94
No. Blows	34	28	21	18				
Moisture Content, W_c (%)	67.66	68.89	70.78	72.03		36.27	34.20	34.85
LL= W_c at 25 Blows and PL= Average of PL at Trial 1, 2, and 3	LL= 69.91%					PL= 35.11 %		
	PI=LL-PL= 29.29							

Liquid Limit Determination

y = -0.2685x + 76.619

Water Content (%) vs Number of Blows
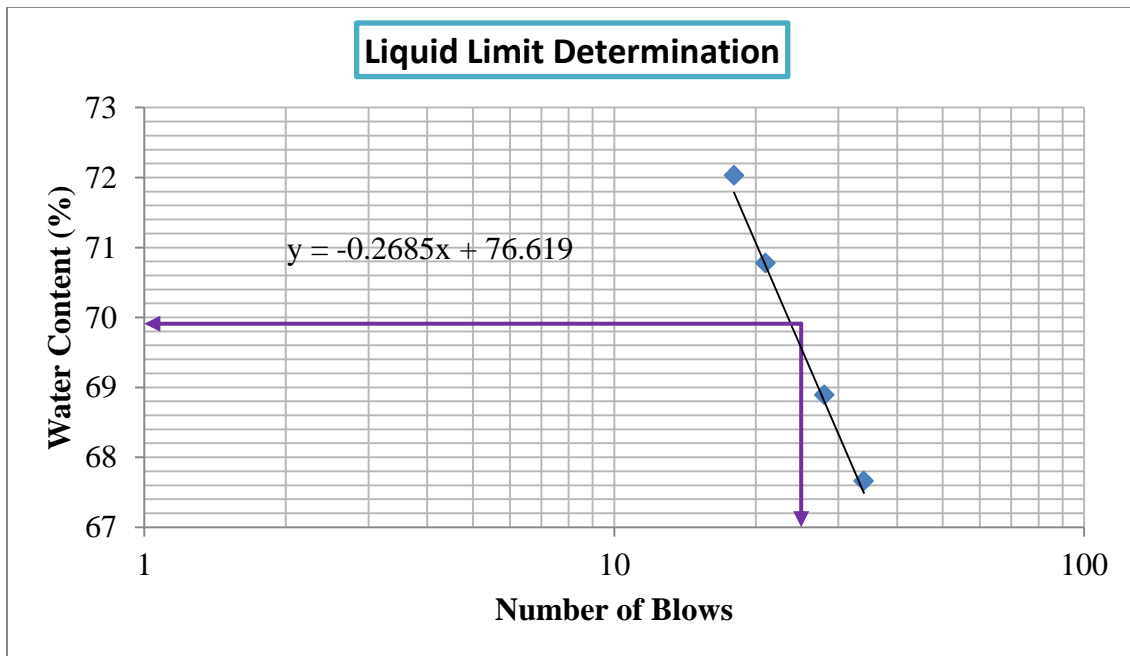
Table A4.6 Datasheet for Atterberg Limit Analysis For TP4 at 2.7 m

Determination	Liquid Limit					Plastic Limit		
Trial Number	1	2	3	4		1	2	3
Can Code	C14	L1	R34	C8		A7	O1	B12
Wt. of Can, W_C (G)	5.97	19.58	17.34	5.82		19.87	18.06	16.60
Wt. of Wet Soil + Can, W_{wsc} (G)	23.09	35.73	34.12	22.15		25.19	24.18	23.52
Wt. of Dry Soil + Can, W_{dsc} (G)	16.31	29.22	27.32	15.48		23.83	22.63	21.76
Wt. of Water, W_w (G)	6.78	6.51	6.80	6.67		1.36	1.55	1.76
Wt. of Dry Soil, W_d (G)	10.34	9.64	9.98	9.66		3.96	4.58	5.16
No. Blows	32	28	23	21				
Moisture Content, W_c (%)	65.57	67.53	68.14	69.05		34.34	33.84	34.11
LL= W_c at 25 Blows and PL= Average of PL at Trial 1, 2, and 3	LL= 67.70 %					PL= 34.10%		
	PI=LL-PL= 19.69							

Liquid Limit Determination

$y = -0.2486x + 73.911$

Water Content (%)

Number of Blows

105
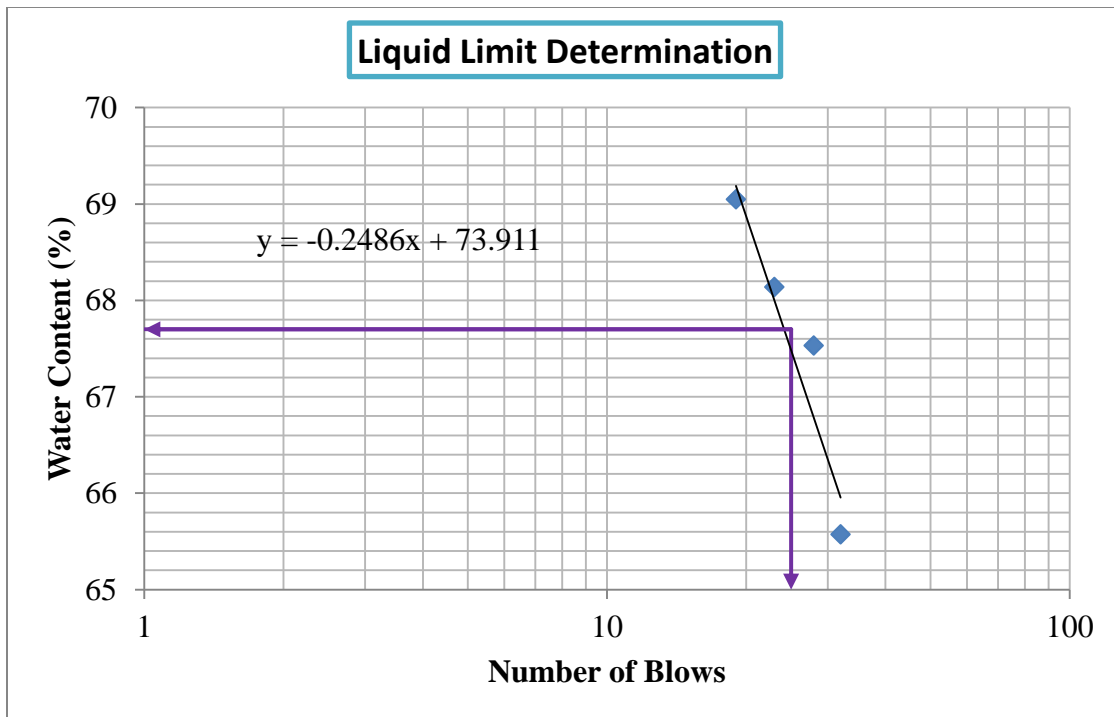
Table A4.7 Datasheet for Atterberg Limit Analysis For TP5 at 2 m

Determination	Liquid Limit					Plastic Limit		
Trial Number	1	2	3	4		1	2	3
Can Code	A3-2	A7	C8	B10		A12	C14	H
Wt. of Can, W_C (G)	16.39	19.88	17.44	9.61		16.12	5.97	19.33
Wt. of Wet Soil + Can, W_{wsc} (G)	31.65	31.23	30.85	21.78		22.69	12.12	23.62
Wt. of Dry Soil + Can, W_{dsc} (G)	25.48	26.58	25.26	16.61		21.01	10.52	22.51
Wt. of Water, W_w (G)	6.13	4.65	5.59	5.17		1.68	1.60	1.11
Wt. of Dry Soil, W_d (G)	9.09	6.70	7.82	7.00		4.89	4.55	3.18
No. Blows	33	27	22	20				
Moisture Content, W_c (%)	67.44	69.40	71.48	73.86		34.36	35.16	34.91
LL= W_c at 25 Blows and PL= Average of PL at Trial 1, 2, and 3	LL= 70.77 %					PL= 34.81%		
PI=LL-PL= 29.50								

Liquid Limit Determination

$y = -0.4607x + 82.292$

Water Content (%) vs Number of Blows
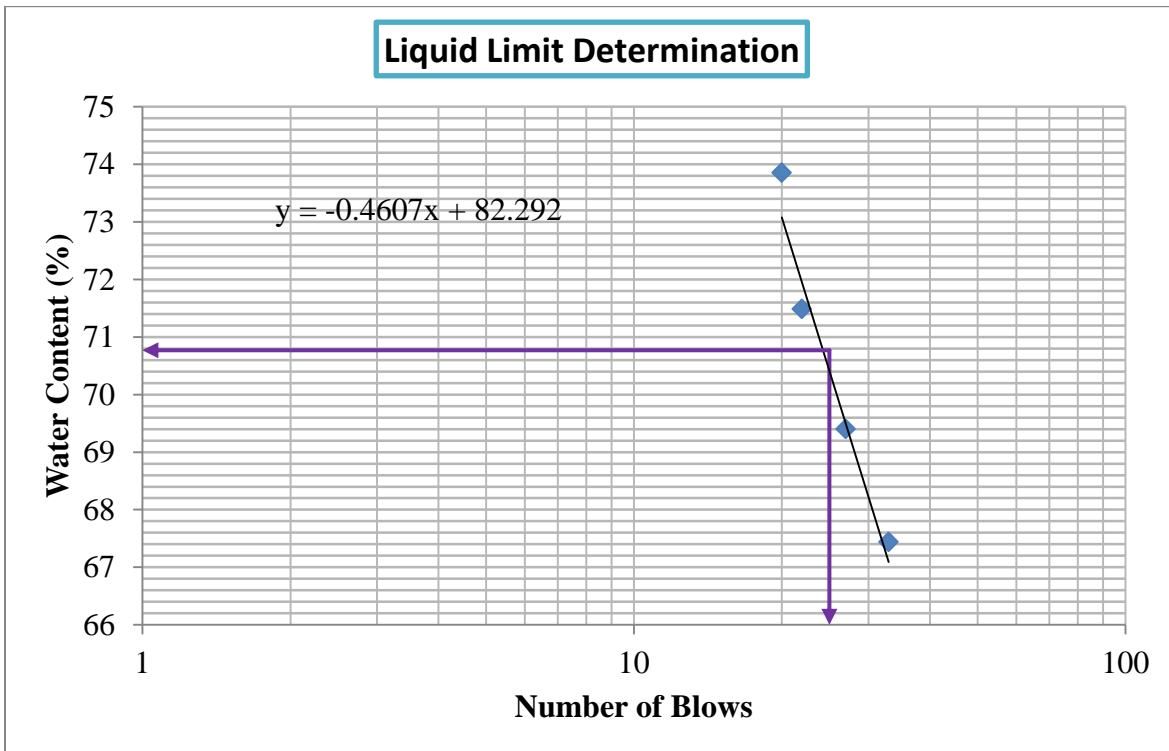
Table A4.8 Datasheet for Atterberg Limit Analysis For TP5 at 2.7 m

Determination	Liquid Limit					Plastic Limit		
Trial Number	1	2	3	4		1	2	3
Can Code	A113	A1	D5-2	R1		C8	O1	L1
Wt. of Can, W_C (G)	6.47	6.28	5.42	5.82		5.83	18.06	19.58
Wt. of Wet Soil + Can, W_{wsc} (G)	20.99	20.12	21.16	25.73		13.29	25.08	25.11
Wt. of Dry Soil + Can, W_{dsc} (G)	15.14	14.51	14.68	17.41		11.56	23.38	23.78
Wt. of Water, W_w (G)	5.85	5.61	6.48	8.32		1.73	1.70	1.33
Wt. of Dry Soil, W_d (G)	8.67	8.23	9.26	11.58		5.73	5.32	4.20
No. Blows	31	27	23	19				
Moisture Content, W_c (%)	67.47	68.17	69.98	71.85		30.19	31.95	31.67
LL= W_c at 25 Blows and PL= Average of PL at Trial 1, 2, and 3	LL= 69.37%					PL= 31.27%		
	PI=LL-PL= 26.52							

Liquid Limit Determination

$y = -0.3734x + 78.701$

(Water Content (%) vs Number of Blows)

107
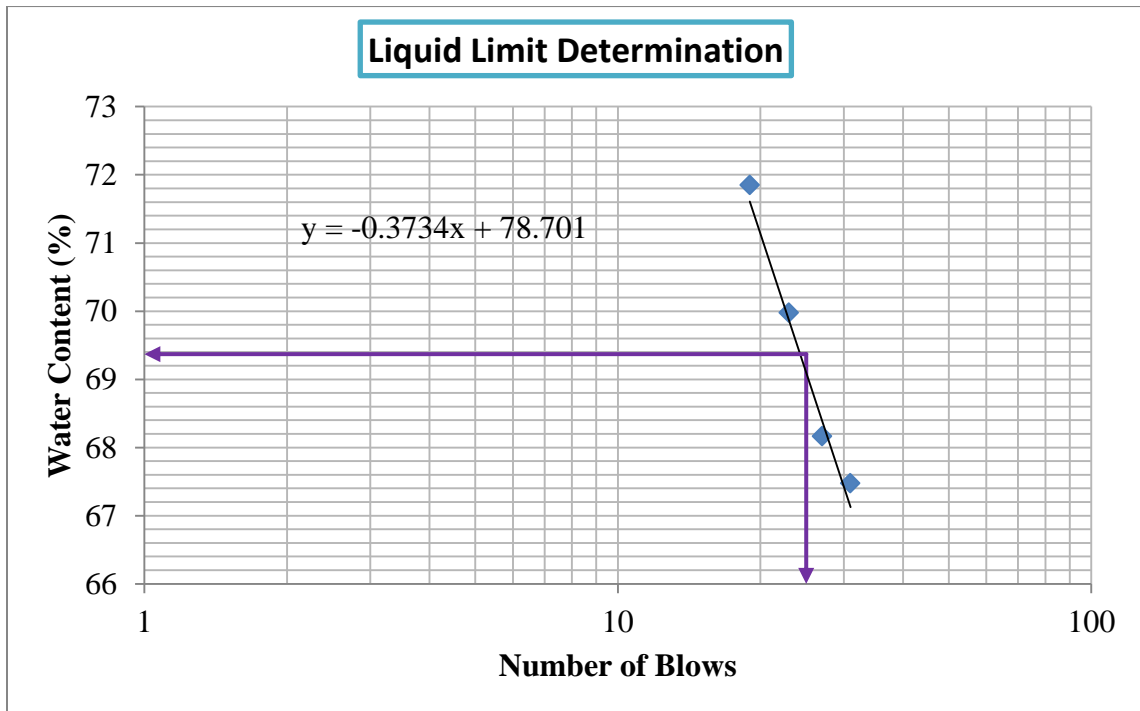
A5. Permeabilty Determination By Falling Head Method

Table A5.1 Datasheet for Permeability Test Results For TP1 at 2.8 m

Falling head Permeability Test				
Trial		01	02	03
Head, h_o	(cm)	95.8	94.3	93.6
Head, h_1	(cm)	75.4	74.7	73.6
Time, t	(s)	2591	2580	2615
Temperature, T	(^{o}c)	21	20	20
Volume,	(ml)	46	48	51
Height deroped	(cm)	20.4	19.6	20
Permeability at T^oc, K_T		2.73E-06	2.67E-06	2.72E-06
R_t for T		0.9761	1.0000	1.0000
Permeability at 20^oC, K_{20}		2.67E-06	2.67E-06	2.72E-06
Average K_{20}	(cm/s)	2.68E-06		

Table A5.2 Datasheet for Permeability Test Results For TP2 at 2.4 m

Falling head Permeability Test				
Trial		01	02	03
Head, h_o	(cm)	95.5	94	96.12
Head, h_1	(cm)	87	86	89.76
Time, t	(s)	4834	4876	5432
Temperature, T	(^{o}c)	21	20	21
Volume,	(ml)	36	38	32
Height deroped	(cm)	8.5	8	6.36
Permeability at T^oc, K_T		1.09E-06	1.03E-06	7.15E-07
R_t for T		0.9998	1.0000	0.9998
Permeability at 20^oC, K_{20}		1.09E-06	1.03E-06	7.15E-07
Average K_{20}	(cm/s)	9.48E-07		

Table A5.3 Datasheet for Permeability Test Results For TP3 at 2.4 m

Falling head Permeability Test			
Trial	01	02	03
Head, h_o (cm)	92.1	91.7	93.66
Head,h_1 (cm)	89	87.65	83.12
Time, t (s)	4200	4201	4200
Temperature, T (^{o}c)	23	22	23
Volume, (ml)	10	11	11
Height deroped (cm)	3.1	4.05	10.54
Permeability at T^{o}c, K_T	1.80E-07	2.38E-07	6.29E-07
R_t for T	0.9993	0.9996	0.9993
Permeability at 20°C, K_{20}	1.80E-07	2.38E-07	6.28E-07
Average K_{20} (cm/s)	3.49E-07		

Table A5.4 Datasheet for Permeability Test Results For TP4 at 2.7 m

Falling head Permeability Test			
Trial	01	02	03
Head, h_o (cm)	89.3	88.5	89.65
Head,h_1 (cm)	57.6	56.9	56.54
Time, t (s)	197	189	196
Temperature, T (^{o}c)	21	22	21
Volume, (ml)	70	72	71
Height deroped (cm)	31.7	31.6	33.11
Permeability at T^{o}c, K_T	6.01E-05	6.31E-05	6.35E-05
R_t for T	0.9998	0.9996	0.9998
Permeability at 20°C, K_{20}	6.01E-05	6.31E-05	6.35E-05
Average K_{20} (cm/s)	6.23E-05		

Table A5.5 Datasheet for Permeability Test Results For TP5 at 2.7 m

Falling head Permeability Test			
Trial	01	02	03
Head, h_o (cm)	91.8	94	93
Head,h_1 (cm)	87	86	89.76
Time, t (s)	4763	4895	5200
Temperature, T (^{o}c)	21	20	21
Volume, (ml)	37	38	33
Height deroped (cm)	4.8	8	3.24
Permeability at T^{o}c, K_T	9.29E-07	1.50E-06	5.62E-07
R_t for T	0.9998	1.0000	0.9998
Permeability at 20°C, K_{20}	9.28E-07	1.50E-06	5.61E-07
Average K_{20} (cm/s)	9.95E-07		

Table A6 DataSheet Forfreeswell Test Result

Designation	Depth (m)	Volume of sample in Kerosene (ml)	Volume of sample in Water (ml)	Free swell (%)
TP1	2.8	12	15	25.00
TP2	2.4	12	16	33.33
TP3	2.4	11	15	36.36
TP4	2.7	11	14	27.27
TP5	2.7	12	17	41.67

A7. <u>Triaxial UU Test Results</u>

<table>
<tr><td colspan="2" rowspan="2">
CDSWC

Company Name:</td><td colspan="4">በኢትዮጵያ የኮንስትራክሽን ዲዛይንና ሱፐርቪዥን ሥራዎች ኮርፖሬሽን
ETHIOPIAN CONSTRUCTION DESIGN & SUPERVISION WORKS CORPORATION</td></tr>
<tr><td colspan="2">Geotechnical Laboratory Report</td><td>Document No.:-
OF/ECDSWC/ 0996</td><td>Issue No;
I</td><td>Page No.
1 of 6</td></tr>
</table>

Title:-

Client Ref. :-	-
Date Received:-	21/04/2021
Reported on :-	29/04/2021

Lab No.	:-	3285/13-3289/13
Submitted by	:-	Mulatu Tamiru
Project	:-	Thesis
Location	:-	Jimma
Test Requested :-		Triaxial UU Test
Reported to	:-	Mulatu Tamiru

No.:-	Test Type	Standard Method	Soil Test Results				
			Lab. No.:- 3285/13 ID:- TP-1-02 Depth(m):- 2.80	Lab. No.:- 3286/13 ID:- TP-2-02 Depth(m):- 2.40	Lab. No.:- 3287/13 ID:- TP-3-02 Depth(m):- 2.40	Lab. No.:- 3288/13 ID:- TP-4-02 Depth(m):- 2.70	Lab. No.:- 3289/13 ID:-TP-5-02 Depth(m):- 2.70
1	Triaxial Test C(KPa) Ø(Degree)	ASTM D 2850	58.51 18.45	68.06 22.56	87.42 17.25	26.07 25.65	153.28 8.02

REMARK :-The samples were collected & submitted to the laboratory by Client.

Processed By :- **Getu M.**
Geotechnical Engineer

Checked By :- **Biruk A.**
Senior Geotechnical Engineer

Approved By : **Getu D.**
Geotechnical Lab S/P Manager

Among The major service Rendered by the Geotechnical and Material Laboratory Testing S/Processes of Ethiopian Construction Design & Supervision Works Corporation.
• In Geotechnical Laboratory:-Testing the engineering properties of Soil Mechanics and Rock Mechanics.
• In Material Testing Laboratory- Testing the engineering properties of various Construction materials, such as Aggregates, Asphalts/Bitumen/, Cements, Rocks,Water, Reinforcement steel bars,Hollow blocks, Bricks, Ceramics, Tiles,Asplalt and Concrete Core

Please make sure that this document is the correct version before use

Figure A7 Summary of Triaxial UU test Results

Company Name:

在ኢትዮጵያ የኮንስትራክሽን ዲዛይንና ሱፐርቪዥን ሥራዎች ኮርፖሬሽን
Ethiopian Construction Design & Supervision Works Corporation

Title:		Document No	Issue No.	Page No.
UU Triaxial Test		OF/ECDSWC/0816	1	2 of 6

Project   :-   Thesis
Client   :-   Mulatu Tamiru
Location   :-   Jimma
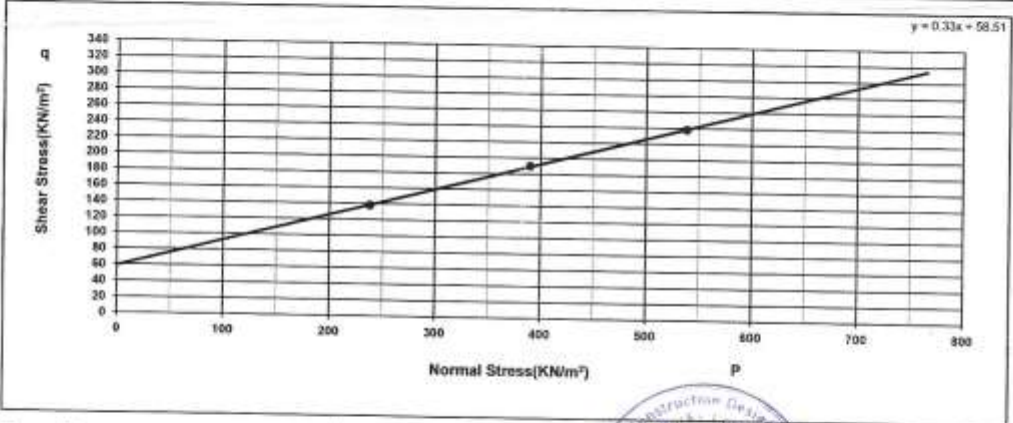Sample ID   :-   TP 1- 02
Depth (m)   :-   2.80

SPECIMEN DATA

Lab No.	3285/13
Initial height (cm)	7.40
Initial Area (cm²)	10.75
Initial Wet Weight (gm)	154.20
Final Dry Weight (gm)	104.80
Moisture content (%)	47.14

Test Type	UU TRIAXIAL TEST
Sample condition	Undisturbed
Initial diameter (cm)	3.70
Initial volume (cm³)	79.58
Bulk density (gm/cm³)	1.938
Dry density (gm/cm³)	1.317

$P =$	$1/2 (s_1 + s_3)$
$q =$	$1/2 (s_1 - s_3)$

Chamber press. (KN/m2)	(s_3)	100	200	300	C (KN/m²)	Ø (Degrees)
Deviator Stress, (KN/m²)	$(s_1 - s_3)$	276	380	476	58.51	18.45

$y = 0.33x + 58.51$

Tested by :-   Yikeber D.
Lab Expert

Processed by:- Getu M.
Geotechnical Engineer

Checked by   Biruk A.
Senior Geotechnical Engineer

Approved by   Getu D.
Geotechnical Lab S/T Manager

Please make sure that this document is the correct version before use

112

Project   :- **Thesis**
Client   :- **Mulatu Tamiru**
Location   :- **Jimma**
Sample ID :- **TP 2- 02**
Depth (m) :- **2.40**

SPECIMEN DATA

Lab No.	3286/13
Initial height (cm)	7.40
Initial Area (cm²)	10.75
Initial Wet Weight (gm)	161.05
Final Dry Weight (gm)	117.85
Moisture content (%)	36.66

Test Type	UU TRIAXIAL TEST
Sample condition	Undisturbed
Initial diameter (cm)	3.70
Initial volume (cm³)	79.58
Bulk density (gm/cm³)	2.024
Dry density (gm/cm³)	1.481

$P =$	$1/2\,(s_1 + s_3)$
$q =$	$1/2\,(s1 - s3)$

Chamber press. (KN/m2)	(s_3)	100	200	300	C (KN/m²)	Ø (Degrees)
Deviator Stress , (KN/m²)	$(s_1 - s_3)$	375	518	659	68.06	22.56

$y = 0.42x + 68.06$

Tested by :- Yikeber D.   Checked by   Birak A.
Lab Expert   Senior Geotechnical Engineer

Processed by:- Getu M.   Approved by   Getu D.
Geotechnical Engineer   Geotechnical Lab S/P Manager

Please make sure that this document is the correct version before use

በኢትዮጵያ የኮንስትራክሽን ዲዛይንና ሱፐርቪዥን ሥራዎች ኮርፖሬሽን
Ethiopian Construction Design & Supervision Works Corporation

Title:	Document No:	Issue No.	Page No.
UU Triaxial Test	OF/ECDSWC/0816	1	4 of 6

Project   :-   **Thesis**
Client   :-   **Mulatu Tamiru**
Location   :-   **Jimma**
Sample ID :-   **TP 3- 02**
Depth (m) :-   **2.40**

SPECIMEN DATA

Lab No.	3287/13
Initial height (cm)	7.40
Initial Area (cm²)	10.75
Initial Wet Weight (gm)	154.60
Final Dry Weight (gm)	110.00
Moisture content (%)	40.55

Test Type	UU TRIAXIAL TEST
Sample condition	Undisturbed
Initial diameter (cm)	3.70
Initial volume (cm³)	79.58
Bulk density (gm/cm³)	1.943
Dry density (gm/cm³)	1.382

$P =$	$1/2 (s_1 + s_3)$
$q =$	$1/2 (s1 - s3)$

Chamber press. (KN/m2)	(s_3)	100	200	300	C (KN/m²)	Ø (Degrees)
Deviator Stress, (KN/m²)	$(s_1 - s_3)$	344	440	524	87.42	17.25

$y = 0.3\mathrm{t}x + 87.42$

Tested by :-   Yikeber D.
Lab Expert

Processed by:- Getu M.
Geotechnical Engineer

Checked by   :-   Biruk A.
Senior Geotechnical Engineer

Approved by   :   Getu D.
Geotechnical Lab & Manager

Please make sure that this document is the correct version before use

Title:		Document No.	Issue No.	Page No.
UU Triaxial Test		OF/ECDSWC/0816	1	5 of 6

Project   :-   Thesis
Client   :-   Mulatu Tamiru
Location   :-   Jimma
Sample ID :-   TP 4- 02
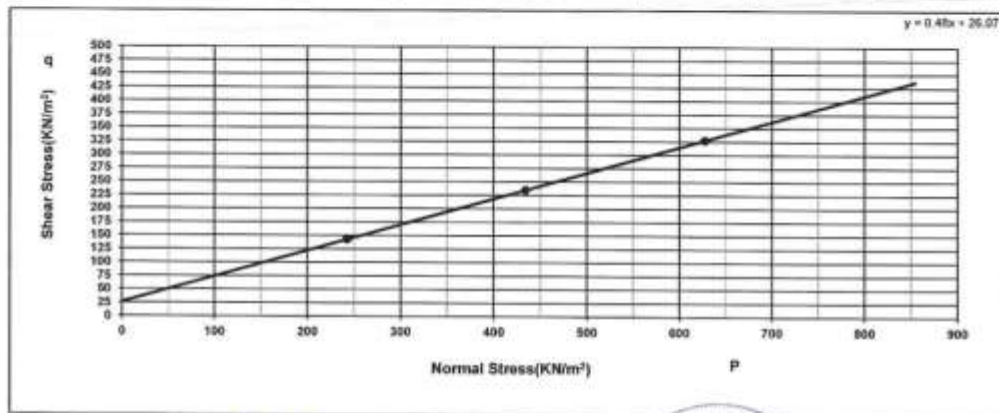Depth (m) :-   2.70

SPECIMEN DATA

Lab No.	3288/13
Initial height (cm)	7.40
Initial Area (cm²)	10.75
Initial Wet Weight (gm)	146.75
Final Dry Weight (gm)	102.60
Moisture content (%)	43.03

Test Type	UU TRIAXIAL TEST
Sample condition	Undisturbed
Initial diameter (cm)	3.70
Initial volume (cm³)	79.58
Bulk density (gm/cm³)	1.844
Dry density (gm/cm³)	1.289

P =	$1/2 (s_1 + s_3)$
q =	$1/2 (s1 - s3)$

Chamber press. (KN/m2)	(s_3)	100	200	300	C (KN/m²)	Ø (Degrees)
Deviator Stress, (KN/m²)	$(s_1 - s_3)$	285	469	654	26.07	25.65

$y = 0.48x + 26.07$

Tested by :-   Mamo H.
Lab Expert

Processed by:-   Getu M.
Geotechnical Engineer

Checked by   Biruk A.
Senior Geotechnical Engineer

Approved by   :-   Getu D.
Geotechnical Lab S/P Manager

Please make sure that this document is the correct version before use.

115

በኢትዮጵያ የኮንስትራክሽን ዲዛይንና ሱፐርቪዥን ሥራዎች ኮርፖሬሽን
Ethiopian Construction Design & Supervision Works Corporation

Title: **UU Triaxial Test**	Document No: OF/ECDSWC/0816	Issue No. 1	Page No. 6 of 6

Project   :-   **Thesis**
Client   :-   **Mulatu Tamiru**
Location   :-   **Jimma**
Sample ID :-   **TP 5- 02**
Depth (m) :-   **2.70**

SPECIMEN DATA

Lab No.	3289/13
Initial height (cm)	7.40
Initial Area (cm²)	10.75
Initial Wet Weight (gm)	157.40
Final Dry Weight (gm)	112.10
Moisture content (%)	40.41

Test Type	**UU TRIAXIAL TEST**
Sample condition	Undisturbed
Initial diameter (cm)	3.70
Initial volume (cm³)	79.58
Bulk density (gm/cm³)	1.978
Dry density (gm/cm³)	1.409

$P =$	$1/2\,(s_1 + s_3)$
$q =$	$1/2\,(s_1 - s_3)$

Chamber press. (KN/m2)	(s_3)	100	200	300	C (KN/m²)	Ø (Degrees)
Deviator Stress . (KN/m²)	$(s_1 - s_3)$	390	424	455	153.28	8.02
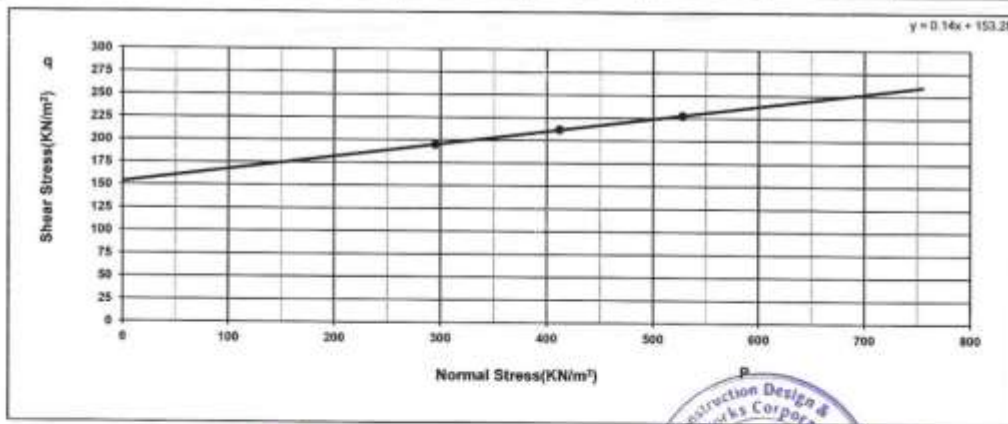
$y = 0.14x + 153.28$

Tested by :-   Mamo H.
Lab Expert

Processed by:- Getu M.
Geotechnical Engineer

Checked by   :-   Biruk A.
Senior Geotechnical Engineer

Approved by
Geotechnical Lab S/D Manager   Getu D.

Please make sure that this document is the correct version before use

116

A7.1 Elastic Modulus determination stress strain curve graph

For Test Pit 1

Figure A7.1 Elastic Modulus determination from stress strain curve of triaxial test for Test Pit 1
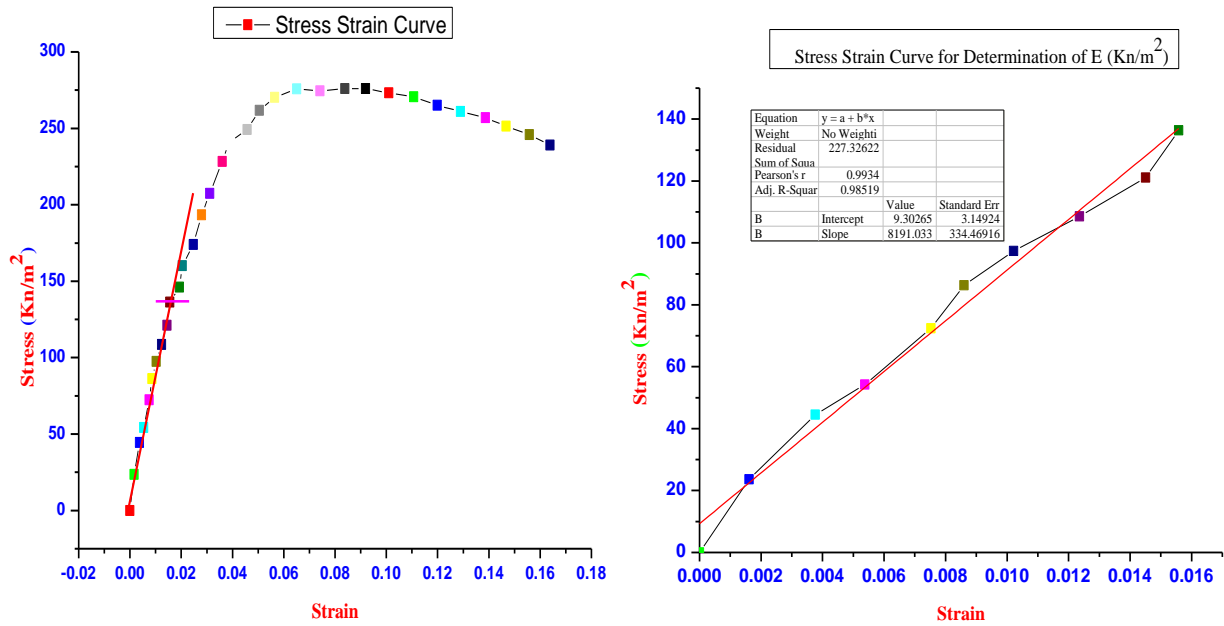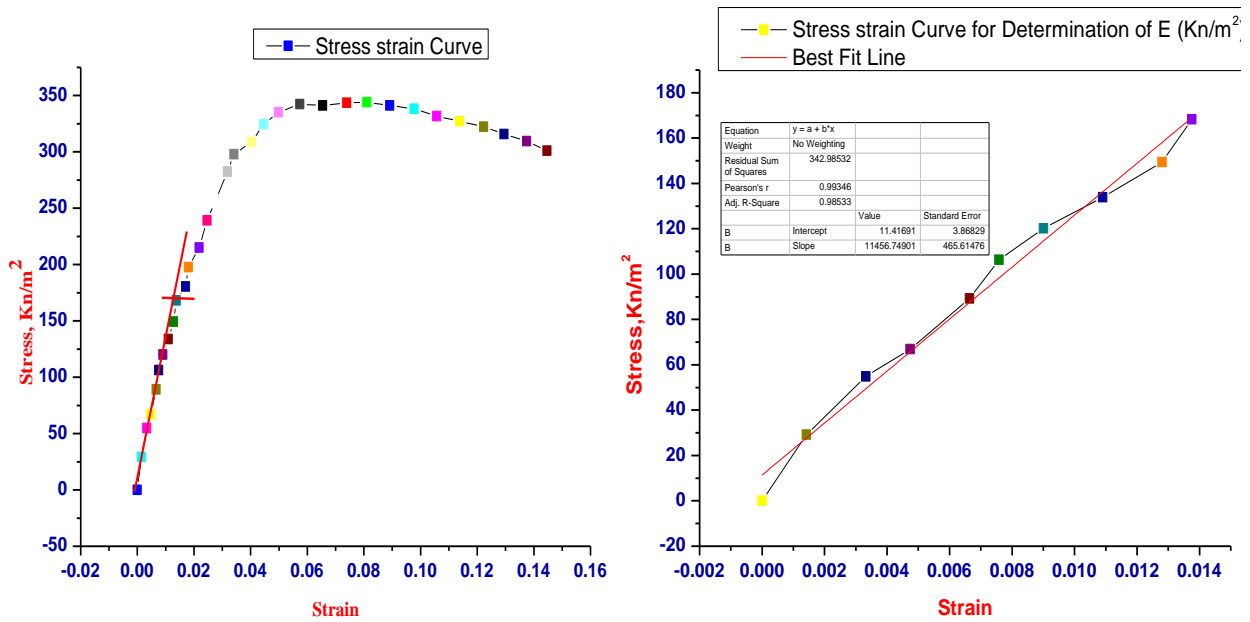
For Test Pit 2

Figure A7.2 Elastic Modulus determination from stress strain curve of triaxial test for Test Pit 2
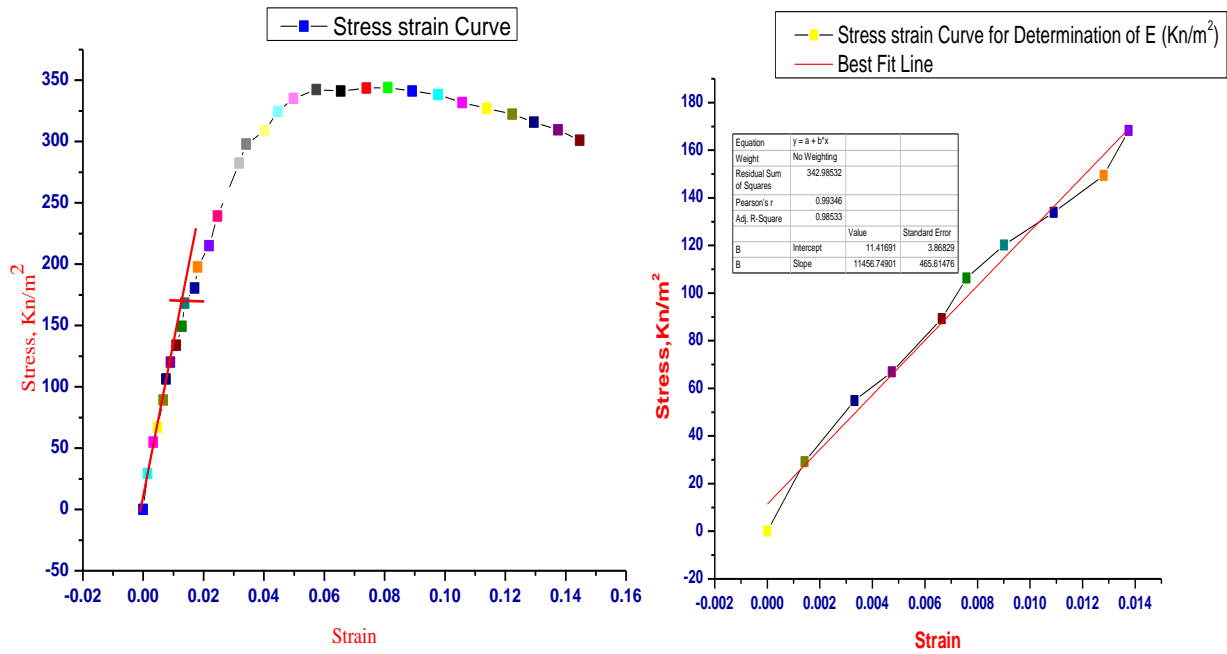
For Test Pit 3

Figure A7.3 Elastic Modulus determination from stress strain curve of triaxial test for Test Pit 3
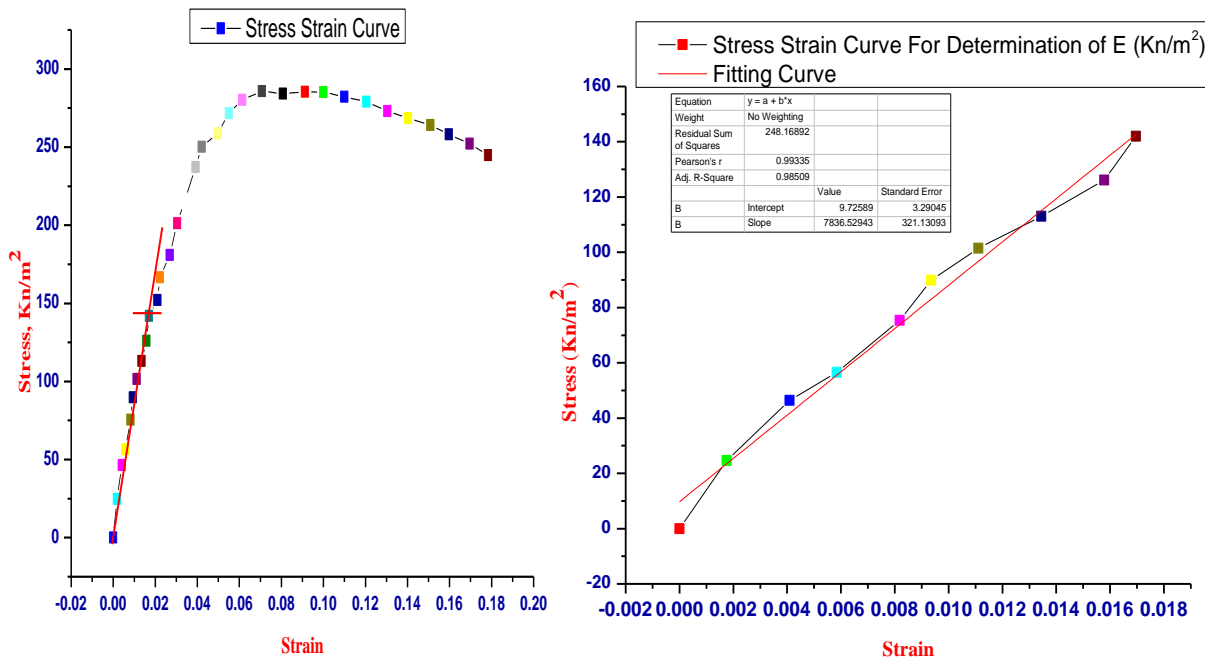
For Test Pit 4

Figure A7.4 Modulus determination from stress strain curve of triaxial test for Test Pit 4

Appendix B. Some Constants Used in Laboratory Test Analysis

Table B.H1 Values of k for use in Equation for Computing Diameter of Particle in Hydrometer Analysis

Temperature,° C	Specific Gravity of Soil Particles								
	2.45	2.50	2.55	2.60	2.65	2.70	2.75	2.80	2.85
16	0.01510	0.01505	0.01481	0.01457	0.01435	0.01414	0.01394	0.01374	0.01356
17	0.01511	0.01486	0.01462	0.01439	0.01417	0.01396	0.01376	0.01356	0.01338
18	0.01492	0.01467	0.01443	0.01421	0.01399	0.01378	0.01359	0.01339	0.01321
19	0.01474	0.01449	0.01425	0.01403	0.01382	0.01361	0.01342	0.1323	0.01305
20	0.01456	0.01431	0.01408	0.01386	0.01365	0.01344	0.01325	0.01307	0.01289
21	0.01438	0.01414	0.01391	0.01369	0.01348	0.01328	0.01309	0.01291	0.01273
22	0.01421	0.01397	0.01374	0.01353	0.01332	0.01312	0.01294	0.01276	0.01258
23	0.01404	0.01381	0.01358	0.01337	0.01317	0.01297	0.01279	0.01261	0.01243
24	0.01388	0.01365	0.01342	0.01321	0.01301	0.01282	0.01264	0.01246	0.01229
25	0.01372	0.01349	0.01327	0.01306	0.01286	0.01267	0.01249	0.01232	0.01215
26	0.01357	0.01334	0.01312	0.01291	0.01272	0.01253	0.01235	0.01218	0.01201
27	0.01342	0.01319	0.01297	0.01277	0.01258	0.01239	0.01221	0.01204	0.01188
28	0.01327	0.01304	0.01283	0.01264	0.01244	0.01255	0.01208	0.01191	0.01175
29	0.01312	0.01290	0.01269	0.01249	0.01230	0.01212	0.01195	0.01178	0.01162
30	0.01298	0.01276	0.01256	0.01236	0.01217	0.01199	0.01182	0.01165	0.01149

Table B.H2 Correction Value Based on Test Temperature

Temperature	21	22	23	25	25.5
Corrections	0.2	0.4	0.7	1.3	1.48

Table B.H3 Different Viscosity Value Based on Temperature

Temperature	19	20	21	22	23	24	25	26
Viscosity, η	0.0103	0.01009	0.00984	0.00961	0.00938	0.00916	0.00895	0.00875

Table B.H4 Values of Effective Depth Based on Hydrometer and Sedimentation Cylinder of Specified Sizes

Hydrometer 151H		Hydrometer 152H			
Actual Hydrometer Reading	Effective Depth, L, cm	Actual Hydrometer Reading	Effective Depth, L, cm	Actual Hydrometer Reading	Effective Depth, L, cm
1.000	16.3	0	16.3	31	11.2
1.001	16.0	1	16.1	32	11.1
1.002	15.8	2	16.0	33	10.9
1.003	15.5	3	15.8	34	10.7
1.004	15.2	4	15.6	35	10.6
1.005	15.0	5	15.5		
1.006	14.7	6	15.3	36	10.4
1.007	14.4	7	15.2	37	10.2
1.008	14.2	8	15.0	38	10.1
1.009	13.9	9	14.8	39	9.9
1.010	13.7	10	14.7	40	9.7
1.011	13.4	11	14.5	41	9.6
1.012	13.1	12	14.3	42	9.4
1.013	12.9	13	14.2	43	9.2
1.014	12.6	14	14.0	44	9.1
1.015	12.3	15	13.8	45	8.9
1.016	12.1	16	13.7	46	8.8
1.017	11.8	17	13.5	47	8.6
1.018	11.5	18	13.3	48	8.4
1.019	11.3	19	13.2	49	8.3
1.020	11.0	20	13.0	50	8.1
1.021	10.7	21	12.9	51	7.9
1.022	10.5	22	12.7	52	7.8
1.023	10.2	23	12.5	53	7.6
1.024	10.0	24	12.4	54	7.4
1.025	9.7	25	12.2	55	7.3
1.026	9.4	26	12.0	56	7.1
1.027	9.2	27	11.9	57	7.0
1.028	8.9	28	11.7	58	6.8
1.029	8.6	29	11.5	59	6.6
1.030	8.4	30	11.4	60	6.5
1.031	8.1				
1.032	7.8				
1.033	7.6				
1.034	7.3				
1.035	7.0				
1.036	6.8				
1.037	6.5				
1.038	6.2				

Table B.H5 Density of water and correction factor, K for various temprature (for specific gravity)

Temperature °C	Density of water (g/ml)	Correction Factor, K
16	0.99897	1.0007
17	0.99880	1.0006
18	0.99862	1.0004
19	0.99843	1.0002
20	0.99823	1.0000
21	0.99802	0.9998
22	0.99780	0.9996
23	0.99757	0.9993
24	0.99732	0.9991
25	0.99707	0.9988
26	0.99681	0.9986
27	0.99654	0.9983
28	0.99626	0.9980
29	0.99597	0.9977
30	0.99567	0.9974

Appendix C. Numerical Validation for Factor of Safety values and softwares
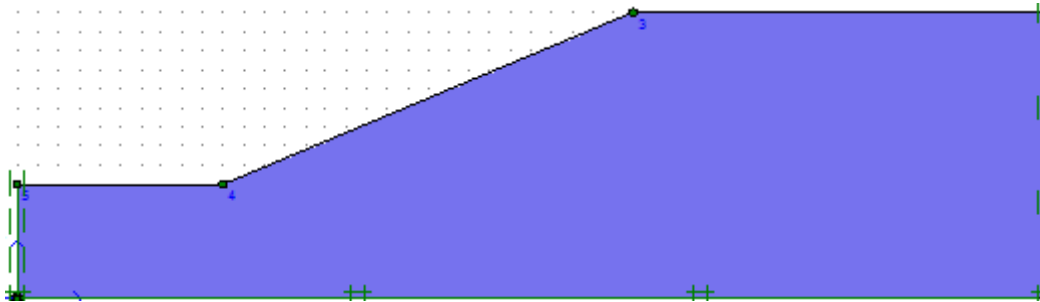

Figure C1. Geometric model used for validation (Fredlund and Krahn, 1977)

Table C1. Material Properties used by Fredlund and Krahn (Zhang *et al.*,2013)

Material	E (Mpa)	v	Υ (kn/m^3)	C (Kn/m^3)	ϕ
Soil	10	0.25	18.8	29	20

Table C2. FS by different investigators for slope by Fredlund and Krahn (1977)

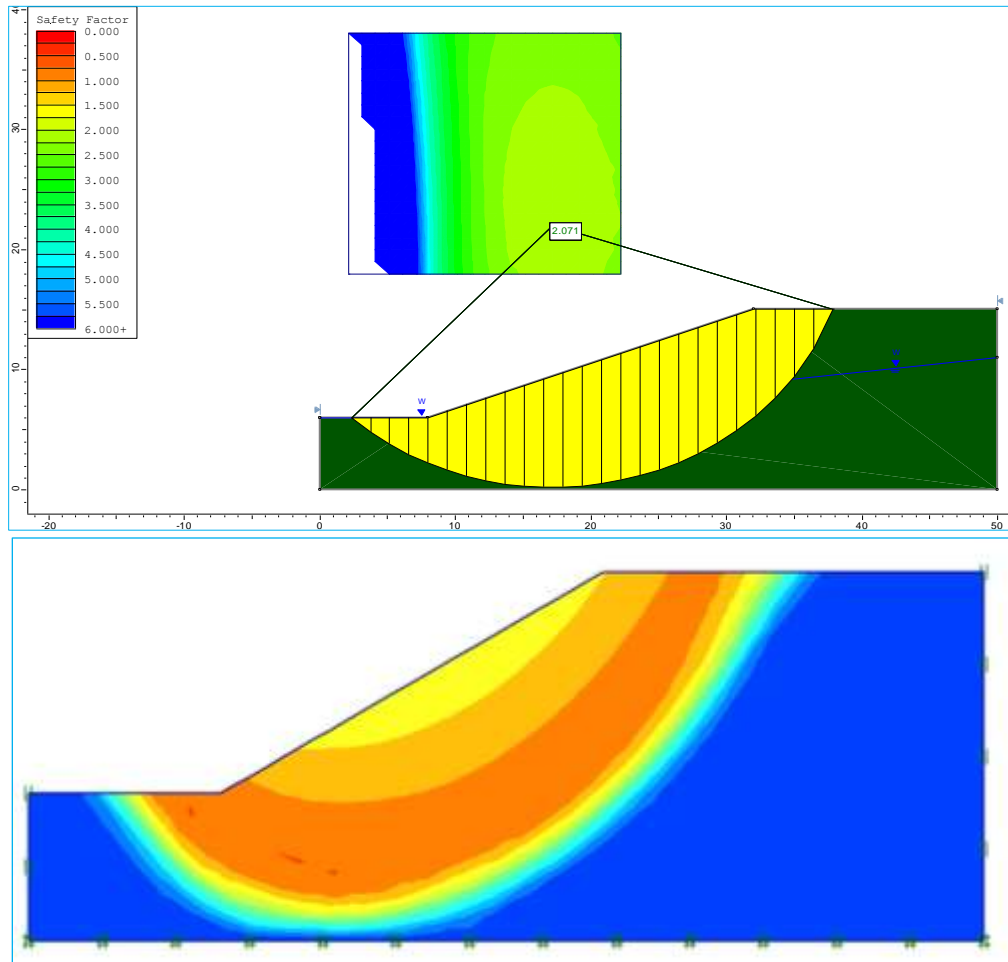| Method and Software	Referance	FS
2D (Average)	Fredlund and Krahn, (1977)	2.034
3D LEM	Zhang, (1988)	2.122
3D UB-LAM	Chen at al., (2001b)	2.262
3D LEM	Chen at al., (2003b)	2.187
3D LEM CIARA	Hungr, (1987)	2.167
3D - FEM	Griffits and Marquez (2007)	2.170
3D – FEM ABAQUS	Nian et al., (2012)	2.150
3D - FDM	Zhang et al., (2013)	2.180
2D – FEM - PLAXIS	Present Solution	2.148
2D – LEM - SLIDE	Present Solution	2.071

Figure C2. Stability analysis (Slide and Plaxis 2D) used for Validation from Fredlund and Krahn, (1977)

Appendix D. Some Photos Taken During Laboratory and Field works

Figure D1. Photo taken during Geophysical test on the field.

Figure D2. Photos taken during boring test pit.

Figure D3. Photos taken during Specific gravity and Atterberg Limits determination.

Figure D4. Photo taken during Hydrometer analysis testing.